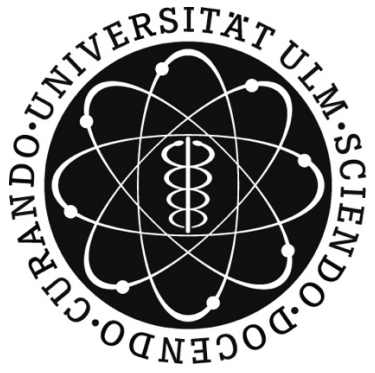

Distinct dynamics of stem and progenitor cells in trauma regeneration

Institute of Molecular Medicine,
University Ulm
Director Prof. Dr. Hartmut Geiger

Dissertation submitted in partial fulfillment of the requirements for the degree of „Doctor rerum naturalium” (Dr. rer. nat.) of the International Graduate School in Molecular Medicine Ulm

Submitted by Mona Vogel
from Göppingen
2020

Chairman International Graduate School in Molecular Medicine Ulm:

Prof. Dr. Bernd Knöll

Thesis Advisory Committee:

Prof. Dr. Hartmut Geiger, *Institute of Molecular Medicine, University Ulm*

Prof. Dr. Markus Huber-Lang, *Institute of Clinical and Experimental Trauma-Immunology, University Hospital of Ulm*

Prof. Dr. Jose Cancelas Perez, *Division of Experimental Hematology, Cincinnati Children's Hospital Medical Center*

External reviewer:

Prof. Dr. Matthias Gunzer, *Institute of Experimental Immunology and Imaging, University Hospital Essen/University of Duisburg-Essen*

&

Prof. Dr. Elvira Mass, *Life & Medical Sciences Institute (LIMES), University of Bonn*

Day doctorate awarded:

25th February 2021

Previous Publications

Parts of the results gained in my thesis have previously been published in the following publications:

Vogel M, Christow H, Manz I, Denkinger M, Amoah A, Schütz D, Brown A, Möhrle B, Schaffer A, Kalbitz M, Gebhard F, Mayer B, Huber-Lang M, Geiger H:

Distinct Dynamics of Stem and Progenitor Cells in Blood of Polytraumatized Patients.

Shock 51: 430–438 (2019)
doi: 10.1097/SHK.0000000000001198

Martin T, Möglich A, Felix I, Förtsch C, Rittlinger A, Palmer A, Denk S, Schneider J, Notbohm L, Vogel M, Geiger H, Paschke S, Huber-Lang M, Barth H:

Rho-inhibiting C2IN-C3 fusion toxin inhibits chemotactic recruitment of human monocytes ex vivo and in mice in vivo.

Arch Toxicol 92: 323–336 (2018)
doi: 10.1007/s00204-017-2058-y

Table of contents

List of Figures

List of Tables

List of Formulas

List of Abbreviations

AIS	**A**bbreviated **I**njury **S**core
ANSP-Score	**A**dditive **N**umber of **SP**Cs
BM	**B**one **M**arrow
CFU –Assay	**C**olony **F**orming **U**nit-Assay
CK	**C**reatine **K**inase
CMP(s)	**C**ommon **M**yeloid **P**rogenitor(**s**)
CXCR4	**C-X-C** Chemokine **R**eceptor type **4**
DAMPs	**D**amage-**A**ssociated **M**olecular **P**attern**s**
DNA	**D**eoxyribo**N**ucleic **A**cid
ECM	**E**xtra**C**ellular **M**atrix
EDTA	**E**thylene**D**iamine**T**etraacetic **A**cid
EGF	**E**pidermal **G**rowth **F**actor
ELISA	**E**nzyme-**L**inked **I**mmuno**S**orbent **A**ssay
EPC(s)	**E**ndothelial **P**rogenitor **C**ell(**s**)
F	**F**emale
FBS	**F**etal **B**ovine **S**erum
FFP	**F**resh **F**rozen **P**lasma
Fig	**Fig**ure
G-CSF	**G**ranulocyte-**C**olony **S**timulating **F**actor
GM-CSF	**G**ranulocyte-**M**acrophage- **C**olony **S**timulating **F**actor
GMP(s)	**G**ranulocyte-**M**acrophage **P**rogenitor(**s**)
GRO	**G**rowth-**R**egulated **O**ncogene
Hb	**H**emoglo**b**in
HBSS	**H**anks' **B**alanced **S**alt **S**olution
HiLiNut	**Hi**gh **L**ate **i**ncrease in **Nu**mbers **u**pon **t**rauma
HSC(s)	**H**ematopoietic **S**tem **C**ell(**s**)
HSPC(s)	**H**ematopoietic **S**tem and **P**rogenitor **C**ell(**s**)
Ht	**H**emat**o**crit
i.p.	**I**ntra**p**eritoneally
ICU	**I**ntensive **C**are **U**nit
IGF-1	**I**nsulin-like **G**rowth **F**actors-**1**
IL	**I**nter**L**eukin
INF-γ	**IN**ter**F**eron-**γ**
ISS	**I**njury **S**everity **S**core
KC	**K**eratinocyte **C**hemoattractant
LDBM	**L**ow **D**ensity **B**one **M**arrow
LDPB	**L**ow **D**ensity **P**eripheral **B**lood
LoLiNut	**Lo**w **L**ate **i**ncrease in **Nu**mbers **u**pon **t**rauma
M	**M**ale
MCP-1	**M**onocyte **C**hemotactic **P**rotein-1

MDC	**M**acrophage-**D**erived **C**hemokine
MIP	**M**acrophage **I**nflammatory **P**rotein
MMPs	**M**atrix **M**etallo**P**roteinase**s**
MSC(s)	**M**esenchymal **S**troma **C**ell(**s**)
n.a.	**N**ot **A**vailable
NETs	**N**eutrophil **E**xtracellular **T**rap**s**
PB	**P**eripheral **B**lood
PBS	Dulbecco's **P**hosphate **B**uffered **S**aline
PDGF	**P**latelet-**D**erived **G**rowth **F**actor
PI	**P**ropidium **I**odide
PRBC	**P**acked **R**ed **B**lood **C**ell
PT	**P**oly**T**rauma
ROS	**R**eactive **O**xygen **S**pecies
SD	**S**tandard **D**eviation
SDF-1	**S**tromal cell-**D**erived **F**actor-**1**
SEM	**S**tandard **E**rror of the **M**ean
SPC(s)	**S**tem and **P**rogenitor **C**ell(**s**)
SR	**S**hock-**R**oom
Tab	**Tab**le
TBI	**T**raumatic **B**rain **I**njury
TC	**T**hrombocyte **C**oncentrate
TGF-β	**T**ransforming **G**rowth **F**actor-**β**
TNF-α	**T**umor **N**ecrosis **F**actor-**α**
TXT	**T**hora**X** **T**rauma
VEGF	**V**ascular **E**ndothelial **G**rowth **F**actor
WBC	**W**hite **B**lood **C**ell

1. Introduction

1.1 Trauma – Definition, facts and numbers

A trauma is a physical injury of an organism caused by external influences. Penetrating traumata arise when an object pierces the skin and enters the body (Amboss, no date). Blunt trauma is caused due to impact with a blunt object or compression or crushing and leads to shear forces which can cause laceration, abrasions, vascular tears, hollow and solid organ contusions, fractures and ruptures. In Germany, most serious injuries are blunt traumata with 96.2 % of all reported cases in the trauma register (Höfer and Lefering, 2019), and life-threatening injuries are traffic accidents, falls from heights, work and sport accidents and to a minor extent suicides and violent crimes.

Ten percent of deaths worldwide are due to trauma (Chang et al., 2016). The Deutsche Gesellschaft für Unfallchirugie registered 32,580 shock-room patients which needed intensive care in the aftermath of an accident in the year 2018. 17,664 patients were severely injured. 3,481 of the registered patients died, 36 % in the first 24 h (Höfer and Lefering, 2019). Trauma is the leading cause of death in people under 40 in the high income countries (Weber et al., 2019). A deadly trauma causes an average loss of 35 years in Germany, that is more than caused by malignant neoplasms (16 years) and cardiovascular diseases (13 years) (TraumaRegister DGU, 2009).
The cost estimation per treatment day for severely injured patients was approximately 902 € and added up to 13,833 € per patient. The costs for rehabilitation and the loss of salary are not included. These numbers clearly indicate the need for research into mechanisms of trauma and trauma regeneration to improve therapeutic approaches to reduce the social-economic burden.

Trauma can be inflicted on a large number of organs with distinct types of effects. To establish treatment guidelines for different injury patterns and to compare trauma outcome between trauma centers the severity of the overall trauma is classified in standardized ways. For this, the **I**njury **S**everity **S**core (ISS) and the **A**bbreviated **I**njury **S**cale (AIS) are applied. For the AIS, each injury of a body part is scored on

a six-point scale which provides the lethality risk of the injury. One indicates a minor injury with a low lethality risk and six is a fatal injury. The body is further subdivided into different regions. Detailed lists how to assign the AIS value for a specific body region are available to standardize the score between different trauma centers (Association for the Advancement of Automotive Medicine, 2019). The AIS values are also needed to calculate the ISS. The ISS is calculated out of the three injuries with the highest assigned AIS values. For the ISS, AIS scores are squared and then the three values are added together to obtain the ISS (ISS = highest AIS^2 + second highest AIS^2 + third highest AIS^2).

An ISS ≥ 16 indicates severe trauma. Multiple injuries at different body regions, of which one or the combination is life-threatening are called **P**oly**T**rauma (PT). The `Berliner definition` of PT states that an ISS ≥ 16 must be reached with at least two relevant injuries (AIS ≥ 3). Furthermore, at least one of the five standardized physiological responses age (≥70 years), hypotension (systolic blood pressure ≤ 90 mmHg), unconsciousness (Glasgow Coma Score ≤ 8), acidosis (base excess ≤ −6.0) and coagulopathy (partial thromboplastin time ≥ 40 s or international normalized ratio ≥ 1.4) must be observed (Pape et al., 2014).

1.2 Molecular mechanism in tissue regeneration

In tissue repair, damaged and lost tissue is replaced by granulation and scar formation, whereas in regeneration the tissue is replaced by functional and specialized cells of the tissue to regenerate the function of the tissue (Watson, no date). The type and severity of injury will strongly influence the outcome and duration of tissue healing which might range from incomplete healing, scarring and fibrosis formation to complete restoration (regeneration). The healing process undergoes four phases: bleeding, inflammation, proliferation and remodeling (**Fig**ure (Fig.) 1).

The first phase after injury aims to end the bleeding and is termed hemostasis. It occurs directly after the injury and is fast. In primary hemostasis blood flow is stopped by vasoconstriction and platelet plug formation, this only takes 1-3 **min**utes (min). In the secondary hemostasis, the blood coagulates and forms the thrombus which is harder and more stable than the primary hemostasis plug (Hick and Hick, 2009).

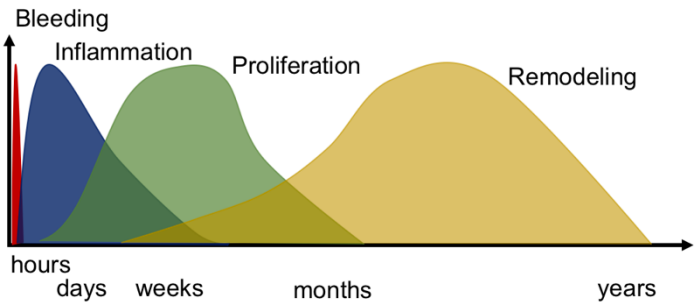

***Figure 1: The four phases of tissue repair**. After tissue damage, there is a relative short-lived bleeding phase followed by the inflammation phase which has a rapid onset and a peak at around 1-3 days. The inflammation can take up to weeks to be completely resolved. The proliferation phase, starting 24-48 h after injury, can have a duration of several month (4-6) and the remodeling phase which can take years indicates the end of tissue repair. The time scale is only a rough estimation and strongly depends on the tissue and the severity of the injury (based on Watson, no date).*

An inflammation phase follows which can last for a few hours up to several weeks. Inflammatory cells, chemical mediators, scaffolding cells and fluids will be found at the side of injury, starting the cleaning and repair progress. Interestingly, the systemic inflammatory response does not only contain immune-stimulating factors but also involves features with immune-suppressive functions. The balance between those features is important to clear the molecular danger signals and to induce repair mechanisms (Huber-Lang et al., 2018).

The proliferation phase can already start 24-48 **h**ours (h) after the injury and reaches its peak 2-3 weeks post injury. Then collagen is produced for scar formation and proliferation of local fibroblasts takes places to strengthen the healing tissue.

In the last phase of repair, which can begin after the first week of injury and which can last up to one year or longer, the recently formed tissue gets replaced by collagen type I. This leads to an organized and functional scar which is able to behave similar to the original tissue. As indicated in Fig. 1, the different phases overlap and are often dependent on each other so that one phase might act as activator/initiator for the other phase (Watson, no date).

1.2.1 Inflammation phase

Every tissue damage leads to an inflammation but not all tissue damage is associated with pathogen infiltration. **D**amage-**A**ssociated **M**olecular **P**attern**s** (DAMPs), like heat shock proteins, high-mobility group box protein 1 or DNA, uric acid and ATP released from damaged cells can also trigger an inflammatory response (Relja and Land, 2019). In the inflammation phase, there are successions of vascular and cellular events, aiming to clean up cell debris and initiating repair processes.

1.2.1.1 Vascular cascade

In the injured vessels, hemostasis is achieved by a strong vasoconstriction and blood thrombus formation (Hick and Hick, 2009). After the injury, damaged tissue, mast cells and resident macrophages release prostaglandins, leukotrienes and histamines which activate endothelial and smooth muscle cells (Kumar V et al., 2012). Smooth muscle cells relax which leads to vasodilation and an increased but slower blood flow in the blood vessels. Additional, dormant capillaries open up to increase blood flow through their capillary bed. Endothelial cells constrict thereby gaps between the normally tightly associated endothelial cells open up which increases permeability of blood vessels. Furthermore, endothelial cells release p-selectins which are then expressed on their surface. Increased blood volume and the slower blood flow together with the expression of selectins increases the migratory abilities of **W**hite **B**lood **C**ells (WBC).

1.2.1.2 Cellular responses

Necrotic and stressed cells as well as damaged **E**xtra**C**ellular **M**atrix (ECM) release DAMPs which trigger inflammation via the nuclear factor 'kappa-light-chain-enhancer' of activated B-cell (NF-κB) pathway or interferon-regulatory factors (Relja and Land, 2019). The activated tissue resident immune cells and non-hematopoietic cells release chemoattractants which serve as additional signals for neutrophils and monocytes to migrate into the damaged tissue.

Neutrophils

Neutrophils are key players of the innate immune system and the first line defenders. In the last years, a high heterogeneity and functional versatility of the neutrophil population was illustrated (Silvestre-Roig et al., 2016). The main

contributions to tissue repair by neutrophils are the phagocytosis of tissue debris and the release of growth or pro-angiogenic factors. Upon migration and activation neutrophils are also able to generate **R**eactive **O**xygen **S**pecies (ROS), release proteolytic enzymes, antimicrobial proteins and can form **N**eutrophil **E**xtracellular **T**rap**s** (NETs), which can in some cases induce tissue damage (Mayadas et al., 2014). The response of the neutrophils is most likely context-dependent, and the mechanisms which result in the conversion of neutrophil action from physiological tissue repair and regeneration to pathological tissue damage and chronic diseases still need to be investigated (Wang, 2018).

Over time, neutrophils become apoptotic and are cleared by macrophages. This process starts a feed-forward pro-resolution program that is characterized by the release of tissue-repairing cytokines such as **T**ransforming **G**rowth **F**actor-**β** (TGF-β) and **I**nter**L**eukin (IL) -10 (Julier et al., 2017). In addition, there is evidence that neutrophils are also involved in the modulation of the adaptive immune response by interacting with T-cells at the side of inflammation and migration into lymph nodes (Leliefeld et al., 2015).

Monocytes and Macrophages

Next to a small number of tissue macrophages, a large number of circulating Ly6C^{high} monocytes get recruited to the site of injury, where they differentiate into macrophages. Dependent on the microenvironment, macrophages take on a pro-inflammatory, pro-tissue healing, pro-fibrotic or an anti-inflammatory, anti-fibrotic, pro-resolving and tissue regenerating phenotype (Wynn and Vannella, 2016). Therefore, macrophages have a critical role in the regulation of all stages of repair. In the initial phase after injury macrophages release chemokines, **M**atrix **M**etallo**P**roteinase**s** (MMPs) and other inflammatory mediators which drive the inflammation. They phagocytize cell debris, neutrophils and other apoptotic cells.

After the early inflammation phase, the pro-inflammatory macrophages switch to a tissue healing phenotype. The now dominant pro-tissue healing macrophages produce growth factors, promote cell proliferation and recruitment of fibroblasts as well as stem and progenitor cells, mediate blood vessel formation and ECM production by myofibroblast differentiation.

A dysfunctional or deregulated monocytes/macrophage response has detrimental effects on tissue repair and regeneration. While pro-inflammatory macrophages

enhance tissue damage and impair tissue healing, the continued activation of the pro-tissue healing phenotype is involved in the development of pathological fibrosis. An overview of the initial response from neutrophils and monocytes is illustrated in Fig. 2.

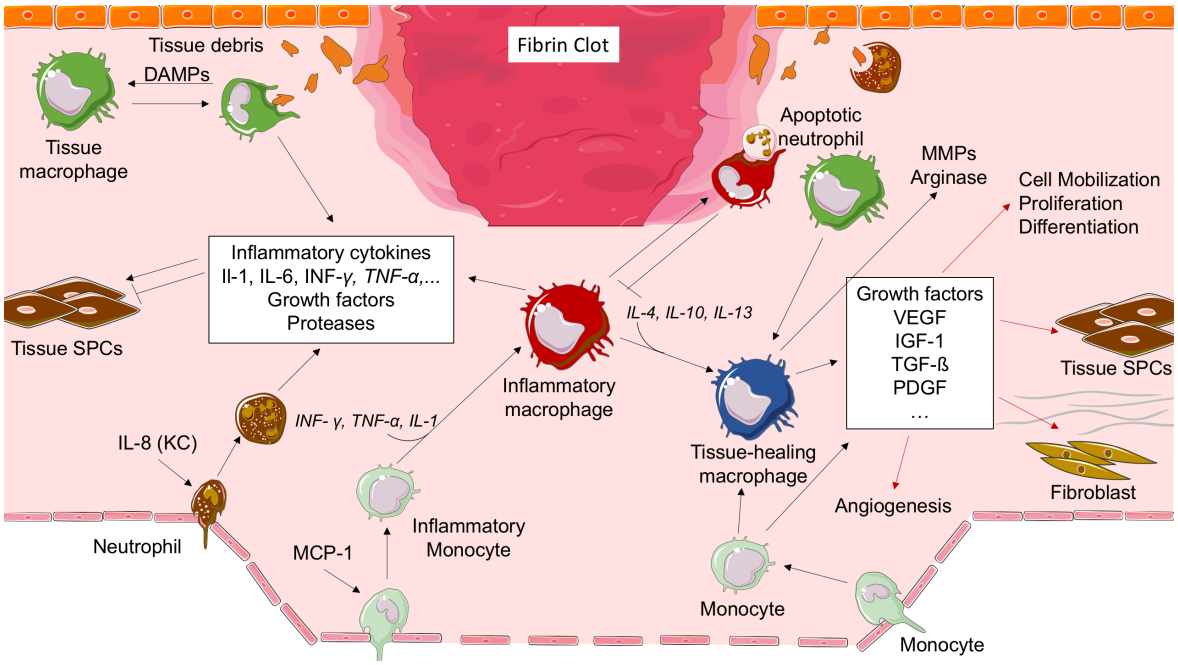

***Figure 2**: **Initial immune response of neutrophils and monocytes/macrophages.** Release of chemical mediators regulate the immune responses of the immune cells. INF-γ = **IN**ter**F**eron-**γ**, TNF-α = **T**umor **N**ecrosis **F**actor-**α**, VEGF = **V**ascular **E**ndothelial **G**rowth **F**actor, IGF-1 = **I**nsulin-like **G**rowth **F**actors-**1**, PDGF = **P**latelet-**D**erived **G**rowth **F**actor, KC = **K**eratinocyte **C**hemoattractant, MCP-1 = **M**onocyte **C**hemotactic **P**rotein-1. (Based on Julier et al., 2017; Image generated with Servier Medical Art (http://smart.servier.com/), licensed under a Creative Common Attribution 3.0 Generic License (https://creativecommons.org/licenses/by/3.0/)).*

Lymphocytes

Neutrophils and monocytes that infiltrate the damaged tissue are associated with the inflammation phase, while lymphocytes (B- and T-cells) are more closely associated with the following proliferation and remodeling phases (Park and Barbul, 2004).

$CD4^+$ regulatory T-cells have the ability to induce anti-inflammatory, pro-repair macrophages, partly through arginase, IL-10 and TGF-β pathways (Liu et al., 2011). Additionally, $CD4^+$ regulatory T-cells are shown to reduce acute lung injury fibroproliferation by decreasing fibrocyte recruitment (Garibaldi et al., 2013). The γδT-cell type is especially important for tissue healing. In the absence of γδT-cells skin wound healing is not effective (Havran and Jameson, 2010). A specific subset of the γδT-cells is further primed to secrete growth factors and cytokines (Ramirez

et al., 2015). For example, the secretion of IL-17A by γδT-subset cells enhances osteoblast function in bone injury and the production of IL-22 mediates proliferation and migration of epithelial cells in various tissues (Kumar P et al., 2012).

B-cells, next to their potential as antibody-producing plasma cells, might be able to modulate the local immune response by the secretion of pro- and anti-inflammatory cytokines and by presenting antigens to T-cells (Li et al., 2016). They are also shown to infiltrate a bone fracture site, accelerating bone fracture healing by producing osteoprotegerin (Könnecke et al., 2014). Goodchild et al. (2009) could show that the application of B-cells promotes tissue regeneration after acute myocardial infarction and in chronic and acute wound healing the application of mature B-cells also speeds up wound healing, enhances angiogenesis, reduces scar formation, increases collagen deposition and maturation and supports nerve growth (Sîrbulescu et al., 2017).

1.2.2 Lung regeneration

An insult to the lungs, direct or as a consequence of remote organ injury and/or hemorrhagic shock, damages lung tissue and vessels leading to an active bleeding and the release of DAMPs. The bleeding and the following clot formation reduce oxygenation and perfusion of alveolar capillaries. Acute lung injury still remains the leading cause of acute respiratory distress syndrome, morbidity and death in patients who have suffered trauma (Huber-Lang et al., 2018).

DAMPs and the activated coagulation system induce the innate immune response, leading to the migration of first neutrophils, followed by monocytes, which differentiate on-site into macrophages. Neutrophils start with the clearance of cell debris and DAMPs, release granules, inflammatory mediators and proteases, generate ROS and form NETs (Grommes and Soehnlein, 2011). Proteases and ROS promote barrier degradation by inducing alveolar epithelial cell apoptosis and pulmonary microvascular endothelial cell injury. This leads to a disruption of the air-blood-barrier, formation of edema in the extra-alveolar space, intra-alveolar accumulation of protein-rich fluids and the formation of hyaline membranes which further impairs gas exchange and blood oxygenation (Huber-Lang et al., 2018). Neutrophils undergo early apoptosis and are cleared away by alveolar macrophages and the inflammation starts to resolve. Alveolar macrophages initiate the innate immune response and, dependent on the posttraumatic

microenvironment and the progress made in cell debris clearance, they can switch to an anti-inflammatory phenotype (Robb et al., 2016). They phagocyte apoptotic neutrophils and release anti-inflammatory cytokines inducing tissue remodeling.

Remodeling processes and repair mechanisms to regenerate normal alveolar surface and healthy gas exchange are complex and multifactorial. They include the recovery of the epithelial layer, clearance of inflammatory signals and edema from the airspace, remodeling of the interstitial matrix and repair of the endothelial layer (Gill et al., 2017). For the recovery of the epithelial layer alveolar type II cells seem to play a central role. They are able to proliferate and to differentiate into alveolar type 1 cells (Kapanci et al., 1969). Furthermore, application of type II alveolar cells reduced fibrosis formation in bleomycin injured lungs (Serrano-Mollar et al., 2007, Wada et al., 2012, Guillamat-Prats et al., 2014). Additionally, it was proposed that mesenchymal stem cells (Hayes et al., 2015) or rare lung progenitor cells are involved in producing type II alveolar cells and thereby improving alveolar repair.

Pulmonary microvascular endothelial cells need to proliferate and need to re-establishment the inter-endothelial junctions to remodel and repair the damaged endothelium and to form a leak-resistant barrier (Bhattacharya and Matthay, 2013). Suzuki et al. (2016) showed that there are resident endothelial cells in the lung which are able to undergo endothelial-to-mesenchymal transition to a highly proliferative progenitor-like cell while others (Mao Sun-Zhong et al., 2015) illustrated that bone marrow-derived endothelial progenitor cells are recruited to the injured lung to support the restoration of barrier functions. After the regeneration of the epithelial and endothelial cell layer a clearance of alveolar fluid takes place by epithelial sodium channels and the NA/K-ATPase in both alveolar type I and II epithelial cells (Hummler et al., 1996, Lin et al., 2016). To repair the alveolar wall interstitium, residual interstitial edema needs to be removed and an intact interstitial compartment needs to be generated by deposition of fibrin and collagen fibers from fibroblasts (Olczyk et al., 2014).

While the regeneration of the single compartments is of highest importance, a complete restoration of the lung and thus lung function requires a crosstalk among the individual components of the alveolar barrier. For example, a crosstalk among macrophages, monocytes and epithelial cells promotes epithelial remodeling (Chen et al., 2014) or, pulmonary microvascular endothelial cells stimulate the proliferation of alveolar epithelial cells (Ding et al., 2011).

1.2.3 Immunomodulation therapies in trauma regeneration

PT patients manifest with a higher mortality rate, longer stays in **I**ntensive **C**are **U**nit (ICU) and higher expenses than non-PT patients with the same ISS (Rau et al., 2017). Late post injury complications like multiple organ dysfunction syndrome or persistent inflammation, immunosuppression, and catabolism syndrome are commonly observed (Probst et al., 2009, Gentile et al., 2012). Severe or multiple injuries like in PT often induce a complex immune response which might contribute to these post injury complications and prevent a timely and full regeneration. Modulating the body's own immune response to reduce tissue damage in organs and to repair and regenerate these damaged tissues is a new prospective in the field of trauma regeneration. For instance, the anti-inflammatory macrophage phenotype could be induced by the application of decellularized ECM which positively influenced the wound immune microenvironment (Badylak et al., 2008). Sadtler et al. (2016) found out that the tissue derived ECM scaffolds are able to support polarization towards the anti-inflammatory macrophage phenotype by meditating a strong Th_2 answer. Another immunomodulation avenue is to provide anti- or pro-inflammatory cytokines to regulate the immune response. Hyaluronic acid and TNF-α induced early healing after burn injury in rats (Friedrich et al., 2014) or Prostaglandin E_2 locally applied by a cholesterol bearing pullulan nanogel was supporting bone regeneration in mice (Kato et al., 2007).

However, immunomodulation therapies in trauma regeneration are still in their infancy. For a safe and beneficial use of immunomodulation for enhancing trauma regeneration the host response to injury and shock needs to be first understood in much more detail.

1.3 Stem and progenitor cells (SPCs) in trauma regeneration

Distinct types of adult stem cells have been found in up to 20 distinct tissues of the body. These rare cells are characterized by their ability to self-renew and differentiate into more committed progenitor cells or functional mature cells of a tissue or organ system. Stem cells can be categorized by their potency. Adult stem cells are mostly categorized as multipotent or oligopotent, they differentiate into the cells of a specific organ system. Normally they are located in specialized niches, where they are protected from external harmful stimuli. They are kept in a quiescent

state until they are activated by an appropriate activation signal (Montagnani et al., 2016).

Transient amplifying progenitor cells retain an undifferentiated state, their function is the generation of a sufficient amount of specialized progeny for tissue maintenance (Stripp, 2008). However, while they keep the ability to proliferate and to differentiate, they lose the ability for self-renewal, thus they are not able to provide long-term potential. Systems like skin, intestine and the hematopoietic system are strongly dependent on stem cells to keep tissue homeostasis throughout a lifetime. Tissue-specific adult **S**tem and **P**rogenitor **C**ell**s** (SPCs) are able to regenerate tissue after injury. Localized and circulating SPCs are attracted to the site of an injury. These SPCs are thought to promote the following function in tissue repair: they replace dead cells through differentiation, they produce soluble factors, such as chemokines, cytokines and growth factors promoting anti-inflammatory and cell-protective effects and they stimulate self-regenerative and repair processes (Pati et al., 2015) (Fig. 3).

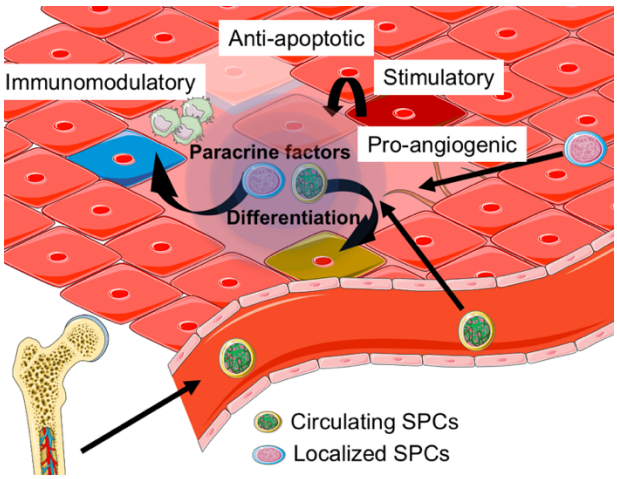

Image generated with Servier Medical Art (http://smart.servier.com/), licensed under a Creative Common Attribution 3.0 Generic License (https://creativecommons.org/licenses/by/3.0/).

Figure 3: Stem and progenitor cells in tissue repair.
The injured tissue releases DAMPs and chemical factors like chemokines and cytokines. Localized and circulating SPCs are attracted to the site of injury. SPCs are also shed into peripheral blood from the bone marrow, increasing the availability of SPCs. At the site of injury SPCs replace damaged or dead cells by differentiation. They release paracrine factors promoting angiogenesis, cell survival and immunomodulation mostly anti-inflammatory. Furthermore, they stimulate endogenous tissue repair and regeneration.

For example, stem cells in the hair follicle bulge migrate towards an epidermal injury and take on an epidermal phenotype generating short-lived 'transient amplifying' cells which are responsible for acute wound repair (Ito et al., 2005). In another instance, adult human renal progenitor cells support the regeneration of acute tubular and glomerular damage, through paracrine mechanisms and differentiation

(Bussolati and Camussi, 2015) and surviving intestinal stem cells are able to regenerate entire crypts after total body irradiation (Kim et al., 2017).

In some tissues, for example in the lung, already differentiated cells can also be stimulated to proliferate under stress conditions like injuries. These cells are called facultative progenitor cells and they manifest with a highly infrequent proliferation. Upon injury, these cells can undergo transition to a continuous proliferation state and they are suggested to possess the ability to go from a differentiated state to an undifferentiated state and vice versa between normal and injury/repair conditions (Stripp, 2008).

Next to the local tissue-specific SPCs it is also thought that the recruitment of other SPC populations is part of tissue regeneration. Upon injury DAMPs, cytokines, chemokines and growth factors are released from the damaged tissue, mediating migration of SPCs towards the injured tissue (**Tab**le (Tab.) 1 List of factors that enhance migration and mobilization of SPCs). SPCs are also shed into the **P**eripheral **B**lood (PB), mostly out of the **B**one **M**arrow (BM), to increase SPCs in circulation which might then migrate to sites of injury. **M**esenchymal **S**troma **C**ell**s** (MSCs), **H**ematopoietic **S**tem and **P**rogenitor **C**ell**s** (HSPCs) and **E**ndothelial **P**rogenitor **C**ell**s** (EPCs) are shown to have a beneficial effect for tissue regeneration (Porada et al., 2016, Kamei et al., 2017,Han et al., 2008). In the next section an overview over MSCs, HSPCs and EPCs and their possible roles in tissue repair is thus given in detail.

Table 1: Factors that enhance migration and mobilization of SPCs
*GRO = **G**rowth-**R**egulated **O**ncogene, G-CSF = **G**ranulocyte-**C**olony **S**timulating **F**actor, GM-CSF = **G**ranulocyte-**M**acrophage-**C**olony **S**timulating **F**actor, MIP = **M**acrophage **I**nflammatory **P**rotein, SDF-1 = **S**tromal cell-**D**erived **F**actor-**1**.*

SPC Population	Mobilizing and migration factors	Reference
MSCs	GRO, IL-1 β, IL-6, IL-8, MCP-1, MIP-1 α, MIP-1 β, SDF-1, TNF- α, VEGF	(Ghaffari-Nazari, 2018, Xing et al., 2014, Fu et al., 2019)
HSPCs	G-CSF, GM-CSF, GRO-β, IL-8, IL-33, MCP-1, MIP-1 α, SDF-1, VEGF	(Pelus and Fukuda, 2006) Si et al., 2010, Kim et al., 2014, Cencioni et al., 2012)
EPCs	G-CSF, GM-CSF, GRO-β, IL-6, IL-8, SDF-1, VEGF	(Tilling et al., 2009, Fan et al., 2008)

1.3.1 Mesenchymal Stroma Cells (MSCs)

MSCs are multipotent and able to differentiate into all non-hematogenous cells in the mesoderm lineage like osteoblasts, chondrocytes and adipocytes. They are mostly localized in the BM, but they can be found in all tissues, partly in a perivascular localization (Crisan et al., 2008). To a certain extent, functionality of MSCs differs dependend on the tissue source (Klimczak and Kozlowska, 2016). The International Society for Cellular Therapy defined minimal criteria for the identification of MSCs in humans (Dominici et al., 2006). In animal model's markers for their identification are still controversially discussed in the literature.

MSCs are able to migrate. Trafficking of endogenous MSCs to injured tissues is implied to be a part of the natural self-healing response (Lin et al., 2017). Following an injury, MSCs are found in higher numbers in the peripheral circulation in mice (Wan et al., 2012) and humans (Wiegner et al., 2018). Furthermore, endogenous or venously applied MSCs can be traced to the site of injury (Oh et al., 2018, Kitaori et al., 2009, Wan et al., 2012), indicating that MSCs migrate towards the site of injury also via PB. Both mobilization and migration are controlled by cytokines or chemokines. Tab 1 provides an overview over some of the chemical factors influencing MSC mobilization and migration. Mechanical factors like ECM stiffness, vascular cyclic stretching or hemodynamic forces on vessel walls also influence the migration process (Fu et al., 2019).

After migration to an injured tissue, MSCs can promote regeneration. There are several mechanisms described how MSCs support regeneration. For example, it is shown that MSCs release paracrine factors which promote angiogenesis (Selvasandran et al., 2018), protection against apoptosis (Li et al., 2020) and immunosuppression (Ren et al., 2008). Paracrine factors have also beneficial effects on tubular cell repair in kidneys (Imberti et al., 2011) or assist in burn wound healing (Oh et al., 2018). Furthermore, MSCs can support regeneration through direct differentiation. They can for example differentiate into tissue fibroblasts assisting in the generation of the ECM, or differentiate into $CD31^+$ endothelial cells in skin regeneration (Li et al., 2017) or trans-differentiate into neuronal cells (Hermann et al., 2004) or hepatocytes (Ye et al., 2015).

Recently, it was also discussed that the engulfment of MSCs by host phagocytic cells plays a central role for the MSC-transmitted immunomodulatory effects

(Hoogduijn and Lombardo, 2019) as engulfment of MSCs results in, among other things, a higher expression of IL-10 and TGF-β and a lower expression of TNF-α (Witte et al., 2018).

In summary, MSCs exhibit both regenerative and immunomodulatory abilities.

MSCs can be easily harvested from diverse tissues like BM, muscle and adipose tissue and be expanded in vitro. Together with their "robustness" which enables freeze-thaw cycles and their lack of the expression of MHC II molecules which reduced their antigenicity, MSCs are promising cell therapeutics that might be used in multiple novel therapeutic approaches – including trauma regeneration.

1.3.2 Hematopoietic Stem and Progenitor Cells (HSPCs)

Hematopoietic **S**tem **C**ells (HSCs) are among the best characterized somatic stem cells. HSCs form in a process that is termed hematopoiesis all types of blood cells. HSCs and progenitors can be identified by distinct combinations of cell surface markers. This allows hematopoiesis to be organized in a hierarchy. HSCs are at the top of the hierarchy, they are able to self-renew and to differentiate into all blood cells. Early progenitors, the direct progeny of HSCs, are still able to differentiate into all lineages but have lost their ability for self-renewal. Late progenitors, like **C**ommon **M**yeloid **P**rogenitors (CMPs) or **G**ranulocyte-**M**onocyte **P**rogenitors (GMPs) are mostly uni- or oligopotent and might only be able to differentiate into one specific blood lineage.

HSPCs are mostly localized in the BM. There are also found in small numbers in other tissues like muscle, liver, spleen and PB. There is a steady trafficking of HSPCs from bone marrow into blood and back to bone marrow. Massberg et al. (2007) proposed a concept of HSPC mediated immunosurveillance. They could show that BM derived HSPCs enter the blood to subsequently migrate into multiple peripheral organs. HSPCs then stay for at least 36 h before they enter the lymphatic system to return to the blood and eventually back to the BM. Tissue resident HSPCs might give rise to innate immune cells while they are tissue residents.

In the BM, HSCs reside in specific stem cell niches, where they are mostly kept quiescent. Both the stem cell niche as well as HSC intrinsic factors react to changes in the balance of blood cells. Both then promote the activation of HSCs leading to proliferation and/or differentiation. HSPCs are discussed to be the ´driving cells´ of an immune response, because they react directly and immediately to infections and

inflammatory signals (King and Goodell, 2011). HSCs are for example activated by INF-γ (Baldridge et al., 2010), HSCs and early progenitors have also a critical role in inflammatory granulopoiesis upon sepsis (Ueda et al., 2009) and there is an emergency machinery of stem-like megakaryocyte-committed progenitors that can counteract platelets depletion during inflammation (Haas et al., 2015). Thus, HSCs control hematopoietic tissue homeostasis and respond to stressors like microorganisms, bleeding and inflammation.

Upon tissue injury and disease, there is an increase in the frequency of HSPCs in peripheral circulation (Massa et al., 2005, Gehling et al., 2010). Mobilization and migration factors of HSPCs are listed in Tab. 1. Furthermore, in animal models HSPCs migrate to the damaged/non-functional tissue and support regeneration (Si et al., 2010, Lagasse et al., 2000, Gussoni et al., 1999). The role of HSPCs in tissue regeneration is as of yet not completely understood. Differentiation into effector cells might be one way how HSPCs can support repair mechanisms. Si et al. (2010) demonstrated that lineage negative hematopoietic cells differentiate into M2 macrophages in injured liver. In another example, Kim et al. (2011) showed that HSPCs proliferate and then differentiate into mature neutrophils in Staphylococcus aureus-infected skin wounds. HSPCs can also influence and modulate the immune function by releasing paracrine factors. For instance, $CD34^+$ human HSPCs are able to generate Th_2 cytokines like IL-5, IL-13, IL-6, and GM-CSF (Allakhverdi and Delespesse, 2012). There is also a cross-talk between endothelial cells and HSPCs for example HSPCs are able to release angiogenic factors, like VEGF-A, which promotes proliferation, survival, motility and remodeling of endothelial cells (Rafii et al., 2016).

HSPCs are thus able to provide effector cells of the immune system and can release paracrine factors that stimulate tissue repair, modulate the immune response and influence vascularization.

1.3.3 Endothelial Progenitor Cells (EPCs)

The first report of BM derived circulating progenitors for the endothelial lineage (EPCs) was published in 1997 by Asahara et al.. Since then many additional publications attempted to shed light on the definition, origin, and function of EPCs. Despite a large number of such publications, many uncertainties remain in the field (Yoder Mervin C., 2010). The vast heterogeneity within the EPC population led to a

new classification in which EPCs are separated in circulating angiogenic cells, myeloid angiogenic cells and endothelial colony forming cells (Medina et al., 2017). However, as most of the publications are based on the older classification in which all cells that are able to differentiate into endothelial cells and which contribute to the formation of new blood vessels were simply termed EPC, the term EPC will still be applied in this work to this heterogeneous cell population.

Upon injury EPCs are found to be enriched in PB. For example, EPCs are increased at day 4 and 7 after **T**raumatic **B**rain **I**njury (TBI) (Wei et al., 2019). EPC numbers are elevated in long bone fractures with a peak at 3 days post injury. The severity of the trauma does not significantly influence the number in long bone fractures. In animal models, also migration of EPC towards the site of injury could be observed (Matsumoto et al., 2008). Thus EPCs, as MSCs and HSPCs, manifest with mobilizing and migratory abilities (Tab. 1). EPCs contribute to tissue repair by direct differentiation into endothelial cells. They can further shed growth factors to initiate the induction and activation of endogenous cells (Kamei et al., 2017). The transplantation of EPCs in a model of skeletal muscle injury induced the expression of VEGF. This could be a reason why enhanced angiogenesis and reduced fibrous scar formation could be observed (Shi et al., 2009). Additionally, human blood derived EPCs improve spinal cord injury regeneration, while again VEGF is upregulated (Kamei et al., 2013). Furthermore, EPCs mediate a better vascularization in a bone defect model, not only by paracrine factors but also because EPCs directly formed new vessels by differentiation (Seebach et al., 2012). EPCs therefore influence vascularization processes by releasing paracrine factors like VEGF. Additionally, they can directly replace lost or form new endothelial cells.

1.4 Stem cell based therapies

The aim of stem cell based therapies is to replace and repair damaged or diseased human cells, tissues or organs to restore functionality. The number of severely traumatized patients and PT patients surviving the early stages of hemorrhage and trauma has increased in recent years (Mira et al., 2018). Yet, the morbidity and mortality from later stage complications after severe injury though remains high (Mira et al., 2018). This demonstrates the need for new therapeutics for intermediate and long-term trauma patients, where so far only limited treatment options are available. A promising avenue are stem cell based therapies. As illustrated in the

last section, adult SPCs contain a high regenerative potential. The idea behind stem cell based therapies is to use this potential to enhance the repair and the function of damaged or diseased tissues.

Studies showed that the number of circulating stem cells is linked to tissue repair and disease progression (Tomoda and Aoki, 2003, Herbrig et al., 2006, Marchesi et al., 2008). If the number of circulating SPCs does play such a central role, increasing this number in trauma by for example mobilization of endogenous stem cells might provide an additional therapeutic effect. Thus, in the next paragraph, mobilization of endogenous adult SPCs as a treatment option in trauma regeneration is discussed. Furthermore, current challenges for stem cell based therapies in trauma regeneration will be addressed.

1.4.1 Mobilization of endogenous SPCs

Next to allogenic or autologous SPC transplantations and localized application of homing factors at the site of injury, mobilization of endogenous SPCs might be another approach to increase the availability of SPCs. Hereby the term mobilization is used for a process in which drugs or cytokines or chemokines are applied to induce the movement of SPCs from their niches into the peripheral circulation (National cancer Institute, no date). From there SPCs can migrate towards the site of injury due to chemotaxis and vascular changes.

Mobilization of endogenous stem cells might be an attractive approach for supporting regeneration upon trauma because SPC transplantation has still several limitations including restricted supply of clinical-grade cells as well as expensive and time consuming in-vitro cell expansion (Pati and Rasmussen, 2017, Herrmann et al., 2015). Furthermore, allogenic cells can be immunogenic, and even the long thought immune privileged MSCs were shown to induce immune responses promoting rejection (Berglund et al., 2017). Some effect on disease and trauma progression upon inducing mobilization of SPCs by pharmacological intervention has been already reported. In acute myocardial infarction (Luo et al., 2013), stroke (Kawada et al., 2006), bone fracture (Toupadakis et al., 2013) and spinal cord (Park et al., 2018), acute kidney (Zuk et al., 2014) and liver injury (Zhai et al., 2018) the pharmacological induced mobilization of SPC improved tissue attrition in mice. A clinically approved drug to induce SPC mobilization right after administration (aka

1-2 h after administration) is AMD3100 which uses the SDF-1/ **C-X-C** Chemokine **R**eceptor type **4** (CXCR4)-axis to induce mobilization.

1.4.1.1 The SDF-1/CXCR4-axis

The CXC chemokine SDF-1 is produced by many BM stroma cell types as well as by many types of epithelial cells (Lapidot and Kollet, 2002). Under physiological conditions, SDF-1 is upregulated in regions of hypoxia within the BM, most likely mediated by the transcription factor Hypoxia-inducible factor-1 α (Ceradini et al., 2004). Cells migrate in response to concentration of SDF-1 and home into the BM. Its receptor CXCR4, a specific G-protein-coupled seven-span transmembrane receptor, is expressed on many cell types including MSCs (Liu et al., 2010), HSCs (Wright et al., 2002) and EPCs (Dai et al., 2011). The SDF-1/CXCR4-axis promotes cell survival, proliferation and differentiation and is thought to be a key regulator of stem cell homing and migration. Wright et al. (2002) for example showed that only SDF-1 yields chemotactic responsiveness of HSCs in vitro compared to a large number of other chemokines. In another instance Kyriakou et al. (2008) illustrated that the overexpression of CXCR4 on MSCs increases BM homing after irradiation and transplantation. In Tie2-lineage cells, which include the EPC population, deletion of CXCR4 lead to a severe reduction of their migratory activity (Kawakami et al., 2015).

Additional evidence for the central role of the SDF-1/CXCR4-axis for SPC migration and/or mobilization stems from injury model systems. For example, SDF-1 is upregulated at the sites of injury in ischemia/reperfusion induced liver injury (Jin et al., 2018), in the ischemic area in the brain after stroke (Hill et al., 2004), in bone fractures coupled to TBI (Liu et al., 2013) or in ligament injuries (Shimode et al., 2009). SDF-1 is thereby most likely released from hypoxic endothelium (Ceradini et al., 2004) and by activated platelets (Massberg et al., 2006). Blocking of SDF-1 in ischemic tissue or of CXCR4 on circulating SPCs inhibits SPC recruitment to sites of injury (Ceradini et al., 2004), whereas an increased tissue concentration of SDF-1 for example by local application further enhances the migration of the SPCs to the site of injury (Tang et al., 2005).

The mobilization of the BM SPCs into PB might be initially induced by a circulating SDF-1 which induces desensitization of the CXCR4 in the BM (Shen et al., 2001). It is a possibility that neutrophils and monocytes in BM generate a proteolytic environment upon AMD3100 stimulation which might be needed for optimal SPCs

release from the BM (Lee et al., 2010). Additionally, Heissig et al. (2002) showed that higher plasma levels of SDF-1, VEGF or G-CSF induce the release of MMP-9, which is required for the release of BM derived cells. The migration towards the damaged area might be promoted by the binding capacity of immobilized SDF-1 around ischemic blood vessels which may overcome the desensitization (Peled et al., 1999, Rennert et al., 2012). Therefore, the SDF-1/CXCR4-axis might mediate both retention and mobilization of SPCs in BM and tissue specific adhesion and migration into tissue upon injury.

1.4.1.2 AMD3100

The CXCR4 antagonist AMD3100 is a small molecular weight bicyclam that binds partly to the binding pocket of SDF-1 on CXCR4 preventing SDF-1 interaction (Scholten et al., 2012). AMD3100 treatment induces the release of HSPCs, already after 15 min a significant increase in PB is seen and the highest numbers of HSPCs are observed at about 1 h after administration (Broxmeyer et al., 2005). EPCs and MSCs can also be mobilized into the peripheral circulation by AMD3100 (Frank et al., 2012a, Frank et al., 2012b). AMD3100 also mediates a release of leukocytes from the BM (Liu et al., 2015). Neutrophils and monocytes are even mobilized faster than HSPCs. All in all, AMD3100 treatment enables a targeted, reversible and fast mobilization of many types of SPCs. The serum half-life of AMD3100 is only 2-3 h in mice (Jujo et al., 2010). Therefore, the CXCR4/SDF-1-axis regains its normal function relatively fast after administration of AMD3100, so that cells can migrate towards the damaged tissue using again the CXCR4/SDF-1 axis. AMD3100 has been shown to improve regeneration in many pre-clinical injury models (Zhai et al., 2018, Zuk et al., 2014, Luo et al., 2013, Toupadakis et al., 2013, Szpalski et al., 2018, Jujo et al., 2010, Wang et al., 2011, Walter et al., 2015) and only few reports indicate adverse or no effect upon injury and after long-term treatments (Liu et al., 2017, Dai et al., 2010, Toupadakis et al., 2012, Yang et al., 2016). AMD3100 has been already approved (Perixaflor) for clinical application for the mobilization of hematopoietic cells for autologous BM transplantations in patients suffering from non-Hodgkin's lymphoma or multiple myeloma (Choi et al., 2010). Pharmacokinetics and safety studies were already performed and side effects in healthy volunteers are described to be low with no grade 2 toxicity (e.g. Hendrix et al., 2000), so regulatory approval for the use of AMD3100 for other clinical applications might be easier to achieve in comparison to a novel compound.

1.4.2 Challenges in stem cell based therapies

Research on stem cell based therapies for trauma regeneration have only been recently initiated. Studies to determine which group of trauma patients would most benefit from stem cell based therapies and which stem cell types and cell sources are best used have not been performed yet in great detail (Pati and Rasmussen, 2017).

Additionally, potential side effects of stem cell based therapies need to be identified and subsequently minimized. Lukomska et al. (2019) for example lists possible side effects for MSC based transplantations: pro-tumorigenic effects, trigger immune responses, disturbed differentiation and differentiation to undesirable tissues as well as current limitations: short survival after implantation, no spectacular improvements and unspecific optimal doses and route of administration. Therefore, it is not surprising, that even though MSC based clinical trials are currently the majority of stem cell based clinical trials (920 clinical trials by 2019), so far only one MSC based therapy obtained regulatory approval (Hoogduijn and Lombardo, 2019). This highlights the importance of carefully planned (pre-)clinical research based on strong underlying science for testing the efficacy of stem cell based therapies. For example, animal models of trauma should mirror the pathophysiology and the immunology observed in trauma patients to test new therapeutic approaches with the aim to translate the findings into the human system (Weber et al., 2019). Small animal models are most frequently used in trauma research. Single hit, double hit and multiple hit animal models are found in literature. Still, modeling the complex injury pattern of PT with animal models that manifest with a severe response in the acute and the late phase of trauma remains difficult. Only a few standardized PT models exist so far. In those models, inflammatory response is further enhanced than in single trauma models or in the double hits models with selected combinations of two injuries (Weckbach et al., 2012, Weckbach et al., 2013, Gentile et al., 2013). So far, the PT models are only able to address questions of the early inflammatory response and thus provide a good foundation for the evaluation of the early pathophysiology of PT and early therapeutic interventions. Long-term PT models to investigate the late-post injury complications are unfortunately still not available, while applying SPC based therapies in this phase in trauma regeneration could provide an especially interesting therapeutic approach to improve outcomes.

1.5 Aim of the study

Stem cell based therapies and immunomodulation therapies are promising novel avenues to improve tissue repair and regeneration upon trauma. To test whether such therapies indeed might result in beneficial effects, multiple variables need to be addressed. One of them is the timing of intervention. To answer the question of ideal timing, we believe an in-depth determination of dynamics distribution of endogenous SPC and mobilized endogenous SPC post injury will be highly beneficial. Therefore, the major aim of this thesis was to characterize the synchrony of the dynamic changes of the distribution of hematopoietic, endothelial and mesenchymal SCs after injury. So far only a very small number of studies analyzed dynamics of several cell populations (not even SPCs) simultaneously and over a longer time period (days) after trauma. In this work, I followed two lines of research. The aim of the first study was to determine the dynamic distribution of SPCs in blood of polytraumatized patients and to correlate these with trauma outcome to obtain information whether indeed stem cell based parameters might be linked to changes in outcomes. Equally important, dynamics of SPC might serve as a novel diagnostic marker for outcome and incidence of clinical complications. The aim of the second study was to analyze cell dynamics in a trauma mouse model to analyzed the dynamic distribution of SPCs not only in blood but also in the injured tissue and their likely place of origin, the BM. Additionally, another focus of this project was to investigate what influence an enforced change in cell dynamics induced by AMD3100 has on trauma outcome in mice.

2. Materials & Methods

2.1 Materials

2.1.1 Antibodies/Dyes

Table 2: Antibodies for the identification of MSCs and HSPCs, all anti-human.

MSC Staining (human)		
Epitope	**Dilution**	**Manufacturer**
CD14 Vioblue	1:10	Miltenyi Biotec
CD20 Vioblue	1:10	Miltenyi Biotec
CD34 Vioblue	1:10	Miltenyi Biotec
CD45 Vioblue	1:10	Miltenyi Biotec
CD90 Clone 5E10 Pe-Cy7	1:10	BD Pharmingen
CD73 APC	1:10	Miltenyi Biotec
CD105 PE	1:10	Miltenyi Biotec

HSPC Staining (human)		
Epitope	**Dilution**	**Manufacturer**
Anti-hematopoietic lin eFluor 450 cocktail	1:10	eBioscience
CD123 Clone 7G3 PerCP-Cy5.5	1:10	BD Pharmingen
CD34 APC	1:10	BD Pharmingen
CD38 PE	1:10	BD Pharmingen
CD90 Clone 5E10 Pe-Cy7	1:10	BD Pharmingen
CD45RA FITC Ref. A07786	1:20	Beckman Coulter

Table 3: Antibodies for the identification of MSCs, EPCs and HSPCs, all anti-mouse.

MSC Staining (mouse)		
Epitope	**Dilution**	**Manufacturer**
Streptavidin eFluor450	1:100	eBioscience
CD90.2 AF700 Clone: 30-H12	1:75	BioLegend
CD105 APC Clone: MJ7/18	1:75	BioLegend
CD73 PerCP/Cy5.5 Clone: TY/11.8	1:100	BioLeged
Ly-6A/E (Sca-1) APC-Cy7 Clone: D7	1:200	BioLegend
CD51 Pe Clone: RMV-7	1:100	BioLegend
CD44 Pe-Cy7 Clone: IM7	1:100	BioLegend
CD29 FITC Clone: HMß-1	1:100	BioLegend

EPC and HSPC Staining (mouse)		
Epitope	**Dilution**	**Manufacturer**
Streptavidin eFluor450	1:100	eBioscience
CD45 V500 Clone:30-F11	1:100	BD Horizon
Ly-6A/E (Sca-1) Pe-Cy7 Clone: D7	1:200	eBioscience
CD117 (c-Kit) AF700 Clone: ACK2	1:50	eBioscience
CD31 FITC Clone: 390	1:50	BDPharmingen
CD34 eFluor660 Clone: RAM 34	1:50	eBioscience
CD309 (Flk-1) PerCP/Cy5.5 Clone: 89B3A5	1:100	BioLegend

Table 4: Antibodies for the identification of lineage differentiated cells, all anti-mouse.

Lineage Cocktail (mouse)		
Epitope	**Dilution**	**Manufacturer**
B220 Biotin Clone: RA3-6B2	3,34µl/10^7 cells	eBioscience
CD11b (Mac-1) Biotin Clone: m1/70	3,14µl/10^7 cells	eBioscience
Gr-1 Biotin Clone: RB6-8C5	2,86µl/10^7 cells	eBioscience
CD8a Biotin Clone: 53-6.7	5µl/10^7 cells	eBioscience
CD5 Biotin Clone: 53->.3/3	5µl/10^7 cells	eBioscience
Ter-119 Biotin	3,2µl/10^7 cells	eBioscience
CD45 Biotin Clone: 30-F11	2,5µl/10^7 cells	BioLegend
CD31 Biotin Clone: 390	5µl/10^7 cells	Biolegend

Lung Lineage$^+$ Staining (mouse)		
Epitope	**Dilution**	**Manufacturer**
CD45 V500 Clone:30-F11	1:100	BD Horizon
MHCII(I-A/I-E) Pe-eFluor610 Clone: M5/114.15.2	1:200	eBioscience
Ly6G eFluor450 Clone: RB6-8C5	1:100	eBioscience
Ly6C APC-eFluor780 Clone: HK1.4	1:100	eBioscience
CD24 PerCP/Cy5.5 Clone: M1/69	1:100	eBioscience
CD11c Pe-Cy7 Clone: N418	1:100	eBioscience
CD11b AF700 Clone: M1/70	1:200	eBioscience
CD64 APC Clone: X54-5/7.1	1:100	BioLegend

Table 5: Antibodies/dyes for the identification of lung fibroblasts/myofibroblasts, apoptosis and proliferation, all anti-mouse.

Fibroblast/Myofibroblast staining (mouse)		
Epitope	**Dilution**	**Manufacturer**
Ly-6A/E (Sca-1) Pe-Cy7 Clone: D7	1:100	eBioscience
CD49e FITC Clone: 5H10-27(MFR5)	1:50	BioLegend
CD45 Biotin Clone: 30-F11	2,5µl/10^7 cells	BioLegend
CD31 Biotin Clone: 390	5µl/10^7 cells	BioLegend
LYVE1 Biotin Clone: ALY7	1:400	eBioscience
Ter-119 Biotin	3,2µl/10^7 cells	eBioscience
CD326 (Ep-CAM) Biotin Clone: G8.8	1:200	BioLegend
CD146 Biotin Clone: ME-9F1	1:200	BioLegend
Streptavidin eFluor450	1:100	eBioscience

AnnexinV and PI Staining (mouse)		
Epitope	**Dilution**	**Manufacturer**
PI (Propidium iodide)	1:20	Sigma-Aldrich
Fixable Viability Dye eFluor780	1:1000	eBioscience
Annexin V	1:50	BioLegend

2.1.2 Specific chemicals, reagents and drugs

Table 6: Specific chemicals, reagents and drugs

Chemicals, reagents and drugs	Producer
0.9 % NaCl	Fresenius Kabi
AMD3100	Sigma-Aldrich
Annexin V Binding Buffer, 10X concentrate	BD Bioscience
Bupenorphine	Temgesic®
FC-Block	eBioscience
HistopaqueR-1083	Sigma-Aldrich
Human Serum	Lonza
Lymphoprep 1.077 g/ml	Stem cells technologies
Propidiumiodide (PI)	Sigma-Aldrich
Protease Inhibitor Cocktail (mouse)	Sigma-Aldrich
Sevoflurane	AbbVie

2.1.3 Special laboratory equipment

Table 7: Special laboratory equipment

Equipment	Manufacturer
BD FACSAria III cell sorter	BD Bioscience
BD LSRII/Fortessa Flow Cytometry Analyzer	BD Bioscience
Cylinder	Festo
Fluorescence microscope Axio Observer.Z1	Zeiss
GentleMACS Octo Dissociator	Miltenyi Biotec
GME-2811 Gasmischeinheit 4 x Maus	FMI Föhr Medical Instruments GmbH
Hemavet Multispecies Hematology Analyzer	Drew
High-speed valve Hee-D24	Festo
Microplate-Reader	Tecan sunrise
Polyester film (Mylar A 50µm)	DuPont Teijin Films-Mylar
Shaver	Contura
SonoPlus	Bandelin electronics
Ultra-Turrax	IKU

2.1.4 Software & Kits

Table 8: Software & Kits

Software	Manufacturer
AxioVision Rel. 4.8	Zeiss
BD FACSDiva 8.1	BD Biosciences
GraphPad PRISM 7.0	GraphPad Software, Inc.

Kits	Manufacturer
Lung Dissociation Kit, mouse	Miltenyi Biotec
Magnetic multiplex bead assay (human) customized	R&D Systems
Mouse lineage cell depletion kit	Miltenyi Biotec

ELISA – Kits	Manufacturer
Mouse CCL2/JE/MCP-1 DuoSet ELISA	R&D Systems
Mouse CXCL1/KC DuoSet ELISA	R&D Systems
Mouse IL-6 DuoSet ELISA	R&D Systems
Mouse IL-10 DuoSet ELISA	R&D Systems
Mouse TNF-alpha DuoSet ELISA	R&D Systems

2.1.5 Media & Buffer

Dulbecco's **P**hosphate **B**uffered **S**aline (PBS)-A	Dulbecco's PBS without $Ca2^+$, $Mg2^+$ 3 % **F**etal **B**ovine **S**erum (FBS) (Sigma-Aldrich)
PBS-B	Dulbecco's PBS without $Ca2^+$, $Mg2^+$ 0.5 % FBS 2 mM **E**thylene**D**iamine**T**etraacetic **A**cid (EDTA) (AppliChem)
Hanks' **B**alanced **S**alt **S**olution (HBSS)+	HBSS (Phenol Red without Ca2+, Mg2+) (Lonza) 10 % FBS 1 % Penicillin/Streptomycin (100x) (PAN Biotech)
10x Stock Red Cell Lysis Buffer	83.4 g NH_4Cl (Sigma) 10 g $NaHCO_3$ (Roth) 2 ml EDTA (0.5M) add H_2O to 1 l Solution was autoclaved before use
MethoCult-EPCs (Tsukada et al., 2013)	MethoCult SF M3236 (StemCell Technologies) 50 ng/ml recombinant Mouse fibroblast growth factor basic Protein (R&D Systems) 50 ng/ml recombinant Mouse VEGF 164 Protein (R&D Systems)

50 ng/ml recombinant Mouse IGF-1 Protein (R&D Systems)
50 ng/ml recombinant murine EGF (PeproTech)
20 ng/ml Mouse IL-3 (ProSpec)
20 ng/ml murine stem cell-derived factor (ProSpec)
2 U/ml heparin (Ratiopharm)

2.1.6 Mice

Adult (12 weeks) male BL6/C57 mice (Janvier) were used for all experiments. All mice were housed under specific pathogen-free conditions at the Tierforschungszentrum University Ulm. Experiments were performed in compliance with the German Law for Welfare of Laboratory Animals and were approved by the Regierungspräsidium Tübingen (1321).

2.2 Methods human study

2.2.1 Study design and blood collection

For analyzing stem and progenitor cell dynamics in polytraumatized patients a prospective, observational cohort study design was used. The study was approved by the Ethics Committee of Ulm University (number: 94/14) and informed consent was obtained from all patients recruited into the study. Polytraumatized patients admitted to the University Hospital Ulm between 2016 and 2017 with an ISS of over 21 were included. Criteria for exclusion were pregnancy, chronical diseases and age < 18.

Blood collection (EDTA-blood and citrate plasma) was performed by trained personnel immediately after admission to the shock-room (0-3 h) and subsequently at 8 h ± 0.25 h, 24 h ± 1 h, 48 h ± 2 h and 120 h ± 5 h.

From the volunteer group blood was taken once. The group consisted of 31 people (12 males and 19 females) with no recent injuries or illnesses and with a mean age of 32 ± 10 years. For the serial blood sampling 4 healthy volunteers (3 males and 1 female) were chosen and for the cytokine profile, citrate plasma was taken from 10 healthy volunteers (6 males and 4 females) with a mean age of 37±13.

2.2.2 Sample preparation

Citrate plasma was centrifuged at 2200xg for 15 min at 4 °C. Supernatant was aliquoted, frozen and stored at -80 °C until further analysis. EDTA-blood was immediately processed and frequency of circulating stem and progenitor cells was determined. First, cell count and blood parameters were measured by Hemavet950 (Drew). Then exact blood amount was defined before PB was diluted 1:1 with 0.9 % NaCl (Fresenius Kabi). Diluted PB was carefully layered on top of Lymphoprep (1.077 g/ml) (Stemcell technologies) in a ratio of 1:2. After low density centrifugation (26 min, room temperature, 1600 rpm, no brake/acceleration), buffy coat was removed and mononucleated cells were washed twice with PBS-A. Cell count was taken by Hemavet950.

2.2.3 Identification and quantification of MSCs and HSPCs in peripheral blood

$2*10^6$ cells were used for hematopoietic and mesenchymal staining respectively. For MSC staining cells were resuspended in PBS-B in a concentration of 10^7 cells/ml. Antibodies were added as listed in Tab. 2 (left side). Cells were incubated at 4 °C for 20 min and washed twice in PBS-B. After washing cells were resuspended and analyzed by flow cytometry (LSR II, Becton Dickinson).

For the hematopoietic staining cells were resuspended in PBS-A in a concentration of 10^7 cells/ml. To block unspecific binding 10 % of human Serum (Lonza) was added for 15 min at 4°C. Then antibodies were added as defined in Tab. 2 (right side). Cells were incubated for 1 h at 4 °C, washed and analyzed by flow cytometry. Single color controls and unstained samples were prepared freshly for each experiment/antibody. Forward and side scatter was used to exclude cell debris und dead cells. Data analysis was performed with the BD FACS DIVA 8.0.1 software package. Absolute cell number in 1 ml of PB was calculated as shown in formula 1.

$$\text{Absolute cell number (1 ml PB)} = \frac{Cell\ count\ low\ density\ PB}{Recorded\ events\ (flow\ cytometer)} * \frac{SPC\ number\ (flow\ cytometer)}{total\ PB\ volume}$$

Formula 1: Calculation of absolute SPC number in 1 ml of PB.

2.2.4 Determination of inflammatory and mobilizing factors in blood plasma

Frozen aliquots of citrate plasma from PT patients (time points 0-3 h, 24 h, 48 h and 120 h) and healthy volunteers were shipped to the research flow cytometry core CCHMC in Cincinnati, USA. There, plasma concentrations of chemokines and cytokines were determined by human magnetic multiplex bead assay (R&D Systems). Each sample was analyzed in duplicate.

2.2.5 The **A**dditive **N**umber of **SP**Cs (ANSP-Score)

For the calculation of the ANSP-Score the difference in numbers in PB between 0-3 h and 48 h and the difference in number between 48 h and 120 h was calculated for each SPC population. Then those four numbers were added together to get the ANSP-Score (Formula 2 and 3).

$$ANSP - Score\ d(0\ h - 48\ h) = d0\ h - 48\ \mathrm{h\ HSCs} + \mathrm{d0\ h - 48\ h\ MSCs} + \mathrm{d0\ h - 48\ h\ CMPs} + \mathrm{d0\ h - 48\ h\ GMPs}$$

Formula 2: Calculation of the ANSP-Score d(0-3 h - 48 h).

$$ANSP - Score\ d(48\ h - 120\ h) = \mathrm{d120\ h - 48\ h\ HSCs} + \mathrm{d120\ h - 48\ h\ MSCs} + \mathrm{d120\ h - 48\ h\ CMPs} + \mathrm{d120\ h - 48\ h\ GMPs}$$

Formula 3: Calculation of the ANSP-Score d(48 h - 120 h).

2.2.6 Correlation studies

Non-parametric Spearman correlation was performed between numbers of SPCs at different time points, or the amount of the decrease (d0-3 h - 48 h) or the amount of the increase (d48 h - 120 h) and the ANSP-Score versus clinical parameters or cytokine/chemokine values at different time points as well as between clinical parameters and cytokine/chemokine values. Relationships were suggested as correlating if Spearman´s coefficient was larger than 0.7 or smaller than -0.7 and p-values were smaller than 0.05. The p-value hereby indicates how likely a relationship would occur just by chance.

2.2.7 Statistical Analysis

For statistical analysis and data presentation Graph Pad Prism 7.0 was used. Data is illustrated, if not otherwise specified, as mean ± **S**tandard **D**eviation (SD) and Two-Way ANOVA was used for statistical analysis with *p<=0.05, **p<=0.01, ***p<0.001, ****p<0.0001.

2.3. Methods mouse study

2.3.1 Blunt thorax trauma (TXT)

In the blunt **T**hora**X** **T**rauma (TXT) mouse model a single thoracic blast injury was applied to analgesic and anesthetized mice. Therefore, mice were weighted, anesthetized (3.5% Sevoflurane (AbbVie) and 96.5% oxygen mixture) and injected subcutaneously with Buprenorphine (0.03 mg/kg body weight) (Temgesic®). Then mice were fixated on the back, limbs were tightened to a glass fiber plate and thorax was shaved free. Markings for the placement of the high-speed valve (Hee-D-24, Festo, Esslingen) and the cylinder were drawn on the hair free thorax to standardize blast injury (Fig. 4). Blast injury was applied with the opening of a high-speed valve which delivered compressed air into the upper section of a cylinder. The upper section is separated from the lower section of the cylinder with a polyester film (Mylar A 50µm). This polyester film ruptured at a standardized pressure, releasing a reproducible single blast wave towards the nozzle which is centered on the ventral thorax of the animal with a defined distance of 1.5 cm. This setup induces pulmonary contusion with histological and immunological changes as illustrated in previous studies (for example Hafner et al., 2015). Sham procedure included anesthesia, analgesia and fixation and shaving without the application of the blunt chest trauma. Mice were closely monitored for 24 h in which Buprenorphine was given twice (0.03 mg/kg body weight). For sample collection mice were

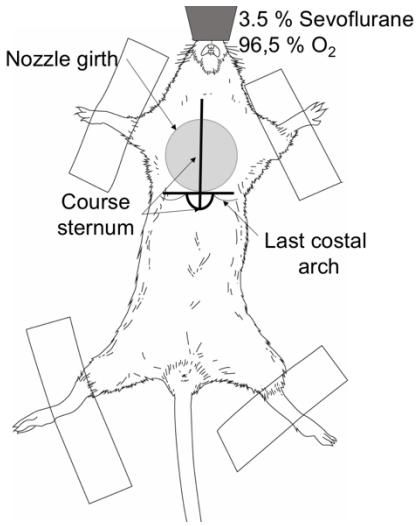

Figure 4: Placement of the cylinder nozzle for the TXT application. *Mice are fixed on their backs and chest is shaved free. Reference lines are drawn: a vertical line in the middle along the sternum and a horizontal line at the origin of the last costal arch. Nozzle is placed according to the drawing.*

sacrificed at the needed time points by using an overdose of Sevoflurane. Mice manifesting a strong cardiac tamponade were not used for further processing.

2.3.2 Polytrauma (PT)

PT mice were provided by the Institute of Experimental Trauma-Immunology, University Hospital of Ulm. In short: mice were anesthetized with a 2.5% Sevoflurane and 97.5% oxygen mixture. For the PT mice were subjected to a TXT, a closed head trauma and a proximal femoral fracture. TXT was performed as described in section 2.3.1, the closed head trauma was generated by a weight drop device (333 g, distance to skull of 2 cm), more details see Flierl et al. (2009). The reproducible closed transverse femoral shaft fracture was induced at the right leg by a weight drop device as well (weight, 50 g; height, 120 cm) (see Bonnarens and Einhorn, 1984). Mice were randomly assigned to the PT or sham group, the sham animals underwent the identical procedure, but no trauma was applied. All mice stayed under anesthesia for the total amount of 2 h then they were sacrificed.

2.3.3 Sample collection and preparation

Mice were euthanized by an overdose of the inhalation anesthetic Sevoflurane. Afterwards, PB was immediately collected by cardiac puncture and stored in EDTA-Monovetten (Sarstedt). For each time point blood from two sham animals and two experimental mice were pooled to obtain enough blood cells for the flow-based analyses. Blood count and composition were measured with the Hemavet950. Exact amount of blood was defined and blood volume was brought to 3 ml with PBS. To isolate mononuclear cells, low density centrifugation (26 min, room temperature, 1600 rpm, no brake /acceleration) on Histopaque-1083 (Sigma-Aldrich) was performed. Buffy Coat was collected. **L**ow **D**ensity **PB** (LDPB) cells were washed and an additional erythrocyte lysis step was applied before cells were resuspended in 0.5 ml HBSS+ and cell count was taken.

For the lung tissue, lungs were flushed through the right heart ventricle with 3-5 ml of cold PBS. Then external tissues and trachea were removed and lung lobes were stored in PBS. To gain single cells the lung dissociation kit from Miltenyi was applied according to protocol. In brief, single lung lobes were flushed and infiltrated with the provided enzyme solution. Using the gentleMACS Octo Dissociator with heater function, tissue was mechanically and enzymatically degraded and single cells were

released. Cell solution was filtered (70 µm) and red cell lysis was performed to get rid of left over erythrocytes. For **E**nzyme-**L**inked **I**mmuno**S**orbent **A**ssay (ELISA) always the same part of the left lung was isolated and immediately frozen down in liquid nitrogen before storing at -80 °C.

BM was gained by isolating and flushing femurs and tibiae of the mice. For the examination of the fold change between TXT and sham animals, BM was isolated from one TXT and one sham mouse, totally four bones (2 x femur, 2 x tibia) were flashed per mouse. Cell count was taken by Hemavet950 and a low density centrifugation same as for PB was performed obtaining **L**ow **D**ensity **BM** (LDBM). Mononuclear cells were collected and washed two times before cell count was taken.

2.3.4 Sample staining for flow cytometry

2.3.4.1 MSC staining

Prepared LDPB was divided in two equal parts, to one part of the LDPB and to $2*10^6$ LDBM cells biotin-labeled anti-CD45 and anti-CD31 as well as biotin-labeled lineage-cocktail was added (Tab. 4 left side) for 30 min at 4 °C. Cells were washed, FC-Block (eBioscience) was applied and antibody mix according to Tab. 3 (left side) was added for 1 h at 4°C. Cells were washed and analyzed by flow cytometry.

2.3.4.2 EPC and HSPC staining

To the other half of the LDPB cells, to $2*10^6$ LDBM cells and to $3*10^6$ lung cells biotin-labeled lineage-cocktail was added (Tab. 4 left side) for 30 min at 4 °C, then cells were washed and resuspended to obtain a concentration of $1*10^6$ cells/ml. After FC-Block incubation, the antibody mix listed in Tab. 3 (right side) was applied for 1 h at 4°C. Finally, cells were washed and before measuring by flow cytometer, **P**ropidium **I**odide solution (PI) (Sigma-Aldrich) was added (1:1000) for live/dead separation. In the evaluation at FACS DIVA an additional size gate for the $Lin^-Sca\text{-}1^+c\text{-}Kit^+$ (LSK) cells in lung tissue was introduced to reduce wrongly identified cells (Fig. 5).

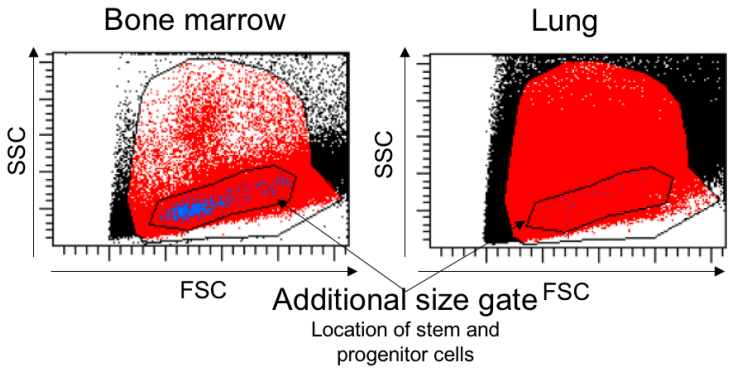

***Figure 5: Size gate introduction to reduce false positive LSK cells in lung tissue. Left side**: Forward and side scatter of LDBM cells, in blue LSK cells are shown, an additional size gate was drawn around them. **Right side:** Defined size gate was used to identify LSK cells in lung tissue.*

2.3.4.3 Mature hematopoietic cell staining in lung tissue

$1*10^6$ lung cells were used. Markers to identify mature hematopoietic cells in the lung tissue were used according to Yu et al. (2016). After FC-Block the antibody mix illustrated in Tab. 4 (right side) was added for 30-45 min on ice. Before analyzing, PI (1:1000) for live/dead staining was applied.

2.3.4.4 Fibroblast/Myofibroblast staining

$2\text{-}3*10^6$ lung cells were incubated with non-fibroblast lineage cocktail (Tab. 5 left side). Cells were washed and FC-Block was added. Subsequently an incubation with anti-Sca-1, anti-CD49e and Streptavidin for 1 h at 4 °C was performed.

2.3.4.5 Sample staining – AnnexinV and PI staining

$2*10^6$ lung cells were incubated with Viability dye eFluor780 (1:1000) (eBioscience) for 30 min. Then the samples were washed and stained in 1xbinding buffer plus Annexin V and Annexin V antibody. Before analysis by flow cytometry (LSRII, Becton Dickinson) PI was added to reach a final concentration of 50 µg/ml, to allow for a quantification of DNA amount. PI gate is non-logarithmic.

2.3.5 Flow cytometry

All samples were measured by a BD LSRII Flow Cytometry Analyzer. Single color controls and unstained samples were prepared freshly for each experiment/sample. Forward and side scatter was used to exclude cell debris and dead cells.

Data were analyzed using BD FACSDIVA software 8.1, obtained cell numbers were used for the calculation of the absolute cell number (formula 1 for PB, formula 4 for lung and PB). For the calculation of the fold change cage mates which only

underwent sham procedure were used (fold change = absolute cell number TXT/absolute cell number sham).

$$\text{Absolute cell number of population n} = \frac{Cell\ count\ isolated\ lung\ cells\ or\ LDBM}{Recorded\ events\ (flow\ cytometry)} * cell\ number\ population\ n\ (flow\ cytometry)$$

Formula 4: Calculation of absolute cell numbers for BM and lung.

2.3.6 EPC-Colony Forming Unit (CFU)-Assay

From 2-4 mice LDBM was isolated and further purified by lineage depletion. For the lineage depletion, Miltenyi lineage depletion kit was used according to manufacturer's protocol. Afterwards cell count was taken by Hemavet950 and EPC/HSPC staining was performed as described previously. EPCs, Flk-1$^+$ and late progenitors were sorted by fluorescence activated cell sorting with a BD ARIA III Sorter. Sorted cells were added to the MethoCult-EPCs (2.1.5 Media & Buffer) (50 cells/100 µl MethoCult-EPCs) and then the cell mix was added to 12-Well plates (500 µl MethoCult-EPCs) or 24-Well plates (200 µl MethoCult-EPCs). Plates were incubated at 37°C and colonies were counted and analyzed between 7 and 21 days. Photos were taken by a Axio Observer Z.1.

2.3.7 Correlation studies

Non-parametric Spearman correlation was performed between the fold change of different tissues for one specific population (same sample, all experiments (n≈46)). Additional correlation studies were performed between the different populations within one tissue (same sample, all experiments (n≈46)). As previous, relationships were suggested as correlating if Spearman´s coefficient was larger than 0.7 or smaller than -0.7 and p-values were smaller than 0.05.

2.3.8 AMD3100 treatment

Traumatized mice were either treated with 5 mg/kg AMD3100 (in 200-300 µl) (Sigma-Aldrich) or PBS (200-300 µl). Solutions were injected **i**ntra**p**eritoneally (i.p.) directly after and/or 6 h post TXT induction.

2.3.9 ELISA

PBS with protease inhibitor (Sigma-Aldrich) was added to frozen lung tissue, then tissue was homogenized with an Ultra Turrax (IKA), followed by sonication for 5 sec, 5 times at 40% power. Homogenate was centrifuged for 15 min at 16000xg at 4 °C and supernatant was aliquoted and stored at -80 °C. Levels of IL-6, IL-10, **K**eratinocyte **C**hemoattractant (KC), MCP-1 and TNF-α (all R&D Systems) were measured by serial ELISA. Manufacture´s protocol was followed.

2.3.10 Statistical Analysis

Data is illustrated, if not otherwise specified, as mean ± **S**tandard **E**rror of the **M**ean (SEM). The SEM indicates the precision of an estimated mean it does not affect the statistical analyses as variance information is still used in the test statistics. The number of biological repeats (n) is given in the figure legend of each experiments. Mice for sham or TXT application were chosen randomly. Two-Way ANOVA was used for statistical analysis with *p<=0.05, **p<=0.01, ***p<0.001, ****p<0.0001. For statistical analysis and data presentation Graph Pad Prism 7.0 was used.

3. Results

3.1 Distinct dynamics of SPCs in peripheral blood (PB) of polytraumatized patients

3.1.1 Patient cohort

To analyze the distribution of SPCs in PB upon PT, blood samples were collected from trauma patients with an ISS of at least 21. Blood was collected immediately after admittance to the shock-room (0-3 h) and after 8 h, 24 h, 48 h and 120 h. In total 8 patients were included in the study with a mean age of 36.75 ± 18 and a mean ISS of 32.5 ± 9.5. Tab. 9 provides an overview of the relevant clinical parameters.

Table 9: Details of the patient cohort. *PT = Polytrauma, ISS = Injury Severity Score, ICU = Intensive Care Unit,* ***F*** *=* ***F****emale,* ***M*** *=* ***M****ale. Based on: Vogel et al.: Distinct Dynamics of Stem and Progenitor Cells in Blood of Polytraumatized Patients. Shock 51: 430–438 (2019). https://journals.lww.com/shockjournal/Fulltext/2019/04000/Distinct_Dynamics_of_Stem_and_Progenitor_Cells_in.5.aspx.*

	Age (years)	Sex	ISS	Infectious complication	Days ICU
PT1	47	F	41 (Thorax 4; neck 5)	Yes (Urinary tract infection)	12
PT2	62	M	21 (Thorax 4; extremities 2; extern 1)	Yes (Wound infection)	10
PT3	23	M	48 (Thorax 4; head 4; extremities 4)	Yes (Pneumonia; wound healing disorder)	18
PT4	19	M	22 (Thorax 3; head 3; extremities 2)	Yes (Urinary tract infection)	12
PT5	48	M	34 (Thorax 4; abdomen 3; extremities 3)	Yes (Wound infection)	30
PT6	18	M	27 (Thorax 3; extremities 3; cervical spine 3)	No	10
PT7	22	M	38 (Thorax 2; abdomen 5; extremities 3)	No	1
PT8	55	M	29 (Thorax 4; head 2; extremities 3)	Yes (n.a.)	5

3.1.2 Identification of distinct types of SPCs

The frequency of HSCs, GMPs, CMPs (late hematopoietic progenitors with endothelial potential (Wara et al., 2011)) and MSCs was analyzed in PB of polytraumatized patients. In Fig. 6 the gating strategies and marker panels of the four analyzed SPC populations are illustrated. The gating strategy enables the measurement of the frequency of HSC, GMP and CMP simultaneously (Fig. 6a), whereas MSCs were measured in an extra panel (Fig. 6b).

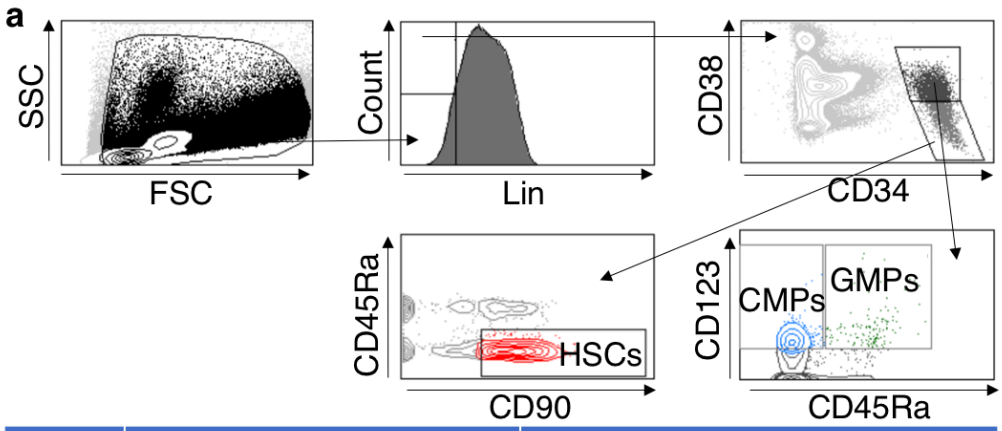

	Negative Marker	Positive Marker
HSCs	Lineage, CD38, CD45Ra	CD34, CD90
GMPs	Lineage	CD38, CD34, CD123, CD45 Ra
CMPs	Lineage, CD45Ra	CD38, CD34, CD123

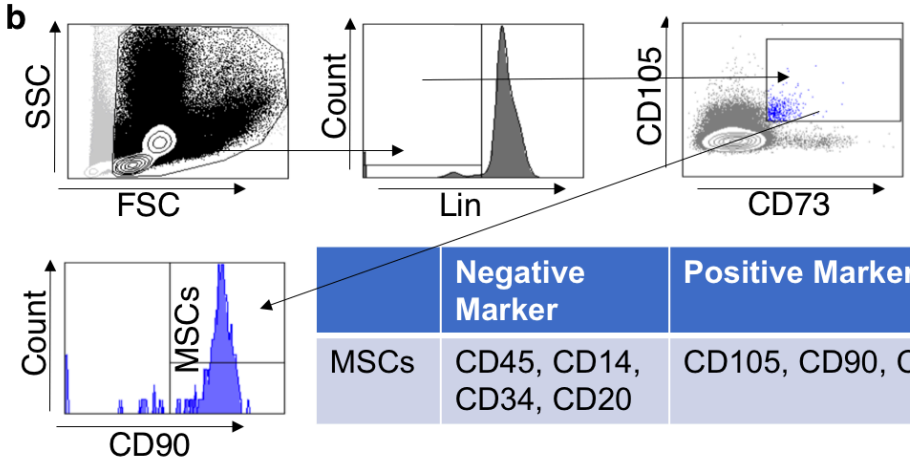

	Negative Marker	Positive Marker
MSCs	CD45, CD14, CD34, CD20	CD105, CD90, CD73

Figure 6: Gating strategies and marker panels to identify the distinct types of SPCs in PB. ***a*** *HSCs, CMPs and GMPs;* ***b*** *MSCs. Used with permission from Wolters Kluwer Health, Inc.: Vogel et al.: Distinct Dynamics of Stem and Progenitor Cells in Blood of Polytraumatized Patients. Shock 51: 430–438 (2019). https://journals.lww.com/shockjournal/Fulltext/2019/04000/Distinct_Dynamics_of_Stem_and_Progenitor_Cells_in.5.aspx.*

3.1.3 SPC numbers in PB of healthy volunteers

To obtain the basal level in PB for the distinct types of SPCs I determined the number of SPCs in PB of 30-31 healthy volunteers (Fig. 7a). The mean age of the healthy cohort was 32.2 ± 9.7 (19 females and 12 males). No recent injuries or illnesses were listed for the healthy volunteers. The measurement revealed an average of 247 ± 136 HSCs, 252 ± 109 MSCs, 83 ± 32 GMPs and 282 ± 200 CMPs per ml of PB. The average of the healthy volunteers was used as a base line for later comparison of the obtained PT SPC numbers. Furthermore, for a small number of controls (n = 4), blood was collected consecutively up to 120 h, similar to the time-axis of collection of the PT patients (Fig. 7b). The number of SPCs in blood in this small subgroup though in general remained constant and did not change over the time interval tested (120 h) and remained within the range of the baseline of the larger cohort of healthy volunteers (Fig. 7a). This implies that the repeated blood collections as well as circadian rhythms do not influence the number of SPCs in blood in healthy volunteers.

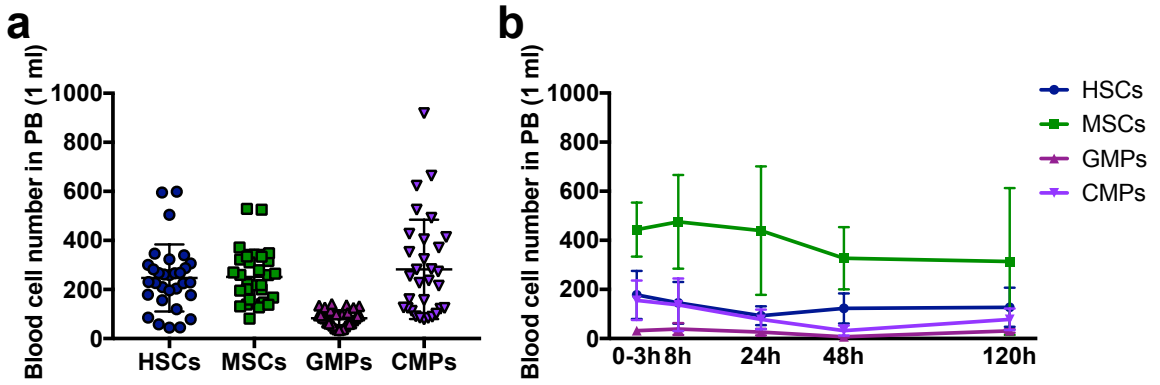

***Figure 7: Number of distinct types of SPCs in 1 ml of PB of healthy volunteers**. **a** SPC numbers were analyzed in 30-31 healthy volunteers, each dot represents one volunteer (mean ± SD; HSCs: 247 ± 136, n=31; MSCs: 252 ± 109, n=30; GMPs: 83 ± 32, n=31; CMPs: 282 ± 200, n=31). **b** Number of distinct types of SPCs (HSCs, MSCs, GMPs, and CMPs) at distinct time points (0-3,8, 24, 48 and 120 h) in healthy volunteers (n = 4; mean ± SD) (based on Vogel et al., 2019a).*

3.1.4 SPC dynamics in PB 0 h - 120 h post PT

Blood was collected at 0-3, 8, 24, 48 and 120 h post PT and SPC numbers in blood were determined and compared to the numbers in healthy volunteers (Fig. 7). These analyses showed an increase in the number of HSCs, MSCs and GMPs in PB at the 0-3 h post PT time point. With respect to CMPs, 3 out of 7 patients presented

with an elevated number in PB at this time point (Fig. 8a-d). After this first initial increase, the number of SPCs in blood decreased, with a nadir at the 24 h post PT time point. For both HSCs and CMPs there was a strong trend towards numbers in blood that were even lower than the healthy control group. The numbers between 24 h and 48 h did not change in a significant manner and stayed at a low level in PB. Then, however an increase was observed between 48 h and 120 h for most SPC populations and patients. For example, there was a significant increase in the number of HSC, MSC and GMP at 120 h post PT. Taken together the data implies on average an inverse bell-shaped pattern for the number of SPCs (HSCs, MSCs, CMPs, GMPs) in blood upon PT (Fig. 8a-d).

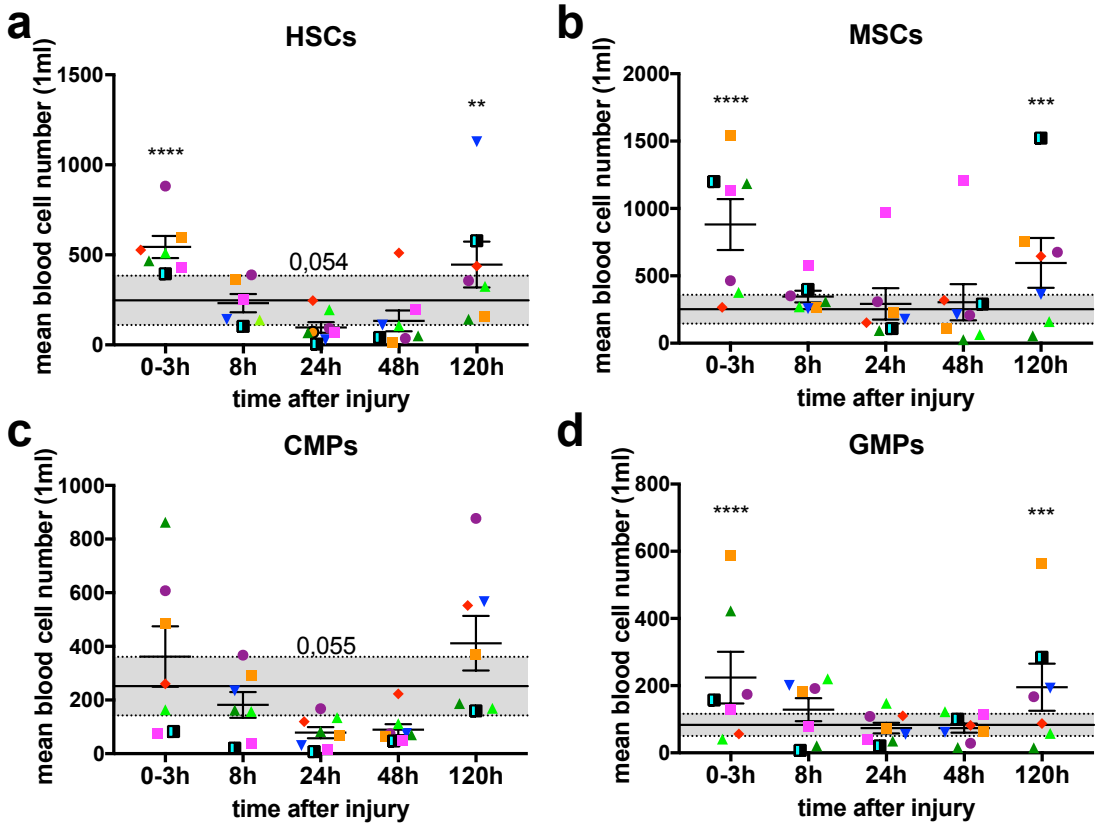

Figure 8: SPC numbers in PB at different time points post injury. *Each colored dot represents a patient, mean values ± SD are indicated for each individual time point. The black dotted lines are the averaged SPC numbers in healthy controls, the grey area the respective standard deviation (exact number see Fig. 7). SPC numbers show for most patients and in most populations an inversed bell-shaped pattern.* ***a*** *HSCs* ***b*** *MSCs* ***c*** *CMPs and* ***d*** *GMP. (Two-Way ANOVA **p≤0.01, ***p<0.001, ****p<0.0001). Adapted with permission from Wolters Kluwer Health, Inc.: Vogel et al.: Distinct Dynamics of Stem and Progenitor Cells in Blood of Polytraumatized Patients. Shock 51: 430–438 (2019). https://journals.lww.com/shockjournal/Fulltext/2019/04000/Distinct_Dynamics_of_Stem_and_Progenitor_Cells_in.5.aspx.*

To obtain additional information on the change of the number of SPCs in a given patient along our time-axis of analysis, we defined and calculated additional novel parameters based on the already existing data: One for the magnitude of decrease in the number of SPCs between the 0-3 h and the 48 h time point (d0-3 h – 48 h, Fig. 9a), another for the magnitude of the increase in number between the 48 h and 120 h time point (d48 h – 120 h, Fig. 9c). Based on these novel parameters, another new parameter could be calculated for individual patients, in which the change in the number for HSCs, GMPs, CMPs and MSCs between the time points were added up to obtain the **A**dditive **N**umber of changes in the number of **SP**Cs (ANSP-Score, Fig. 9b,d). For the change in SPC numbers between 0-3 and 48 h post PT and ANSP-Score, no distinct pattern in individual patients or the group of patients could be observed (Fig. 9a,b). To quantify the increase in SPC numbers between 48 h and 120 h post PT, the number of SPC at 48 h was subtracted from the number of SPC at 120 h (Fig. 9c). As individual patients showed in general either a minor or a major increase in distinct SPCs in this time interval (Fig. 9c), the ANSP-Score of d48 h -120 h identified two groups - one, in which the increase is relatively low between 48 h and 120 h, this group was termed **Lo**w **L**ate **i**ncrease in **Nu**mbers **u**pon **t**rauma (LoLiNut) patients. This group consists of PT 3, 5 and 8. The other group, in which there is a **Hi**gh **L**ate **i**ncrease in **Nu**mbers **u**pon **t**rauma (HiLiNut) consists out of PT 1, 2, 4, 6. There was no difference in the mean ISS score between these two groups. Interestingly though, from the LoLiNut group 2 out of the 3 patients had the longest ICU stay and developed infectious complications such as pneumonia or wound healing problems. The ANSP-Score d48 h – 120 h might thus correlate with long-term clinical outcome. Additional experiments on a much larger cohort of PT patients will be necessary to test this hypothesis.

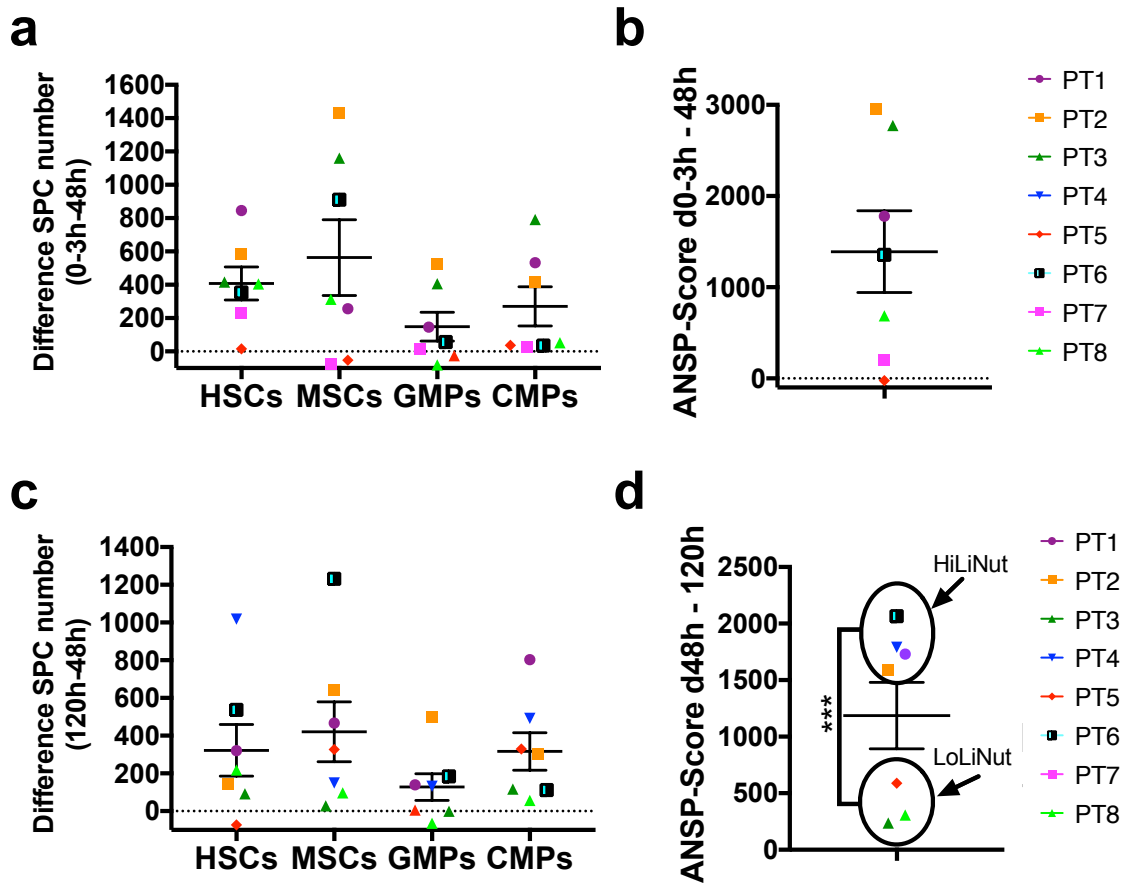

Figure 9: Strength of decrease (d0-3 h – 48 h) and strength of increase (d 48 h – 120 h) in SPCs after PT. a *Difference between the SPC numbers in PB after 0-3 h and 48 h, this phase is characterized by a decrease in SPC number in most populations and for most patients.* ***b*** *ANSP-Score (calculation see 2.2.5) between 0-3 h and 48 h, the ANSP-Score is heterogeneous and mostly positive indicating an overall loss of SPC in PB after injuries.* ***c*** *Difference between 120 h and 48 h time point, this phase is characterized by increased numbers of SPC in PB for most patients.* ***d*** *ANSP-Score (calculation see 2.2.5) between 120 h and 48 h, two separated groups can be identified the low late increase in numbers upon trauma (LoLiNut) group and the high late increase in numbers upon trauma (HiLiNut) group (unpaired t-test ***p<0.001). Adapted with permission from Wolters Kluwer Health, Inc.: Vogel et al.: Distinct Dynamics of Stem and Progenitor Cells in Blood of Polytraumatized Patients. Shock 51: 430–438 (2019). https://journals.lww.com/shockjournal/Fulltext/2019/04000/Distinct_Dynamics_of_Stem_and_Progenitor_Cells_in.5.aspx.*

3.1.5 Correlation between clinical parameters, blood products, fluid balance and SPC numbers in PB post injury

To investigate whether SPC numbers, the ANSP-Score and the strength of decrease/increase were associated with clinical parameters like ISS and days in ICU (listed in Tab. 9), Spearman correlation was applied. These analyses implied that in general there is no correlation among these parameters. Additional analyses

with age of the patients as a novel variable revealed a positive correlation between the number of HSC in PB after 0-3 h (r = 0.75 and p = 0.06) and 24 h (r = 0.81 and p = 0.02) with age. Furthermore, it should be addressed how the administration of fluids and blood products like **P**acked **R**ed **B**lood **C**ell (PRBC) units, **F**resh **F**rozen **P**lasma (FFP) units or of **T**hrombocyte **C**oncentrate (TC) units is influencing SPC numbers in PB. The patients included into the study were all treated according to the S3 guidelines for polytrauma patients (AWMF registry no 012/19), thus obtaining fluids and blood products to compensate the hemodynamically active blood loss. There might be a possibility that simply changes in **H**ema**t**ocrit (Ht) or treatments with blood products and fluids might significantly influence and thus correlate with SPC dynamics in blood upon PT. Tab. 10 lists Ht levels at different time points and the fluids and blood products given to the patients. I did not detect any correlation between Ht values from the patients and the number of SPCs in PB at any time point of analysis. The inverse bell-shaped pattern seen in SPCs was also not confirmed for the Ht time curve. (Tab. 10). In addition, correlations between the number of PRBC, FFP and TC units with the number of SPCs were, with the exception between MSCs 24 h and FFP (Spearman´s r = -0.93 and p = 0.02) and between HSCs d(120 h - 48 h) and TC units (Spearman´s r = -0.91 and p = 0.01) not significant. Finally, the correlation between fluid balance and CMPs 0-3 h in PB (Spearman´s r = 0.79 and p = 0.05) remained the single significant correlation for this parameter. In aggregation, these analyses strongly support that the changes in the number of SPC in PB upon PT are in general independent of any of those parameters (all calculated r- and p-values are found in the appendix Tab. A1).

***Table 10: Details about hematocrit, creatine kinase, given blood products and fluid balance for single PTs**. Ht= Hematocrit, Hb=Hemoglobin, CK = Creatine kinase, FFP = Fresh Frozen Plasma, PRBC = Packed red blood cells Erythrocyte Concentrate, TC = Thrombocyte concentrate, ICU = Intensive Care Unit, F = female, M = male, SR = Shock-Room, n.a. = not available. According to: Vogel et al.: Distinct Dynamics of Stem and Progenitor Cells in Blood of Polytraumatized Patients. Shock 51: 430–438 (2019). https://journals.lww.com/shockjournal/Fulltext/2019/04000/Distinct_Dynamics_of_Stem_and_Progenitor_Cells_in.5.aspx.*

	Hematocrit (Ht/Hb) Vol%	CK (U/l)	Catechol-amines	PRBC	FFP	TC	Fluid balance (ICU first 48h)
PT1	24 h: 23,2 48 h: 26,2 120 h: 22,7	0-3 h: 482 24 h: 1501 48 h: 2170	SR: no Course: n.a.	SR: 2 Course: -	SR: 3 Course: -	SR: - Course: -	+ 2604 ml
PT2	0-3 h: 28 24 h: 28,5 48 h: 25,5 120 h: 24,8	0-3 h: 2163 24 h: 9361 48 h: 7384 120 h: 2554	SR: yes Course: yes	SR: 8 Course: -	SR: 8 Course: -	SR: 2 Course: -	+ 1555 ml
PT3	0-3 h: 29 24 h: 22 48 h: 21 120 h: 24,2	0-3 h: 747 24 h: 2805 48 h: 12042 120 h: 5229	SR: yes Course: n.a.	SR: 24 Course: 1	SR: 25 Course: -	SR: 2 Course: 2	+ 4005 ml
PT4	0-3 h: 40 24 h: 38 48 h: 34 120 h: 33	0-3 h: 635 24 h: 2266 48 h: 2140 120 h: 2078	SR: n.a Course: -	SR: n.a. Course: -	SR: n.a. Course: -	SR: n.a. Course: -	+ 1890 ml
PT5	0-3 h: 28 24 h: 22,4 48 h: 29,3 120 h: 26,5	0-3 h: 737 24 h: 12336 48 h: 15625 120 h: 11870	SR: yes Course: yes	SR: 28 Course: 13	SR: 22 Course: 10	SR: 4 Course: 2	+ 5090 ml
PT6	0-3 h: 28 24 h: 28 48 h: 25 120 h: 24	0-3 h: 375 24 h: 4225 48 h: 5070 120 h: 1841	SR: no Course: n.a.	SR: 10 Course: 2	SR: 10 Course: -	SR: - Course: -	+ 1160 ml
PT7	24 h: 33,3 48 h: 23	0-3 h: 177 24 h: 897 48 h: 2763	SR: - Course: -	SR: 3 Course: 2	SR: 3 Course: 3	SR: - Course: -	+ 620 ml (only 24h)
PT8	0-3 h: 30	0-3 h: 493 24 h: 10084 48 h: 6013 120 h: 1165	SR: n.a. Course: yes	SR: 1 Course: -	SR: - Course: -	SR: - Course: -	+ 1540 ml

3.1.6 Cytokines and Chemokines in PB after PT

To examine if the inverse bell-shaped pattern of the number of SPCs in PB after PT might correlate with the concentration of inflammatory or SPC mobilizing agents in PB, cytokine and chemokine levels were analyzed at 0-3, 24, 48 and 120 h after PT. Additionally, a control group of healthy volunteers was included (Tab. 11). Using multiplex ELISA the following cytokines and chemokines were measured in blood plasma: **E**pidermal **G**rowth **F**actor (EGF), Fractalkine, G-CSF, GM-CSF, Gro-α, Gro-β, IL-1β, IL-6, IL-8, IL-10, IL-33, MCP-1, **M**acrophage-**D**erived **C**hemokine (MDC), MIP-1α, MIP-1β, SDF-1α and VEGF-A (Fig. 10). IL-33, IL-1*β*, GM-CSF and EGF levels were below detection limit and thus not further examined.

Table 11: Cytokine and chemokine levels in PB of healthy volunteers *(n = 10) (based on Vogel et al., 2019a).*

	Mean (pg/ml)	SD
Fractalkine	1184.30	333.65
G-CSF	26.67	23.58
Gro-α	69.48	31.75
Gro-β	14.19	138.22
IL-10	0.24	0.33
IL-6	1.72	1.39
IL-8	4.44	2.22
MCP-1	209.02	54.29
MDC	722.93	214.80
MIP-1α	88.45	54.70
MIP-1β	115.43	113.08
SDF-1α	347.57	337.17
VEGF-A	96.61	19.42

For the inflammatory cytokines IL-6, IL-8, MCP-1 and IL-10, a significant increase was detected at the 0-3 h time point post trauma when compared to the control group. The level of IL-6 and IL-8 remained increased after 24 h post PT, while MCP-1 peaked again at 48 h. Other cytokines that have been previously linked to mobilization of SPCs, like Gro-α, Gro-ß and G-CSF were upregulated at the 0-3 h time point, too. Interestingly, VEGF-A and MDC were increased only at the 120 h time point after PT. Levels of SDF-1α though did not change in PT patients compared to the controls at any of the time points analyzed. In general, no cytokine or chemokine manifested with an inverse bell-shaped pattern over the 120 h time interval, as seen for the SPC populations (Fig. 10). Taken together, this data imply that there is likely a complex interplay among distinct chemokines and cytokines that influence the number of SPC in PB upon PT.

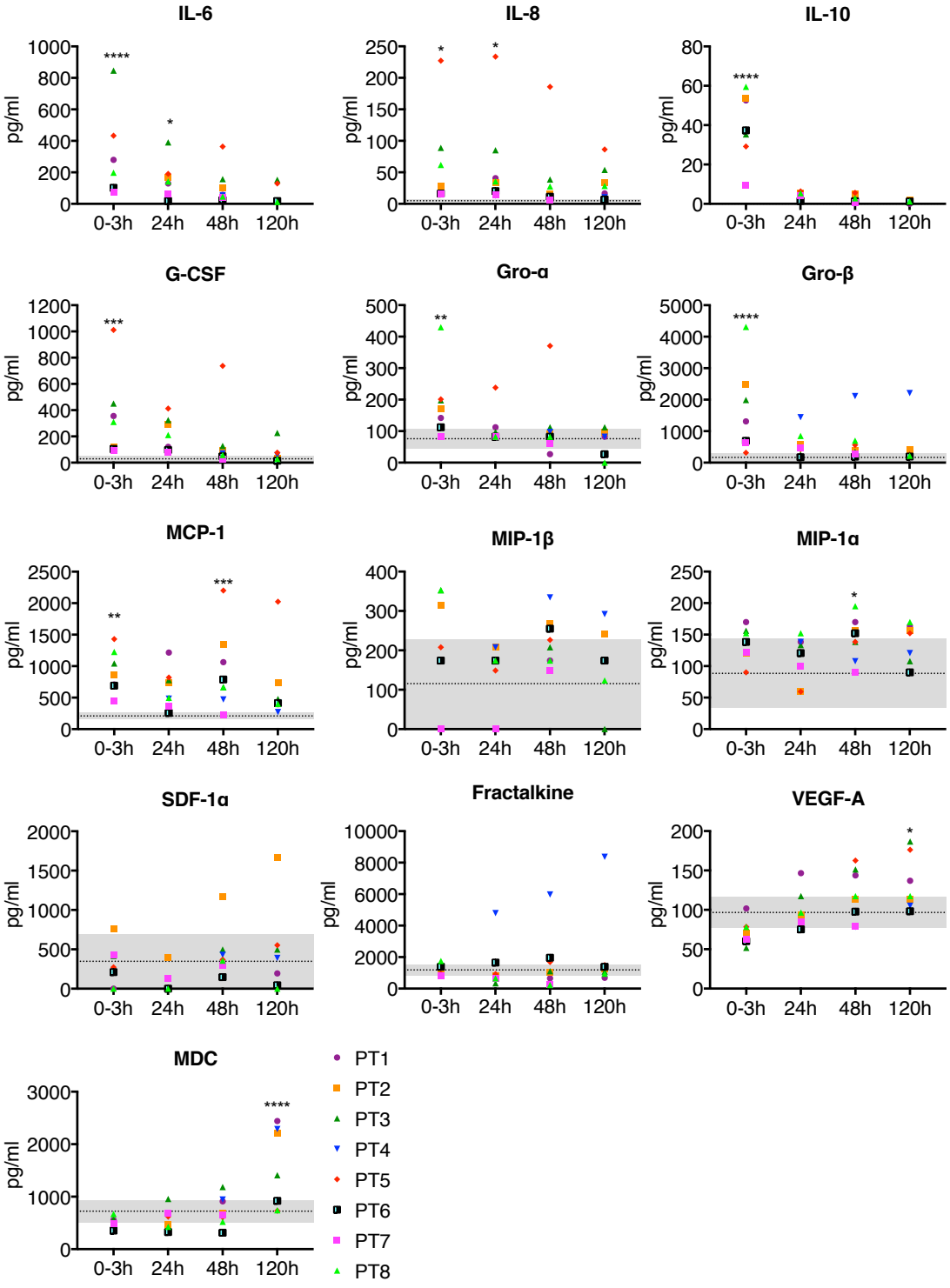

Figure 10: Inflammatory and mobilizing factors in blood plasma over a time period from 0-3 h to 120 h post injury. *The black dotted lines are the averaged blood concentrations in healthy controls the grey area the respective standard deviation (Tab. 11). Each dot marks the plasma concentration in an individual PT at the specific time point (Two-Way ANOVA between healthy control group and PT group, *p≤0.05 **p≤0.01, ***p<0.001, ****p<0.0001) (based on Vogel et al., 2019a).*

Cytokine and chemokine concentrations in PB were also grouped according to the ANSP-Score of the patient (LoLiNut and HiLiNut group) (Fig. 11). In the LoLiNut group pro-inflammatory cytokines like IL-6, IL-8 and G-SCF and the damage parameter **C**reatine **K**inase (CK) (primarily a marker for muscle injury and measured by default in ICU, listed Tab. 10) were increased at the early stages of trauma (at 0-3 h IL-6, IL-8 and G-CSF, at 24 h IL-8 and at 48 h CK), thus high levels of these cytokines at early time points after trauma are associated with a low increase in SPC numbers at 48 h to 120 h. MDC though was the only factor that presented with a higher concentration at the 120 h time point in HiLiNuts. These data link the elevated level of MDC to a high ANSP-Score (Fig. 11). It is thus a possibility that the change in level of MDC might be linked to trauma outcome.

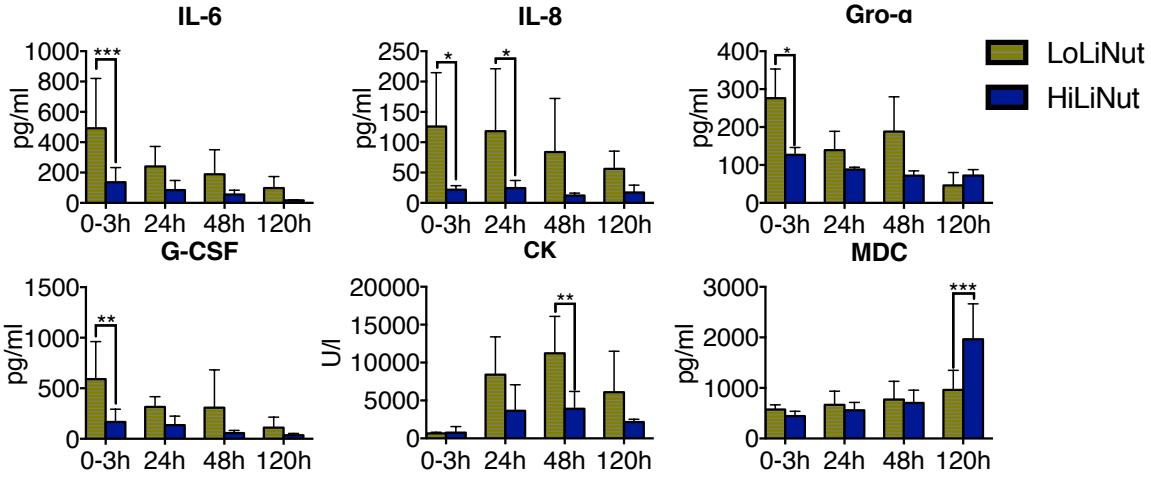

Figure 11: Cytokine and Creatine kinase concentration separated by the ANSP-Score. *The different cytokine/CK values in blood plasma at different time points after polytrauma, in LoLiNut group (low increase in SPC numbers between 48 h and 120 h) and HiLiNut group (strong increase in SPC numbers between 48 h – 120 h) are presented (mean ± SD; Two-Way ANOVA p≤0.05 **p≤0.01, ***p<0.001, ****p<0.0001). Adapted with permission from Wolters Kluwer Health, Inc.: Vogel et al.: Distinct Dynamics of Stem and Progenitor Cells in Blood of Polytraumatized Patients. Shock 51: 430–438 (2019). https://journals.lww.com/shockjournal/Fulltext/2019/04000/Distinct_Dynamics_of_Stem_and_Progenitor_Cells_in.5.aspx.*

3.1.7 Correlations between cytokines/chemokines, clinical parameters and SPC numbers in PB upon injury

To investigate correlations between cytokine concentrations and SPC numbers and ANSP-Scores, another set of Spearman correlations was performed. Only a few significant correlations were identified. For example, there was a correlation between VEGF-A at 0-3 h and the number of HSCs at 0-3 h and 24 h (Spearman´s

r = 0.79; p = 0.05 and r = 0.86; p = 0.02). We also found that the level of IL-8, Gro-α, MCP-1 and G-CSF at 0-3 h positively correlated to the number of CMPs at 48 h (Spearman´s r = 0.79; p = 0.05, r = 0.82; p = 0.03, r = 0.82; p = 0.03 and r = 0.86; r = 0.02, respectively). Higher levels of CK, IL-6, G-CSF, IL-8 as well as VEGF-A at the 48 h time point were associated with a lower increase in HSC numbers between 48 h and 120 h (Spearman´s r = -0.96; p = 0.00, r = -0.82; p = 0.03, r = -0.79; p = 0.05, r = -0.96; p = 0.00 and r = -0.86; p = 0.02) (Appendix Tab. A2).
Finally, correlations between clinical parameters, blood products, fluids and cytokines were investigated. Strikingly, G-CSF levels correlated with the length of stay in ICU at 0-3 h, 48 h and 120 h time point (Spearman´s r = 0.88; p = 0.01, r = 0.77; p = 0.03 and r = 0.80; p = 0.01, respectively). The other basic parameters like ISS or age did not persistently correlate with the analyzed inflammatory and mobilizing factors. Also, there were no correlations between number of FFP units provided and the concentrations of cytokines, indicating that given plasma did not influence cytokine levels in PB. The level of CK showed a correlation with the level of multiple cytokines, including G-SCF, Gro-α, IL-6, IL-8, IL-10 and MCP-1 (Appendix Tab. A3).

In conclusion, the recurrent, inverse bell-shaped pattern of SPCs in PB in the first 120 h post PT is highly interesting and suggests that SPCs are mobilized at distinct time points. The interplay between different inflammatory and mobilizing factors that might direct the dynamic changes in the number of SPC in PB upon trauma remain still to be identified. However, the identification of LoLiNuts and HiLiNuts and the differential cytokines levels between those groups imply a strong relationship between the level of those cytokines and the number of SPC in PB.

3.2 Distinct dynamics of SPCs and leukocytes in a mouse model of blunt thorax trauma (TXT)

The recurrent inverse bell-shaped pattern of the distinct SPC populations after PT and the annotation in HiLiNut and LoLiNut patients associated to trauma outcome provide novel rationale for investigations into what role SPC mobilization might play in trauma regeneration. I therefore established a trauma mouse model. In this setting I can obtain a better understanding for the role of SPCs in trauma regeneration as I can also investigate and analyze the injured tissue. Furthermore,

I can manipulate SPC numbers with pharmacological interventions. However, first, a basic understanding of what the cell dynamics look like after injury in the mouse are needed to detect differences and similarities to the human situation and to identify time points for manipulating SPC numbers to improve outcome. Thus, cell number fluctuations were analyzed in PB, BM and lung tissue 0.2 h, 2 h, 6 h, 12 h, 24 h, 48 h and 168 h after blunt thoracic injury. I analyzed the cell dynamics of three distinct types of MSCs, EPCs, HSCs and early and late hematopoietic progenitors. Additionally, leukocytes (lymphocytes, monocytes and neutrophils) numbers were measured to obtain a better understanding on the inflammatory response and to identify suitable time-points post trauma for immune modulating therapies.

3.2.1 Gating strategies and marker panels

In contrast to human MSCs, murine MSC remain somewhat less defined with respect to their cell surface marker profile in literature. Published protocols for the identification of murine MSCs are thus quite heterogenous with respect to appropriate marker combinations, and distinct populations are identified by overlapping, but also distinct types of markers. To identify the different MSC populations after injury gating strategies and marker panels were defined (Fig. 12). All MSC populations were gated for CD31, CD45 and anti-hematopoietic lineage cocktail (listed in Tab. 4) negativity (Qian et al., 2012, Winkler et al., 2010). MSC 1 population has been described in several publications (e.g. Winkler et al., 2010) and is characterized by Sca-1 and CD51 expression. The three-lineage differentiation potential of this population was previously confirmed in the laboratory (Guidi et al., 2017). MSC 2 ($CD29^+$, $CD105^+$ and $Sca\text{-}1^+$) and MSC 3 ($CD29^+$, $CD44^+$, $CD90^+$ and $Sca\text{-}1^+$) populations are defined via commercially available MSC identification kits from the companies Novus and Abcam. However, the three-lineage differentiation and thus stem cell potential for all three of these MSC populations have been verified only in BM derived MSCs (Fig. 12 left panel). It is known though that the potential of MSCs identified with the same marker combination but isolated from distinct tissue is not always identical (Petrenko et al., 2020). Due to their low number of MSCs in PB, and the number of cells currently necessary for the differentiation assay, verification of the potential via ex vivo differentiation would require hundreds of mice and was thus not performed. As markers that identify MSCs are also found

in non-MSC cells of the lung, the number of MSC frequency in the lung could not be determined.

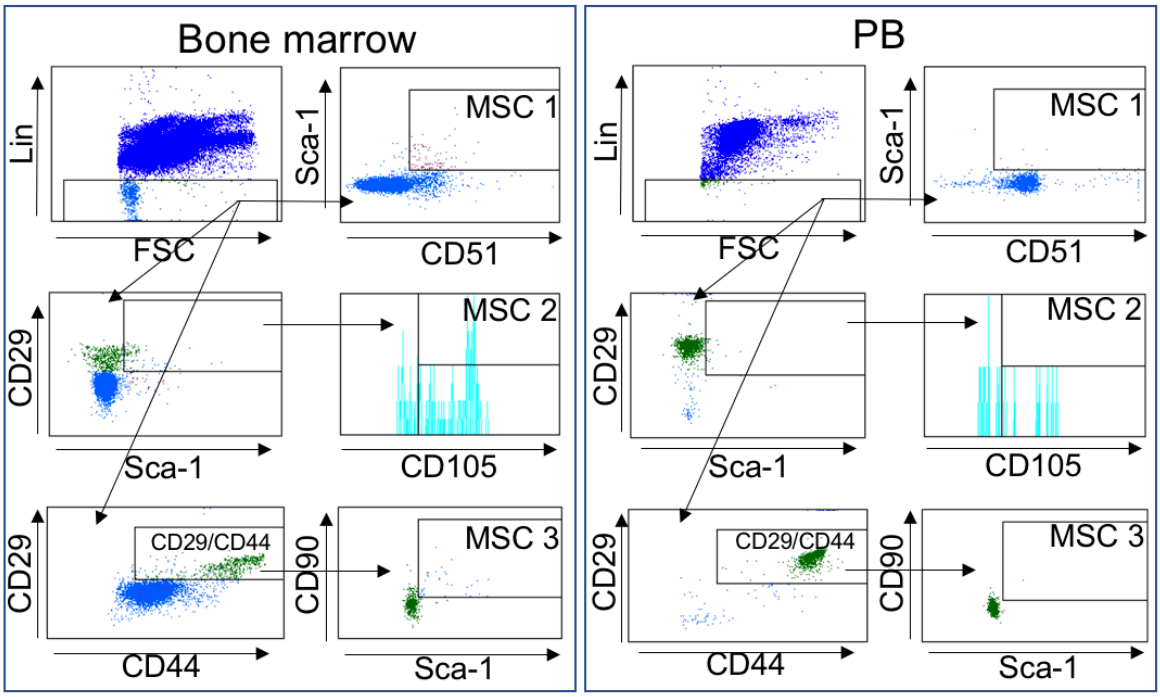

	Negative Marker	Positive Marker
MSC 1	CD45, CD31, Lineage	Sca-1, CD51
MSC 2	CD45, CD31, Lineage	Sca-1, CD29, CD105
MSC 3	CD45, CD31, Lineage	CD44, CD29, Sca-1, CD90

Figure 12: Gating strategy and marker panel for the different MSC populations. *Out of the Lin$^-$ cells (CD45, CD31 and hematopoietic lineage negative) three different populations were isolated, markers for identification are shown in the panel.* ***Left:*** *gating of BM derived cells;* ***Right:*** *gating of PB derived cells.*

Together with the determination of the number of MSCs, different HSPC populations in the three tissues BM, PB and lung were also examined. HSCs are the best characterized adult stem cell population, the marker panel and gating strategy is provided in Fig. 13. For HSCs (Lin$^-$, Sca-1$^+$, c-Kit$^+$ and CD34$^-$) long-term potential and lineage differentiation was verified by transplantation models in our lab (Vogel et al., 2019b). Early progenitors (Lin$^-$, Sca-1$^+$, c-Kit$^+$ and CD34$^+$) and late progenitors (Lin$^-$, Sca-1$^-$ and c-Kit$^+$) were also quantified, as they also show a high mobilization and migratory ability. The BM gating strategy to identify these populations (Fig. 13 left panel) was also used for cells from PB and the lung. As anticipated, the number

of HSPCs in PB was really low (Fig. 13 middle panel). For lung tissue, an additional gate was introduced to identify the CD45$^+$ cells (Fig. 13 right panel).

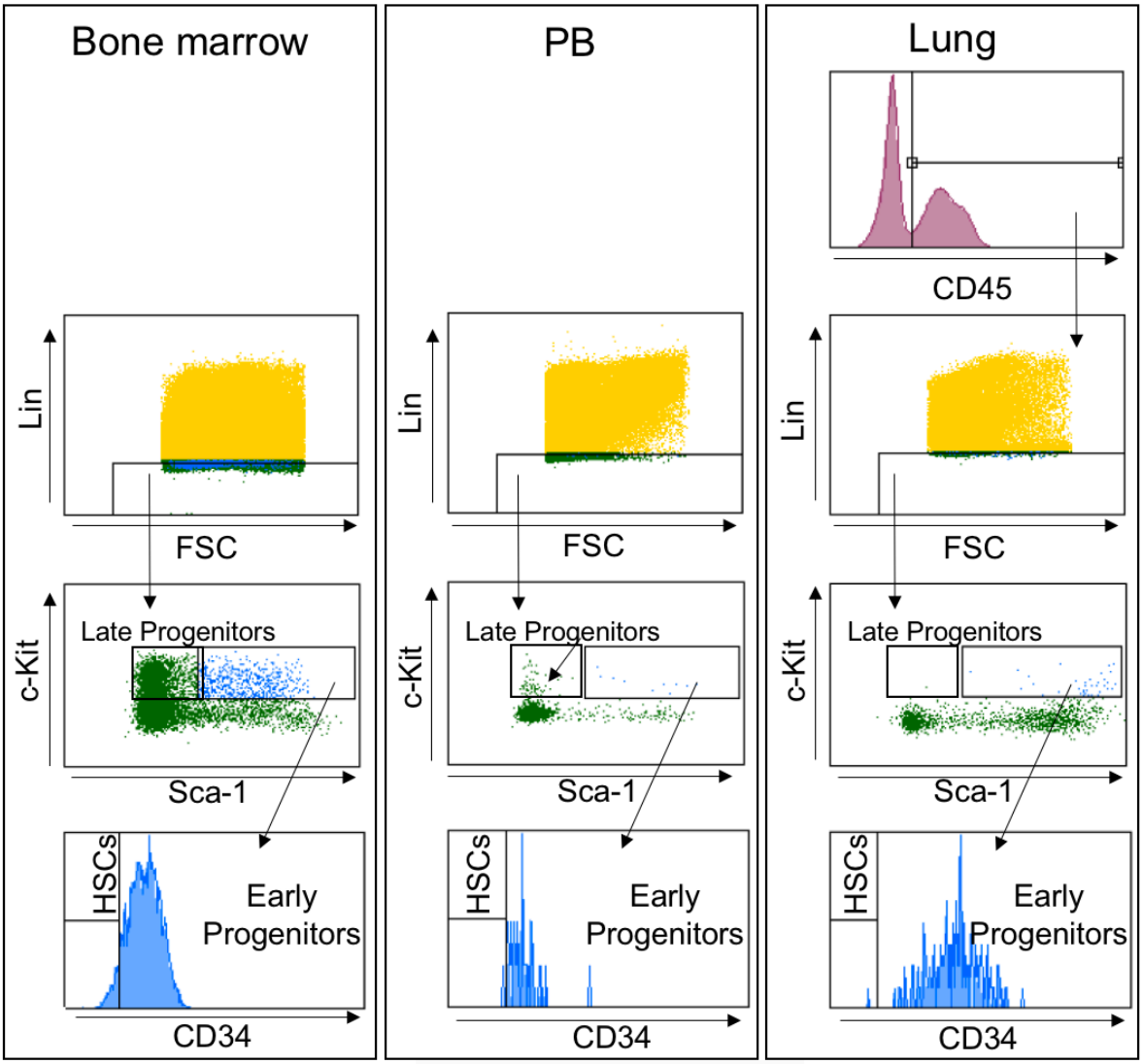

	Negative Marker	Positive Marker
Late Progenitors	PI, Lineage Cocktail	C-Kit
Early Progenitors	PI, Lineage Cocktail	Sca-1, c-Kit, CD34
HSCs	PI, Lineage Cocktail, CD34	Sca-1, c-Kit

Figure 13: Gating strategy and marker panel for HSPC populations. left: *Gating of BM derived cells* ***Middle:*** *gating of PB derived cells* ***Right:*** *gating of lung cells, here an additional size gate (see 2.3.4.2) and CD45 gate were established to identify the hematopoietic cells. Markers for the different populations are shown in the table.*

Within the HSPC panel, cells with endothelial potential (Flk-1$^+$, CD34$^+$, c-Kit$^+$) could also be identified according to the gating strategy illustrated in Fig. 14a. Lung tissue presented with the highest number of EPCs (Fig.14a), while again, as anticipated

the number was very low in both BM and PB. This gating strategy for cells with endothelial potential was previously utilized by Zhang et al. (2006). I confirmed the endothelial differentiation potential within that population in a CFU assay on BM derived EPCs (Fig. 14b).

a

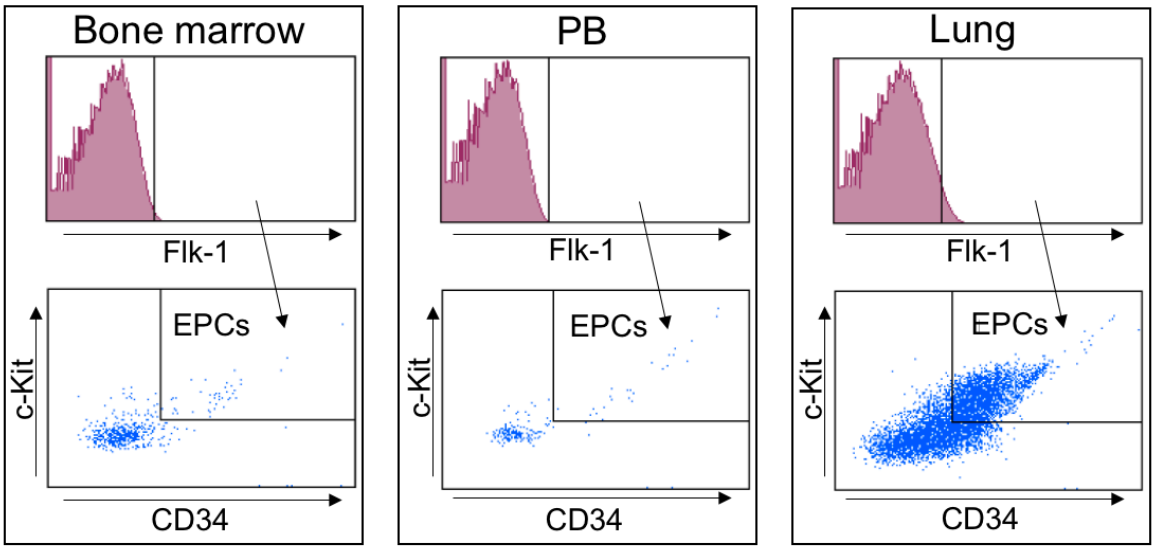

	Negative Marker	Positive Marker
EPCs	PI	Flk-1, CD34, c-Kit

b

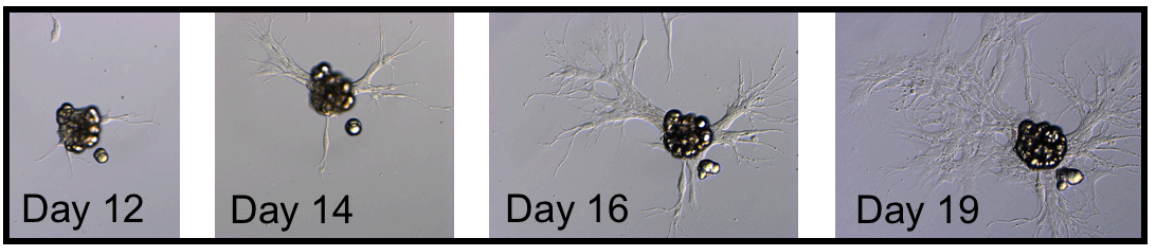

Figure 14: Gating strategy and marker panel for EPCs. a *Illustrated is the gating of the EPCs in the different tissues.* ***Left:*** *Bone marrow* ***middle:*** *PB and* ***right:*** *Lung* ***b*** *CFU of BM derived EPCs after different time points, verifying endothelial potential of the chosen panel.*

Finally, in the TXT animal model, mature hematopoietic cell populations were also quantified. The change in number of lymphocytes, monocytes and neutrophils were investigated. Mature hematopoietic cells were identified in PB and BM by a Hemavet950 cell counter. For lung tissue, the gating strategy to identify lymphocytes, monocytes and neutrophils introduced by Yu et al. (2016) was used (Fig. 15). In this scheme, neutrophils were characterized by Ly6G expression and monocytes by expression of CD11b and CD64. Lymphocytes do neither express Ly6G nor CD11b and CD11c.

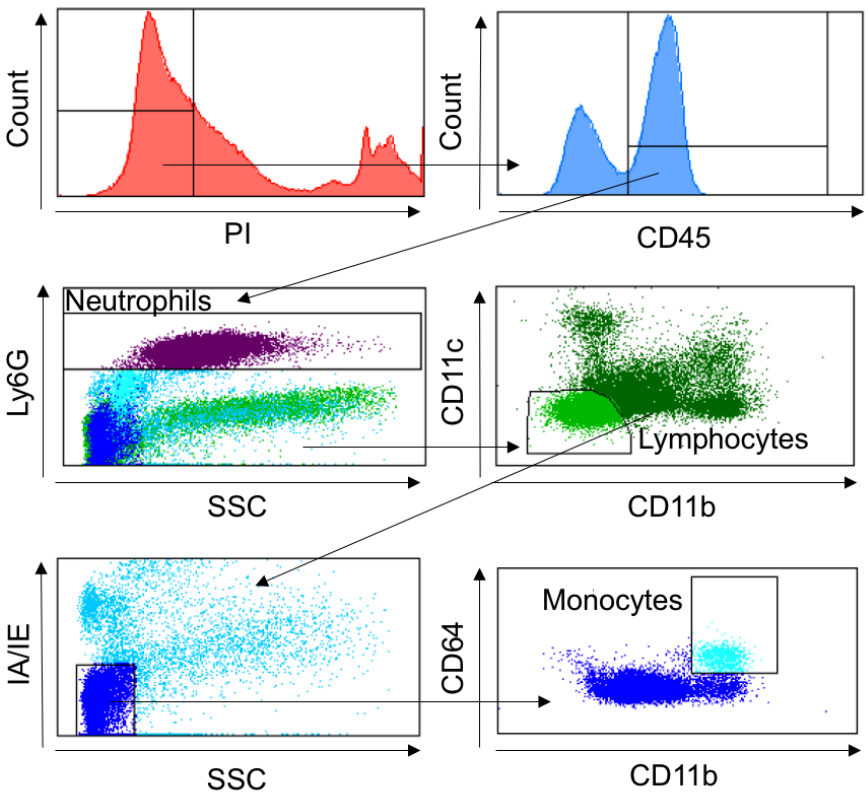

	Negative Marker	Positive Marker
Neutrophils	PI	CD45, Ly6G
Monocytes	PI, Ly6G, IA/IE	CD45, CD11b, CD64
Lymphocytes	PI, Ly6G, CD11b, CD11c	CD45

Figure 15: Gating strategy and marker panel of mature hematopoietic cells in lung tissue. *Isolated lung cells were stained and gated for the distinct cell types. PI staining was applied to obtain alive cells and CD45 to isolate hematopoietic cells. Marker for the different populations are shown in the table below.*

Taken together I established flow panels and gating strategies for three different MSC populations (for PB and BM), HSCs, early and late hematopoietic progenitors, EPCs and mature hematopoietic cells (for PB, BM and lung tissue).

3.2.2 Cell dynamics in polytrauma versus single TXT

Similar to our studies in humans, I determined the number of SPCs in PB of a PT mouse model (TXT, TBI, bone fracture) and a TXT only mouse model. The TXT mouse model, where a single blast is applied on the thoracic area of the mouse, has the advantage of an increased throughput rate for the analysis of the animals. The observation period after the trauma is in addition not limited, enabling the

determination of a cell dynamic curve over a longer time frame. The TXT mouse model is defined by both a local and systemic inflammatory response (Perl et al., 2006). The murine PT model, which more closely resembles human PT, is showing a strong systemic inflammatory response and is a very short-lived model (analysis only up to 4 h post trauma possible), with a high exclusion rate due to immediate death upon trauma. The relative change in the number of the distinct SPC populations 2 h post trauma is shown in Fig. 16. The relative change was calculated by dividing absolute cell number in traumatized animals by the absolute cell number in sham treated animals. Sham treated animals were housed in the same cage and the same procedures (analgesic and narcotics) were applied without inflicting an insult. The WBC count was elevated in the TXT, but interesting not the PT model (Fig. 16a). The change in mesenchymal, hematopoietic and endothelial SPCs however, were similar between the two model systems (Fig. 16b-d). As the PT model results in changes in the number of SPCs in blood that were almost identical to the changes seen in the TXT model, subsequent analyses were focused on the TXT model which allows for a long-term observation of changes in the number of SPCs in blood and tissues, and will thus allow, in the long-term, to test for the influence of SPCs on trauma outcome.

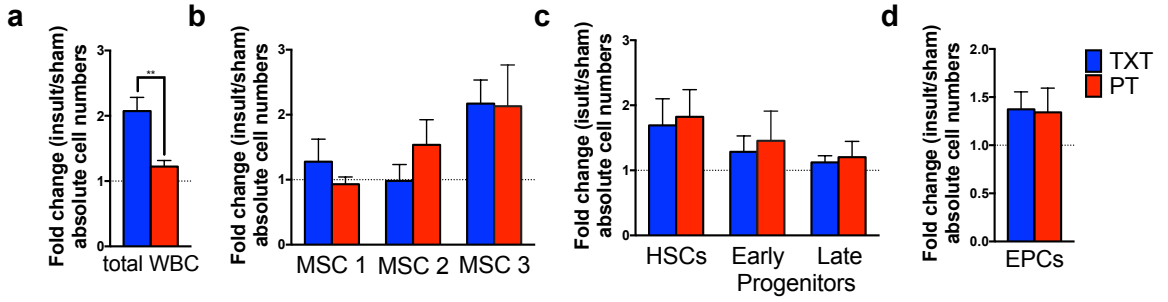

Figure 16: SPC numbers in PB in PT and TXT mouse model 2 h after injury. a *total WBCs obtained by Hemavet950* ***b*** *MSCs numbers in PB* ***c*** *HSPCs in PB* ***d*** *EPCs in PB (mean ± SEM; n = 2-7; One-way ANOVA **p≤0.01).*

3.2.3 Changes of the number of SPCs in PB upon TXT

PB was collected at 0.2 h (10 min), 2 h, 6 h, 12 h, 24 h, 48 h and 168 h after induction of the trauma by cardiac puncture. Overall, there was no significant change in the number of MSCs, HSCPs or EPCs at any given single time-point post trauma (Fig. 17).

The number of the MSC1 and MSC3 populations though showed a dual wave-like pattern that peaked at 2 h (2.9-fold MSC1 and 2.2-fold MSC3) and 24 h (2.4-fold MSC1 and 3.4-fold MSC3). The MSC2 population presented with a slightly different dual-wave distribution, with an elevation of their number at 12 h and 24 h (3.3-fold). In aggregation, all three characterized types of MSCs presented with a number elevated compared to controls at 24 h post trauma, which might imply that indeed the number of MSCs might be elevated in PB upon trauma at this time-point. The number of HSPCs in PB resembled over the whole time course of the analysis (2 h to 168 h post induction of trauma) an inverse bell-shaped pattern (trend) which was though not as pronounced as the change in the number of SPCs in PB seen upon PT in humans (Fig. 8). Additional experiments will therefore be necessary to determine the validity of this observations in a larger cohort of animals.

2 h after TXT there was a significant increase in the number of monocytes (3.3-fold) neutrophils (4-fold) and lymphocytes (1.8-fold), which returned to controls levels already at 6 h post trauma induction. Only neutrophils showed a slight second wave (increase in numbers, 2.9-fold) at the 24 h time point (Fig. 17d).

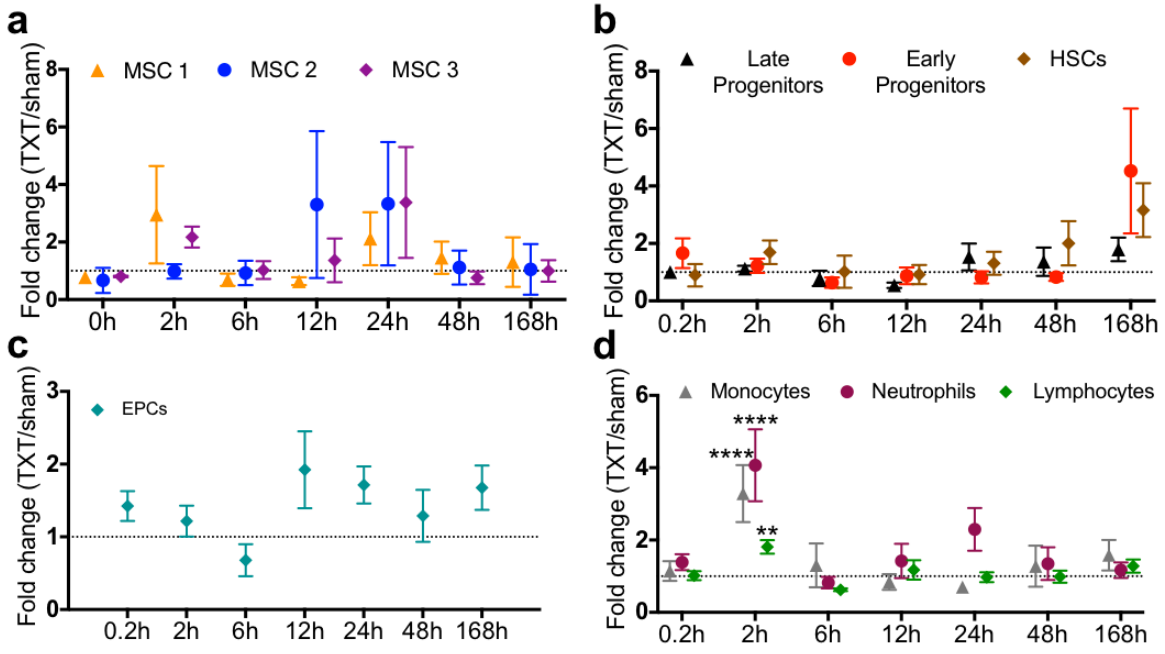

Figure 17: Cell dynamics after TXT in PB. *SPC numbers in PB at different time points post TXT. Given is the fold change calculated by dividing the TXT cell number through the sham cell number, per group two animals were pooled to obtain enough blood.* ***a*** *MSCs* ***b*** *HSPCs* ***c*** *EPCs* ***d*** *Mature hematopoietic cells (mean ± SEM; n = 5-7; Two-Way ANOVA **p≤0.01, ****p≤0.0001).*

3.2.4 Changes of the number of SPCs in BM upon TXT

In a next step, I determined the change in the number of SPCs in BM upon TXT (Fig. 18). BM might be the likely source of circulating SPCs in blood. Similar to the blood analyses, I did not detect a significant change in the number of SPCs for a given time-point post TXT induction, with the exception of a significantly elevated number of late hematopoietic progenitors in BM 2 h post trauma induction. The number of HSCs and early progenitors was also elevated at this time-point (1.8 and1.9 fold, Fig. 18b). Also, similar to blood analyses, all of the three MSCs subtypes analyses showed a trend towards elevated numbers in BM (Fig. 18a, 1.6 to 2-fold). Interestingly, the number of mature hematopoietic cells in BM was mostly unaffected by TXT in BM (Fig. 18d). In summary, TXT does not affect to a great extent the number of SPCs and mature hematopoietic cells in BM.

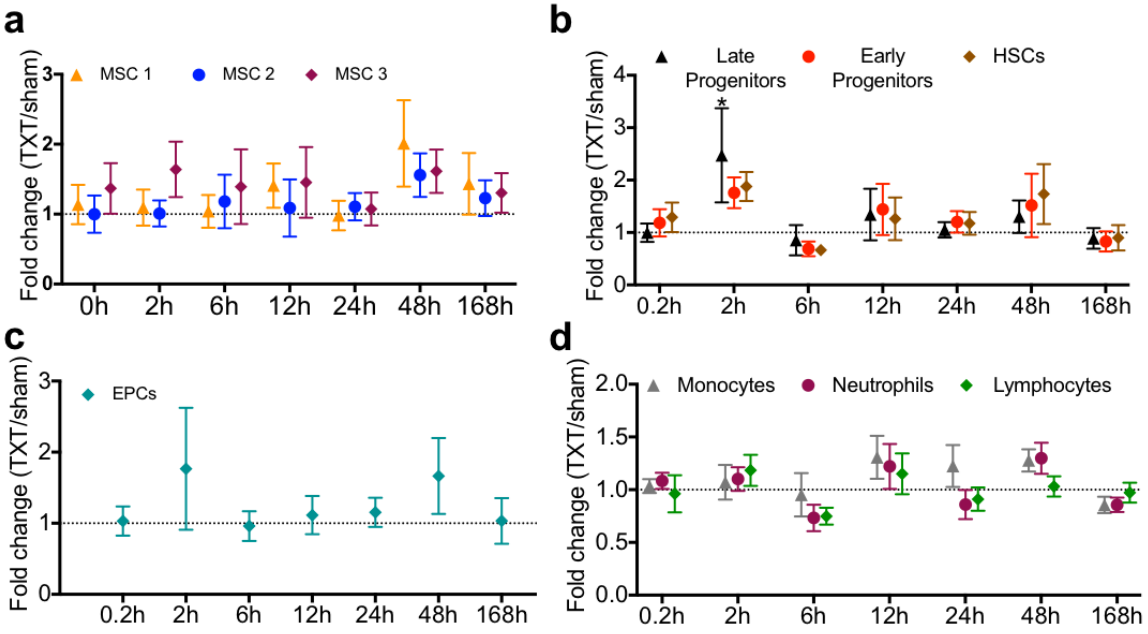

Figure 18: Cell dynamics after TXT in BM. *Cell numbers in BM after TXT application over a time period of 168 h, BM was isolated from one mouse. Fold change is calculated dividing TXT numbers through sham numbers.* ***a*** *MSCs* ***b*** *HSPCs* ***c*** *EPCs* ***d*** *Mature hematopoietic cells (mean ± SEM; n = 5-7; Two-Way ANOVA *p≤0.05).*

3.2.5 Changes of the number of SPCs in the lung upon TXT

Finally, the change in the number of SPCs upon TXT was also determined in the lung, the target tissue of the trauma (Fig. 19).

In the lung, the number of HSCs was elevated 48 h post trauma (3.2 fold), together with an increase, though smaller, in the number of early and late progenitors (Fig. 19a) Similar to all other tissue, the number of EPC did not change in the lung between 0.2 h and 168 h post trauma (Fig. 19b). Mature hematopoietic cells were, similar to blood, significantly elevated 2 h post injury (monocytes 4.6-fold, lymphocytes 2.1-fold and neutrophils 13.2-fold) compared to sham treated controls and also returned to levels similar to controls already 6 h post TXT (Fig. 19c). This data might imply that HSPCs in lung contribute to a late (48 h and later) repair phase, while in the initial inflammatory phase primarily inflammatory cells are increased in lung.

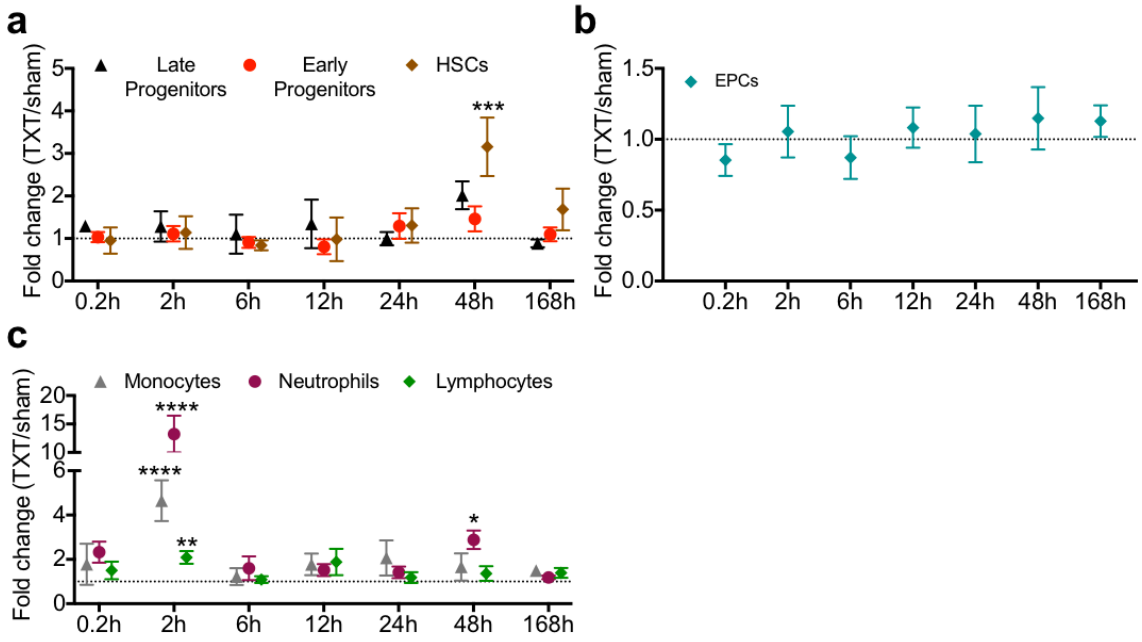

Figure 19: Cell dynamics after TXT in lung tissue. *Cell numbers were analyzed by flow cytometry at different time points after TXT induction in total lung tissue of one mouse.* ***a*** *HSPCs* ***b*** *EPCs* ***c*** *Mature hematopoietic cells (mean ± SEM; n = 5-7; Two-Way ANOVA *p≤0.05; ***p≤0.001; ****p≤0.0001).*

3.2.6 Correlations between distinct cell populations and between different tissues

I also tested whether correlation between changes in number of cells in any given tissue exist in individual animals which might be otherwise blunted by the relatively high level of variability of the data in each experimental group. In BM, changes in the number of HSCs, early and late hematopoietic progenitors did correlate (Appendix Tab. A4). However, the relative change in a specific cell population in one tissue did not correlate with the change of the same cell population in another

tissue (Appendix Tab. A5). Changes in the number in one tissue are thus likely not directly linked to changes in another tissue.

3.3 Manipulation of SPC dynamics in the early phase of TXT does not improve parameters linked to regeneration.

I finally tested whether enforced pharmacological mobilization of endogenous SPCs early (0-6 h) post TXT will i) influence the dynamic changes in the number of SPCs in PB and tissue and whether this ii) might correlate with changes in the parameters linked to trauma outcome. To this end, the short-time (hours) mobilizer drug AMD3100 (i.p. 5 mg/kg) was used (see 1.4.1.2). I applied in these first round of experiments AMD3100 directly post TXT and 6 h after TXT induction (Fig. 20). Those two time points were chosen as I found them of interest based on my investigations on the synchronous dynamics of different SPC populations and leukocytes. I applied AMD3100 directly after injury because we can further increase SPC numbers at the peak of initiation of inflammation and the circulation of inflammatory cells and 6 h post TXT because we found a nadir in PB at this time point for most SPC populations.

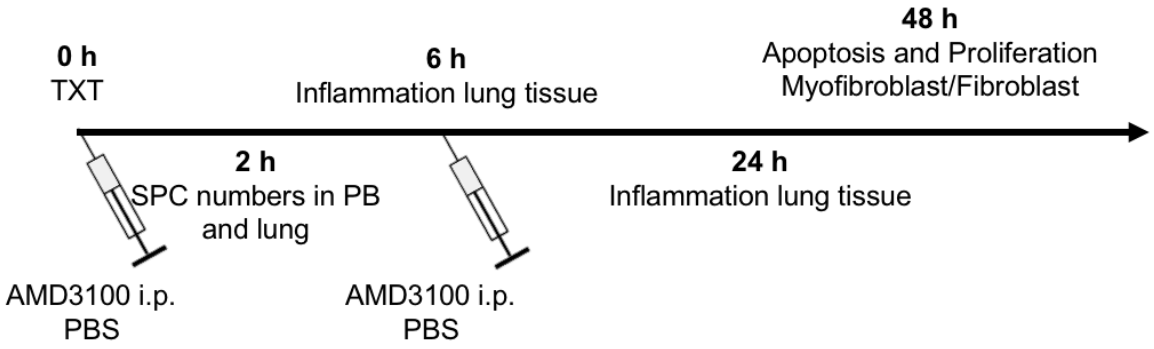

Figure 20: Overview of the analysis for how AMD3100 treatment is influencing tissue repair after TXT induction. *2 h after TXT application and AMD3100 treatment cell numbers were analyzed in PB and lung tissue, at 6 h and 24 h inflammatory responses were investigated by measuring cytokine levels in lung tissue, and at 48 h post TXT regeneration parameters like apoptosis, proliferation and myofibroblast/fibroblast ratio were examined.*

3.3.1 Modulation of the number of SPC in trauma by SPC mobilization

I first determined in as much AMD3100 resulted in an increase in the number of SPCs as well as mature hematopoietic cells in PB of TXT animals at 2 h after application of AMD3100 relative to controls (TXT without AMD3100). AMD3100 resulted in a significant increase in the number of early hematopoietic progenitors

(9.1-fold increase) and HSCs (9.7-fold increase) in PB, while there was only a trend for higher numbers of late progenitors (4.9-fold) and EPCs (5.8-fold). Interestingly, the number of both MSC3 (0.5-fold) and MSC2 (0.6-fold) cells was on average reduced in PB (Fig. 21a). Mature hematopoietic cells presented also with an increase in PB 2 h after TXT plus AMD3100 treatment (lymphocytes 2.5-fold, monocytes 4-fold and neutrophils 3-fold). In the lung there was, similar to PB, an increase in the number of monocytes (5.1-fold) and neutrophils (3.8-fold). The number of HSPCs did not increase in the lung 2 h after AMD3100 application and the number of EPCs was actually reduced by 50% (Fig. 21b). In conclusion, AMD3100 mobilizes especially HSPCs into the peripheral circulation in the TXT animal model, while only the numbers of leukocyte subsets were elevated in the lung.

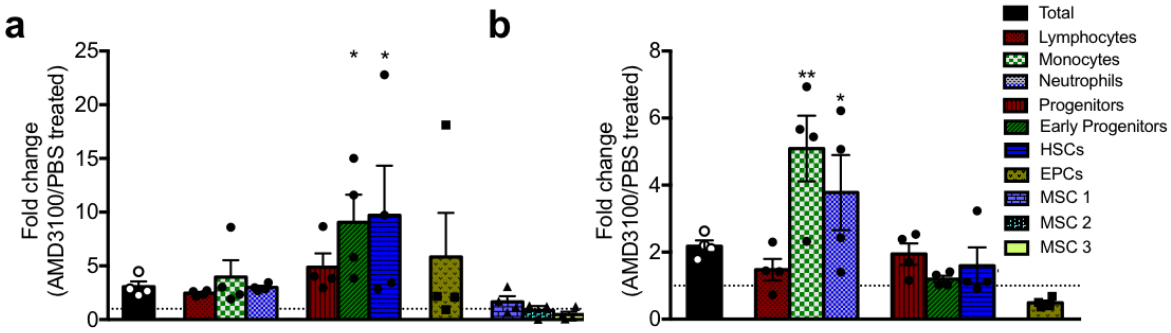

Figure 21: Modulation of SPC numbers in PB and lung tissue by AMD3100. *Directly after TXT induction AMD3100 or PBS was i.p. injected. 2 h later cell numbers were measured and fold change was calculated by dividing absolute cell numbers found in AMD3100 treated animals through the cell numbers in PBS treated animals* ***a*** *PB* ***b*** *lung tissue (mean ± SEM; n = 4; One-Way ANOVA *p≤0.05, **p≤0.01).*

3.3.2 Inflammatory response in AMD3100 treated animals

AMD3100 resulted in an increase in the number of leukocytes as well as HSPCs and EPCs in PB in TXT animals over control. We next analyzed whether this increase might correlate with a changed inflammation or enhanced lung tissue repair upon trauma, as predicted by our overall hypothesis. The inflammatory status was determined by analyzing the concentration of the inflammation-associated cytokines IL-6, IL-10, KC, TGF-α and MCP-1 in lung tissue. It has been previously reported that those cytokines were associated with inflammation upon TXT in the mouse (Knöferl et al., 2003, Niesler et al., 2014, Hafner et al., 2015, Perl et al., 2006). Interestingly, there was no change in the level of these cytokines 6 h after

trauma initiation in combination with AMD3100 induced mobilization compared to controls (TXT only) (Fig. 22a). In another set of experiments cytokine levels in the lung were determined 24 h post TXT. With respect to application of AMD3100, an additional time point (6 h post TXT) for AMD3100 delivery was added to the experimental set-up, which resulted in a total of 4 groups: PBS treated or AMD3100 treated at both time points (0 h and 6 h), AMD3100/PBS treated (0 h AMD3100 and 6 h PBS) and PBS/AMD3100 treated (0 h PBS and 6 h AMD3100). Similar to above, animals treated with AMD3100 did not show any significant difference in the concentration of these cytokines in the lung (Fig. 22b). In summary, administration of AMD3100 to TXT animals either right after trauma initiation or 6 h post did not reduce markers of inflammation in lung tissue of TXT mice.

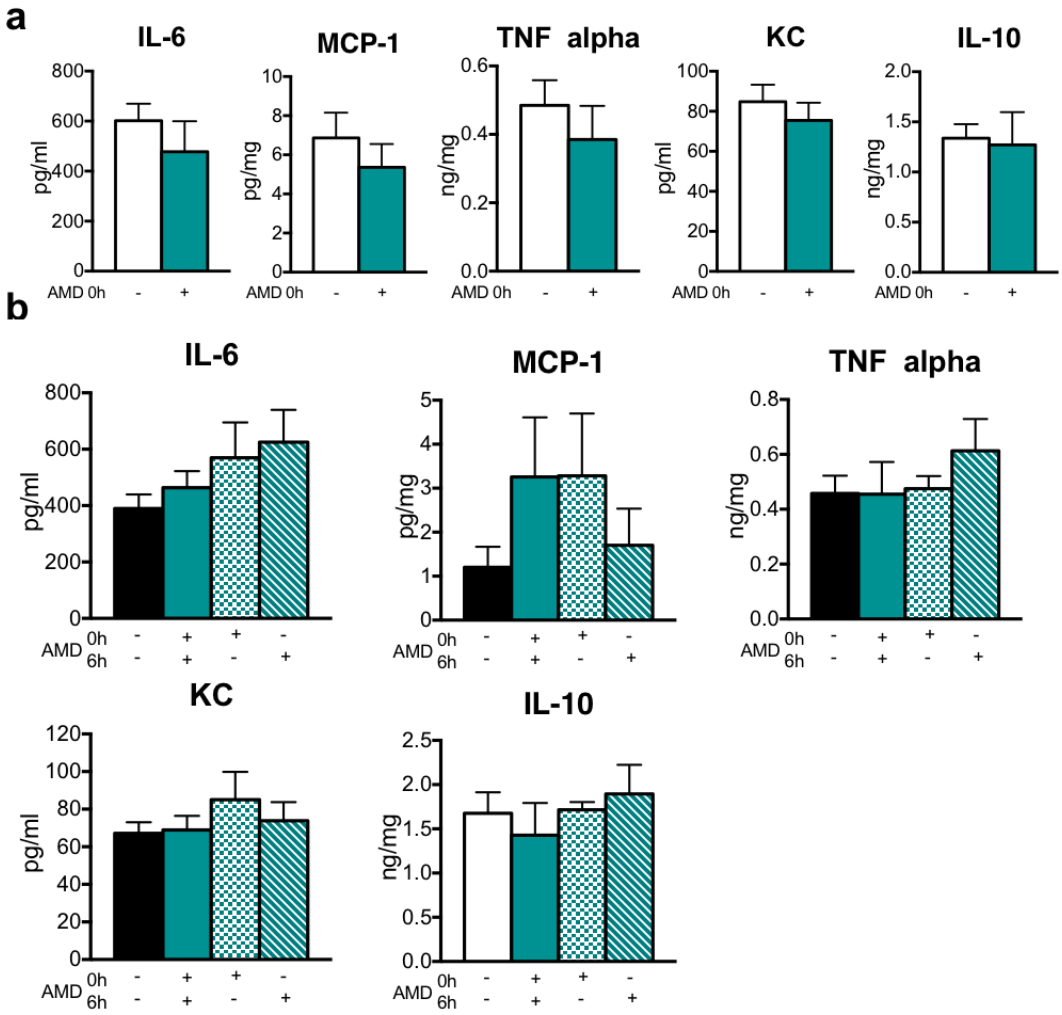

Figure 22: Inflammatory response after TXT and AMD3100 treatment. *Cytokine and chemokine levels in lung tissue were measured by serial ELISA after TXT application and injection with AMD3100 or PBS.* ***a*** *6 h after TXT induction and AMD3100 treatment* ***b*** *24 h after TXT induction, different treatments were applied as illustrated (n = 5-7; mean ± SEM; One-Way ANOVA).*

3.3.3 Proliferation and Apoptosis upon AMD3100 treatment

Apoptosis contributes to tissue damage and inflammation. Proliferation, migration and differentiation of local or BM derived progenitor cells are important steps in tissue repair (Rennert et al., 2012). 48 h after TXT induction, the level of apoptosis was determined by Annexin V staining (Fig. 23a). Levels of apoptosis remained unaffected by AMD3100. An increase in the number of mature hematopoietic cells and/or HSCPs in PB and lung upon AMD3100 administration does not alter apoptosis. The percentage of cells in S-phase of the cell division cycle was measured by PI staining at 48 h post TXT, when the regeneration phase (characterized by proliferation) of the tissue repair process has been already started (Fig. 23b). While the frequency of proliferating cells was significantly decreased in the TXT animals in comparison to sham treated animals, there was no change in between experimental groups treated with AMD3100 and controls (TXT plus PBS only). AMD3100 does therefore not increase proliferation or decrease apoptosis in the lung 48 h post TXT.

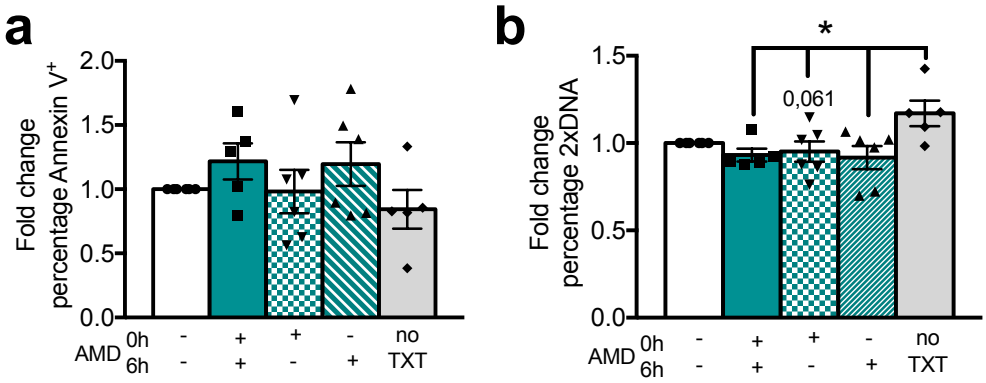

Figure 23: Apoptosis and proliferation in lung tissue 48 h after TXT induction and AMD3100 treatment. a *Percentage of Annexin V$^+$ cells in lung tissue was measured by flow cytometry, fold changes was calculated by dividing through the percentage of PBS treated animals.* ***B*** *DNA amount was measured by PI staining, fold change was calculated by dividing through the PBS treated animals (n = 5-6; mean ± SEM; One-Way ANOVA *p≤0.05).*

3.3.4 Fibroblast/Myofibroblast ratio in the lung in response to AMD3100 treatment

To investigate lung regeneration upon TXT, the percentage of myofibroblasts and fibroblasts in lung tissue 48 h after TXT induction and AMD3100 treatment was measured by flow cytometry (Fig. 24). The persistence of myofibroblasts in inured

lung tissue is associated with fibrosis and scarring and thus impaired lung regeneration (Glasser et al., 2016). Myofibroblasts are identified as Lin^- (fibroblast lineage cocktail Tab. 5), Sca-1^{low} and $CD49e^+$, fibroblasts are Lin^-, Sca-$1^{low/+}$ and $CD49e^{low}$, as shown previously by Akamatsu et al., 2013 (Fig. 24a). As anticipated, there was a significant increase in the frequency of myofibroblasts in all TXT compared to sham treated animals, which significantly reduced fibroblast/myofibroblast ratio in TXT animals (Fig. 24b). The ratio though in TXT animals was not affected by AMD3100. The data confirm that TXT induces myofibroblast formation in the lung, while induction of mobilization of leukocytes and HSCPs has no influence on the ratio with which they are formed or removed, at least up to 48 h post TXT.

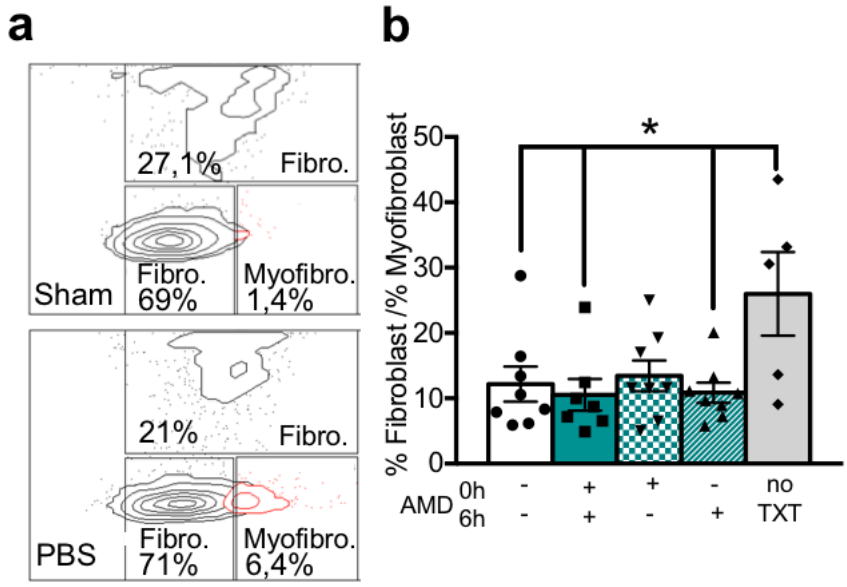

Figure 24: Fibroblast and Myofibroblast ratio 48 h after TXT induction and AMD3100 treatment. ***a*** *Illustrated is the gating for the differentiation between fibroblasts and myofibroblasts* ***b*** *Ratio between fibroblasts and myofibroblasts at 48 h after TXT (n = 7-8; mean ± SEM; One-Way ANOVA *p≤0.05).*

In summary, my data indicate that even though AMD3100 increases the number of leukocytes and HSPCs in PB and to some extent in the lung, this does not affect the inflammatory response nor the regenerative response to TXT in the lung. Thus, mobilization of cells by AMD3100 at 0 h or 6 h post TXT does not affect TXT parameters in the lung linked to trauma outcome.

4. Discussion

Stem cell based therapies are promising approaches in regenerative medicine. Especially MSCs, but also HSPCs and EPCs are investigated for a role in changing trauma outcomes both in animal models and in humans. For example, the endogenous induction or exogenous application of SPCs upon trauma has been associated with improved trauma regeneration in mice as indicated by increased vascularization, improvement in the cytokine profile and an accelerated healing (for example Wang et al., 2011, Allakhverdi and Delespesse, 2012, Seebach et al., 2012). Another new and interesting avenue to improve trauma outcome are immunomodulation therapies (Julier et al., 2017). Recently, Martin et al. (2018) showed that chemotactic neutrophil recruitment into a damaged lung can be reduced by applying a Rho-inhibiting C2IN-C3 fusion toxin. So far though, only moderate clinical success was achieved with either of these approaches, likely due to the uncomplete understanding of the mechanisms by which stem cells and immune cells contribute to trauma outcome. Here, I hypothesized first that endogenous SPCs are mobilized to PB and the site of injury at distinct time-points post trauma to likely affect trauma outcome, and then secondly, that providing elevated levels of endogenously SPCs at distinct time point post trauma via mobilization might improve trauma outcome.

4.1 Distinct dynamics of SPCs in PB of polytraumatized patients

We first investigated the number of distinct types of SPC in PB of PT patients over the first 120 h post PT. I developed a novel experimental protocol to simultaneously detect multiple types of SPCs in PB upon PT. The simultaneous detection of these SPCs in blood provided novel insight into the role of coordinates changes in SPCs upon trauma and suggested a novel role for SPCs for the regeneration phase (48 h onwards) in human PT regeneration.

Previously, it was already demonstrated that disease, injury and multiple types of traumata result in an elevated (higher than steady state levels) number of distinct types of SPCs in PB (for example: Massa et al., 2005, Ramírez et al., 2006, Mansilla et al., 2006). The change in the number of SPCs in PB of humans reported though varies from study to study, likely due to different sample preparation protocols and marker panels used to identify the target cell population. For example, Massa et al. (2005) used only CD45 and CD34 expression plus morphologic qualities as markers

for HSPCs (defined by the International Society of Hematotherapy and Graft Engineering (Sutherland et al., 1996)). Skirecki et al. (2019), in their study of SPC dynamics in septic shock patients, included CD45, CD34, CD133, CD38 and a lineage cocktail, to identify human HSCPs. In this study, I used the established marker panel for HSCs with CD34, CD38, CD45ra, CD90 and lineage cocktail (e.g. Wisniewski et al., 2011).

The very definition as well as the characterization of human EPCs in PB still remain a matter of debate in itself (Del Papa and Pignataro, 2018). For this reason, I omitted the analysis of EPCs in the human studies. As published results also demonstrate that CMPs and GMPs themselves and thus hematopoietic cells can support angiogenesis and are able to trans-differentiate into endothelial cells (Wara et al., 2011), I included these populations in my analysis. The introduction of minimal requirements to identify human MSCs by the International society for cellular therapy addressed the problem of comparability between studies on MSCs (Dominici et al., 2006). For MSC detection I used the phenotyping kit from Miltenyi that fulfils these minimal requirements.

As discussed in Vogel et al. (2019a) the inverse bell-shaped pattern of the number of SPCs in PB identified would suggest that in general, in the first hours upon PT an active mobilization or a mechanical release of the SPCs takes place. The strong decrease between 0-3 h and 48 h might be due to migration of SPCs into the damaged tissue or dramatically reduced mobilization, and the increase between the 48 h and 120 h time point might be either related to a reduced recruitment of SPCs to other tissues or an increase in mobilization.

The early increase in the number of SPC in PB might be due to the release of inflammatory and migratory cytokines and chemokines. IL-6, IL-8, IL-10, G-CSF, Gro-α, Gro-β and MCP-1 were all upregulated in PB early on after PT. IL-8, G-CSF and Gro-β are well known mobilizers of the different types of SPCs (reviewed in (Richter et al., 2017, Tilling et al., 2009, Rennert et al., 2012). It also has been shown that MCP-1 is able to recruit MSCs in gliomas (Xu et al., 2010) and is linked to MSC homing in a mouse model of cardiac ischemia (Belema-Bedada et al., 2008). Correlations between changes in the number of SPC between 0-3 h and 48 h and individual cytokine though were not identified, implying that a combination of

cytokines might underlay this mobilization, or indeed there might be no connection between the cytokines tested and the change of the number of SPCs in blood. At the later time points tested (48 h -120 h post PT), the concentrations of VEGF-A and MDC were elevated. VEGF-A is linked to angiogenesis, vasodilation and vascular permeability (Shibuya, 2011). It also has mobilizing effects on EPCs (Pitchford et al., 2009) and HSPCs (Tashiro et al., 2013). MDC is linked to Th_2 lymphocyte, monocyte, monocyte-derived dendritic cell, and natural killer cell recruitment (Godiska et al., 1997, Mantovani et al., 2000). Thus, further research on the role of MDC on mobilization of SPCs could be of interest. The elevated concentration of G-CSF, IL-6, IL-8 and VEGF-A at 48 h negatively correlated with a change in the number of HSCs between 48 h and 120 h post injury, while the concentration of MCP-1, IL-8, Gro-α and G-CSF at 0-3 h time point correlated positively with the number of CMPs at 48 h post PT. It is thus a possibility that changes in cytokines in the early phase of trauma might indirectly affect mobilization of SPCs later in trauma.

The synchrony of mobilization patterns between SPC populations in individual PT patients prompted me to introduce a novel parameter, the additive number of stem and progenitor cells (ANSP-Score). Looking at the difference of the ANSP-Score in the 48 h-120 h interval post PT, two distinct types of patients emerged. One group with a strong increase in the ANSP-Score between 48 h and 120 h (HiLiNuts) and another group where barley/no changes between the ANSP-Score at those time points (LoLiNuts). While trauma-impact parameters like the ISS were almost similar for the two groups, out of the three patients of the LoLiNut group, 2 patients had the longest stay in the ICU, the highest remaining CK values at 48 h/120 h and presented with pneumonia or wound healing defects. We thus speculate that change in the ANSP-Score between 48 h to 120 h post PT could be novel parameter for trauma outcome and thus a prognostic parameter. The number of patients included in the study though remains a strong limiting factor for drawing definitive conclusions. The interesting concept of HiLiNuts and LoLiNuts needs therefore to be further evaluated with a higher number of patients to validate the role and predictive value of the ANSP-Score.

The two patient groups also presented a distinct cytokine/chemokine profile. In the LoLiNut group, a strong initial elevation of pro-inflammatory cytokines/chemokines (IL-6, IL-8 and G-SCF) was observed, suggesting again that elevated levels of

cytokines linked to inflammation early on after trauma might negatively influence SPC mobilization to PB at 120 h post PT. MDC was the only cytokine that correlated positively with the ANSP-Score at 120 h in the HiLiNut group, suggesting that MDC might indeed positively affect that increase in SPCs in blood at this time point post PT.

4.2 Distinct dynamics of SPCs and leukocytes in the TXT mouse model

I determined the number of SPCs in blood and other tissues in mice after TXT to obtain information on the synchronous dynamics of these cell populations and to identify time points for interventions that will increase the number of circulating SPCs to most likely positively affect trauma outcome. I simultaneously examined cell dynamics of three different MSC populations, EPCs, HSCs, early and late hematopoietic progenitors, neutrophils, monocytes and lymphocytes in PB, BM and the lung in a mouse model of TXT. The recruitment of BM derived SPCs to the sites of tissue damage has been already previously associated with tissue repair (for example Mao Sun-Zhong et al., 2015). While the TXT mouse model is a highly standardized and well established animal model system, the data among identical repeats of experiments still showed a relatively high level of variation (Fig. 17), which renders testing for the significance of differences in the number of SPCs difficult. In addition, the number of MSCs in PB in mice are in general quite low, even after trauma, which results itself in a higher level of variance among individual experiments. The very standardized blast wave to induce the trauma still resulted in slightly different injury patterns in the lung of individual mice, as for example variations in hematoma formation or a lack thereof was observed within the lung tissue of identically treated animals. Thus, it remains a possibility that small differences in the nature of the lung injury might have a strong influence on SPC mobilization. Testing this hypothesis would require more in-depth analyses on the correlation of the type of lung damage and SPC mobilization in a very large number of animals.

Within the TXT model, I made the following main and thus likely critical observations: i) The number of HSPCs increases in BM by 2 h post injury. Yet, HSC division 2 h after initiation of stimulation is highly unlikely because HSCs are generally in a very quiescent state (Yamada et al., 2013). HSCs might thus simply relocate. Another,

less likely possibility might be that HSCs undergo changes in the expression of surface markers. For example, INF-γ was shown to upregulate Sca-1 expression (Snapper et al., 1991). HSPCs can be directly stimulated by an infection itself (Singh et al., 2008, Takizawa et al., 2011). This finding suggests that HSPCs participate directly in the primary immune response after an infection. They might thus also be activated to mobilize by the early inflammation resulting from the trauma. These results differ from previous findings in which BM-specific fluctuations in HSPC numbers at later time points after trauma were observed (Leitão et al., 2019).

ii) Similar to my analyses in human polytrauma (Vogel et al., 2019a), in PB of TXT animals there was a trend towards an inverse bell-shaped pattern for HSPCs and EPCs after TXT, with a modest increase of their number 2 h and a nadir at 6 h post trauma, followed by an increase at the later time points. This inverse bell-shaped pattern though was much more pronounced in the human patients. While the mouse model thus replicates patterns of the distribution of SPCs seen in humans, the amplitude of the changes is muted compared to human PT. It would be interesting to analyze whether a more severe murine PT model, in which animals can still be followed up to the initiation of the regeneration phase, might show SPCs dynamics in mice even more similar to human PT.

iii) In lung tissue, there was a significant increase in the number of HSCs 48 h after TXT induction, suggesting a role for HSCs in the proliferation/remodeling phase of trauma regeneration. HSPCs can support regeneration by providing effector cells. HSPCs further release paracrine factors that stimulate tissue repair, are able to modulate the immune response and influence vascularization (Allakhverdi and Delespesse, 2012, Si et al., 2010, Rafii et al., 2016).

iv) The numbers of neutrophils, monocytes and lymphocytes were increased 2 h after TXT in PB and lung tissue. This is a clear indication of leukocytosis and thus inflammation. Interestingly though, 6 h post injury leukocytosis was already resolved, with the exception of an additional increase in the number of neutrophils at 48 h post trauma in lung tissue. In recent years, neutrophils have been characterized as a more heterogeneous cell population (Silvestre-Roig et al., 2016), containing also anti-inflammatory cell types. I speculate that at this later time point post trauma (48 h) neutrophils are likely of anti-inflammatory nature.

In conclusion, TXT and also PT induced a strong increase in the number of leukocytes in PB and lung tissue (up to 6 h, PT data is only up to 2 h). The changes in the number of SPCs in PB upon trauma followed in part that of PT patients, although with comparatively muted changes. Differences in the dynamics of SPC within BM and lung were negligible, with the exception of an increase in the number of HSCs in the lung 48 h post trauma.

4.3 Manipulation of SPC dynamics in the early phase of TXT in mice does not improve regeneration parameters.

It has been previously shown that human MSCs improved regeneration in a rat model of TXT when injected right after TXT induction. In this model, inflammatory cytokines and the morphologic injury score were decreased compared to sham treated animals 24 h post TXT (Amann et al., 2018). To the best of my knowledge there are no studies available that describe the influence of an increased number of HSPCs or EPCs on lung regeneration in TXT. I hypothesized that the application of the short-time mobilizer AMD3100 will increase the number of distinct types of endogenous SPCs in PB to then increase their availability for tissue regeneration.
Defining the synchronous dynamics of different SPC populations and leukocytes as discussed above informed the choice of time points post TXT for the application of AMD3100 to increase SPCs. In a first trial, I applied the drug directly after TXT so that a maximal mobilization is reached after 1-2 h. The 2 h post TXT time point was the time point where I found a strong increase of at least leukocytes in PB which indicated a peak in inflammation. Secondly, I chose the time point at the nadir of the number of SPCs in blood (6 h post trauma) to increase the number of SPCs in circulation when they are quite low after TXT.
2 h after TXT induction and AMD3100 treatment the number of HSPCs was highly increased in PB compared to control TXT animals. However, in lung no change in the number of HSPCs was detected. It is a possibility that SDF-1α/CXCR4 axis is still partly blocked by AMD3100 at 2 h post injection (plasma half live of 2-3 h (Jujo et al., 2010)), thus the cells do not migrate into the damaged tissue because chemotaxis via SDF-1a is still inhibited. Liu et al. (2017) for example illustrated that the migration and differentiation of endogenous neuronal stem cells was inhibited by AMD3100 treatment in spinal cord injury. When applied at both 0 h and at 6 h, AMD3100 did also not result in a change in the number of HSPCs in the lung, which

implies additional mechanisms beyond receptor blockage that might mitigate migration of freshly mobilized HSPCs into the injured lung tissue.

All three types of MSC populations were not enriched in PB after treatment with AMD3100. Considering the important role of the SDF-1/CXCR4 axis in the regulation of MSC migration, I expected an increase of their number in PB upon mobilization in TXT. Toupadakis et al. (2013) for example induced a higher number of MSCs in PB after AMD3100 treatment in a bone fracture model. Liu et al. (2018) in contrast could only increase the number of MSCs in PB by pre-treating animals with the hypoxia-mimicking agent cobalt chloride but not by AMD3100 alone. The number of EPCs were also slightly increased in PB upon AMD3100 treatment, which is in accordance to the literature (Frank et al., 2012a). Surprisingly though, I found a reduction of the number of EPCs in lung. Yin et al. (2007) showed that while AMD3100 stimulates mobilization it also reduces EPC functionality in part by inducing apoptosis, which might contribute to the reduction of EPCs in the lung upon AMD3100 administration.

A 4-fold increase of the number of monocytes and neutrophils in lung tissue after AMD3100 treatment under physiological conditions was already previously described (Liu et al., 2015). In these experiments, monocytes and neutrophils mostly from BM were redistributed into secondary lymph organs, lung and blood after AMD3100 applications. I could also observe an approximately 4-fold increase in the number of monocytes and neutrophils in the lung upon AMD3100 treatment compared to control treated TXT mice, which is within a similar range. I expected that the increase in the number of leukocytes in the lung might further increase the inflammatory response in the damaged lung. Interestingly though, in all three treatment groups (0 h AMD3100, 6 h AMD3100 and 0 h / 6 h AMD3100) I did not detect any change in the concentration of a large set of inflammatory cytokines. In addition, biomarkers of regeneration like apoptosis, proliferation and fibroblast/myofibroblast ratio were not affected by the administration of AMD3100 and thus by mobilization of SCPs and leukocytes. The application of AMD3100 at early time points after TXT (0 h - 6 h post trauma) did thus not improve parameters of regeneration in mice. Additional insight on the influence mobilization has on lung regeneration could be gained by sequential examinations of, for example, lung function. Hereby starting points and progression points can be generated within the

same mouse providing insight into dynamics in a single mouse. Metabolic cages which can non-invasively generate information on lung function might be a possibility to obtain this information. It might be also of interest to analyze whether an application of AMD3100 at later time points in the healing progress can improve outcome. I observed an upregulation of HSCs in lung tissue 48 h after TXT application so SPCs might be more involved in the regeneration and remodeling phase of tissue healing.

5. Summary

Worldwide about 10 % of deaths are caused by physiological trauma. We hypothesize that endogenous stem and progenitor cells (SPCs) are mobilized to PB and the site of injury at distinct time-points post trauma to likely affect trauma outcome. Providing elevated levels of endogenous SPCs at distinct time point post trauma via mobilization might improve trauma outcome.

Thus, I analyzed the number of hematopoietic stem cells (HSCs), common myeloid progenitors, granulocyte-macrophage progenitors and mesenchymal stromal cells (MSCs) in PB 0-3 h, 24 h, 48 h and 120 h after polytrauma (PT). The number of SPCs in blood followed a synchronous, inverse bell-shaped distribution. Interestingly, analysis of the change in the number of SPCs in PB between 48 h and 120 h identified two distinct patient groups: Group 1 was characterized by a strong increase in the number of SPCs and group 2 was characterized by an almost absent increase in the number of SPCs compared to their nadir at 24 h – 48 h post PT. The low increase in the number of SPCs was associated with higher levels of pro-inflammatory cytokines at the early phase of trauma. Furthermore, two out of three patients with the almost absent increase in the number of SPCs in blood had severe septic complications and the longest stay in ICU. The data provide a strong indication for further investigations on the role of stem cell mobilization in PT patients and its likely positive impact on trauma outcome.

To then unravel the impact of SPC mobilization on trauma outcome, I determined the number of distinct SPC populations in a time interval of 0.2 h - 168 h simultaneously in PB, BM and lung tissue after inducing a blunt thorax trauma (TXT) in mice. There was an increase in the number of leukocytes 2 h after TXT in PB and lung tissue, which is a clear indication of inflammation. A change in the number of SPCs at all time points analyzed and for all tissues tested though was relatively rare, indicating that SPCs might play a minor role for the inflammatory phase of the healing process. I found a significantly increased number of HSCs 48 h after TXT induction in the lung which might imply a role for HSCs in the remodeling and thus regenerative phase of trauma regeneration.

Application of AMD3100, a short-term mobilizer of stem and mature cells at 0 h and 6 h after TXT further increased the number of hematopoietic SPCs in PB 2 h after treatment compared to control treated TXT animals. However, biomarkers of outcome like inflammatory cytokines were not improved in AMD3100 treated

animals. The data support that treatment with AMD3100 in the early phase after TXT does not affect trauma outcome or lung regeneration, while the effect of mobilization of SPCs at later time-points (after 6 h) post TXT will need to be further investigated.

5.1 Graphical summary

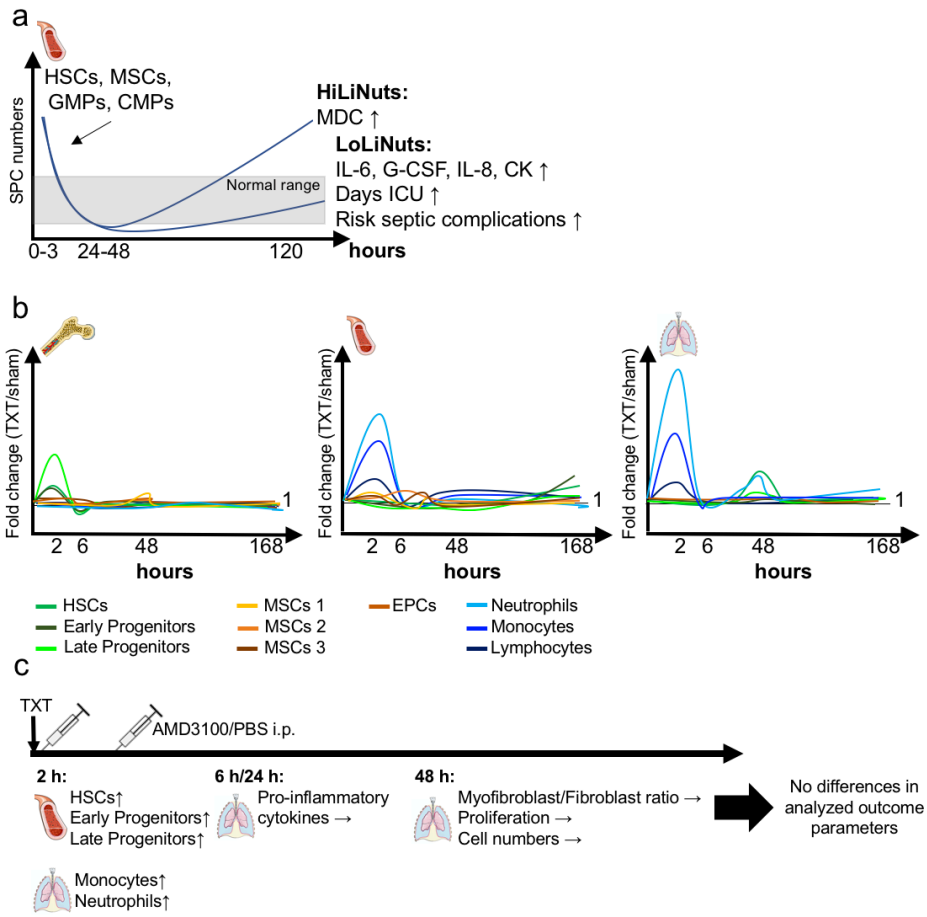

Figure 25: Graphical summary: a Distinct dynamics of SPCs in PB of polytraumatized patients. *Analyzed SPC numbers in PB of nine polytraumatized patients revealed an inverse bell-shaped pattern, recurrent and reproducible between the different patients and populations. Between 48 h and 120 h two distinct patterns can be seen. High late increase in numbers upon trauma (HiLiNuts) group had increased levels of the cytokine MDC in serum 120 post PT. Low late increase in numbers upon trauma (LoLiNuts) group had upregulated levels of pro-inflammatory cytokines in the early phase after trauma, risk for septic complications and days in ICU might be increased.* ***b Distinct dynamics of SPCs and leukocytes in a mouse model of TXT.*** *Fold change, calculated by dividing the absolute number of cells measured in TXT animals through the absolute number of cells measured in sham animals, is given for BM, PB and the injured lung tissue. Distinct cell populations are marked by specific colors, time period ranges from 0.2 h to 168 h.* ***c Manipulation of SPC dynamics in the early phase of TXT does not improve parameters linked to regeneration.*** *Directly or/and 6 h after TXT induction AMD3100 or PBS was applied. SPC numbers were upregulated in PB and inflammatory cells were elevated in lung tissue, this did not alter pro-inflammatory cytokine levels in lung tissue, regeneration parameters like proliferation or myofibroblast/fibroblast ratio were also unaffected by the treatment.*

6. References

1. Akamatsu T, Arai Y, Kosugi I, Kawasaki H, Meguro S, Sakao M, Shibata K, Suda T, Chida K, Iwashita T: Direct isolation of myofibroblasts and fibroblasts from bleomycin-injured lungs reveals their functional similarities and differences. Fibrogenesis & Tissue Repair 6: 15 (2013)

2. Allakhverdi Z, Delespesse G: Hematopoietic progenitor cells are innate Th2 cytokine-producing cells. Allergy 67: 4–9 (2012)

3. Amann EM, Rojewski MT, Rodi S, Fürst D, Fiedler J, Palmer A, Braumüller S, Huber-Lang M, Schrezenmeier H, Brenner RE: Systemic recovery and therapeutic effects of transplanted allogenic and xenogenic mesenchymal stromal cells in a rat blunt chest trauma model. Cytotherapy 20: 218–231 (2018)

4. Amboss: Penetrating trauma. https://www.amboss.com/us/knowledge/Penetrating_trauma (no date) (opened 12/30/2019)

5. Asahara T, Murohara T, Sullivan A, Silver M, van der Zee R, Li T, Witzenbichler B, Schatteman G, Isner JM: Isolation of putative progenitor endothelial cells for angiogenesis. Science 275: 964–967 (1997)

6. Association for the Advancement of Automotive Medicine: AIS 2005/2008 Update Dictionary – Clarification Document (update 10/09/2019). https://www.aaam.org/wp-content/uploads/2019/10/ClarificationDocument.Oct_.10.2019.rev_.pdf (2019) (opened 07/25/2020)

7. Badylak SF, Valentin JE, Ravindra AK, McCabe GP, Stewart-Akers AM: Macrophage Phenotype as a Determinant of Biologic Scaffold Remodeling. Tissue Engineering Part A 14: 1835–1842 (2008)

8. Baldridge MT, King KY, Boles NC, Weksberg DC, Goodell MA: Quiescent hematopoietic stem cells are activated by IFNγ in response to chronic infection. Nature 465: 793–797 (2010)

9. Belema-Bedada F, Uchida S, Martire A, Kostin S, Braun T: Efficient homing of multipotent adult mesenchymal stem cells depends on FROUNT-mediated clustering of CCR2. Cell Stem Cell 2: 566–575 (2008)

10. Berglund AK, Fortier LA, Antczak DF, Schnabel LV: Immunoprivileged no more: measuring the immunogenicity of allogeneic adult mesenchymal stem cells. Stem Cell Res Ther 8: (2017)

11. Bhattacharya J, Matthay MA: Regulation and Repair of the Alveolar-Capillary Barrier in Acute Lung Injury. Annu Rev Physiol 75: 593–615 (2013)

12. Bonnarens F, Einhorn TA: Production of a standard closed fracture in laboratory animal bone. J Orthop Res 2: 97–101 (1984)

13. Broxmeyer HE, Orschell CM, Clapp DW, Hangoc G, Cooper S, Plett PA, Liles WC, Li X, Graham-Evans B, Campbell TB, Calandra G, Bridger G, Dale DC, Srour EF: Rapid mobilization of murine and human hematopoietic stem and progenitor cells with AMD3100, a CXCR4 antagonist. J Exp Med 201: 1307–1318 (2005)

14. Bussolati B, Camussi G: Therapeutic use of human renal progenitor cells for kidney regeneration. Nat Rev Nephrol 11: 695–706 (2015)
15. Cencioni C, Capogrossi MC, Napolitano M: The SDF-1/CXCR4 axis in stem cell preconditioning. Cardiovasc Res 94: 400–407 (2012)

16. Ceradini DJ, Kulkarni AR, Callaghan MJ, Tepper OM, Bastidas N, Kleinman ME, Capla JM, Galiano RD, Levine JP, Gurtner GC: Progenitor cell trafficking is regulated by hypoxic gradients through HIF-1 induction of SDF-1. Nat Med 10: 858–864 (2004)

17. Chang R, Cardenas JC, Wade CE, Holcomb JB: Advances in the understanding of trauma-induced coagulopathy. Blood 128: 1043–1049 (2016)

18. Chen Q, Luo AA, Qiu H, Han B, Ko BH-K, Slutsky AS, Zhang H: Monocyte interaction accelerates HCl-induced lung epithelial remodeling. BMC Pulmonary Medicine 14: 135 (2014)

19. Choi H-Y, Yong C-S, Yoo BK: Plerixafor for stem cell mobilization in patients with non-Hodgkin's lymphoma and multiple myeloma. Ann Pharmacother 44: 117–126 (2010)

20. Crisan M, Yap S, Casteilla L, Chen C-W, Corselli M, Park TS, Andriolo G, Sun B, Zheng B, Zhang L, Norotte C, Teng P-N, Traas J, Schugar R, Deasy BM, Badylak S, Bűhring H-J, Giacobino J-P, Lazzari L, Huard J, Péault B: A Perivascular Origin for Mesenchymal Stem Cells in Multiple Human Organs. Cell Stem Cell 3: 301–313 (2008)

21. Dai S, Yuan F, Mu J, Li C, Chen N, Guo S, Kingery J, Prabhu SD, Bolli R, Rokosh G: Chronic AMD3100 Antagonism of SDF-1α-CXCR4 Exacerbates Cardiac Dysfunction and Remodeling after Myocardial Infarction. J Mol Cell Cardiol 49: 587–597 (2010)

22. Dai X, Tan Y, Cai S, Xiong X, Wang L, Ye Q, Yan X, Ma K, Cai L: The role of CXCR7 on the adhesion, proliferation and angiogenesis of endothelial progenitor cells. J Cell Mol Med 15: 1299–1309 (2011)

23. Del Papa N, Pignataro F: The Role of Endothelial Progenitors in the Repair of Vascular Damage in Systemic Sclerosis. Front Immunol 9: (2018)

24. Ding B-S, Nolan DJ, Guo P, Babazadeh AO, Cao Z, Rosenwaks Z, Crystal RG, Simons M, Sato TN, Worgall S, Shido K, Rabbany SY, Rafii S: Endothelial-Derived Angiocrine Signals Induce and Sustain Regenerative Lung Alveolarization. Cell 147: 539–553 (2011)

25. Dominici M, Blanc KL, Mueller I, Slaper-Cortenbach I, Marini F, Krause D, Deans R, Keating A, Prockop D, Horwitz E: Minimal criteria for defining multipotent mesenchymal stromal cells. The International Society for Cellular Therapy position statement. Cytotherapy 8: 315–317 (2006)

26. Fan Y, Ye J, Shen F, Zhu Y, Yeghiazarians Y, Zhu W, Chen Y, Lawton MT, Young WL, Yang G-Y: Interleukin-6 stimulates circulating blood-derived endothelial progenitor cell angiogenesis in vitro. J Cereb Blood Flow Metab 28: 90–98 (2008)

27. Flierl MA, Stahel PF, Beauchamp KM, Morgan SJ, Smith WR, Shohami E: Mouse closed head injury model induced by a weight-drop device. Nat Protoc 4: 1328–1337 (2009)

28. Frank RR, Jagan S, Paganessi LA, McNulty MA, Sumner DR, Fung HC, Gregory SA, Christopherson KW: Effective Mobilization of Mesenchymal Stem Cells in C57BL/6 Mice Utilizing Single Agent Plerixafor (AMD3100) or in Combination with Neupogen (G-CSF). Biology of Blood and Marrow Transplantation 18: S266 (2012b)

29. Frank RR, Jagan S, Paganessi LA, McNulty MA, Sumner DR, Fung HC, Gregory SA, Christopherson KW: Endothelial Progenitor Cell Mobilization in C57BL/6 Mice Following Treatment with Single Agent or Combination Neupogen (G-CSF), Plerixafor (AMD3100), and VEGF. Biology of Blood and Marrow Transplantation 18: S374 (2012a)

30. Friedrich EE, Sun LT, Natesan S, Zamora DO, Christy RJ, Washburn NR: Effects of hyaluronic acid conjugation on anti-TNF-α inhibition of inflammation in burns. Journal of Biomedical Materials Research Part A 102: 1527–1536 (2014)

31. Fu X, Liu G, Halim A, Ju Y, Luo Q, Song G: Mesenchymal Stem Cell Migration and Tissue Repair. Cells 8: (2019)

32. Garibaldi BT, D'Alessio FR, Mock JR, Files DC, Chau E, Eto Y, Drummond MB, Aggarwal NR, Sidhaye V, King LS: Regulatory T Cells Reduce Acute Lung Injury Fibroproliferation by Decreasing Fibrocyte Recruitment. Am J Respir Cell Mol Biol 48: 35–43 (2013)

33. Gehling UM, Willems M, Schlagner K, Benndorf RA, Dandri M, Petersen J, Sterneck M, Pollok J-M, Hossfeld DK, Rogiers X: Mobilization of hematopoietic progenitor cells in patients with liver cirrhosis. World J Gastroenterol 16: 217–224 (2010)

34. Gentile LF, Cuenca AG, Efron PA, Ang D, McKinley BA, Moldawer LL, Moore FA: Persistent inflammation and immunosuppression: A common syndrome and new horizon for surgical intensive care. J Trauma Acute Care Surg 72: 1491–1501 (2012)

35. Gentile LF, Nacionales DC, Cuenca AG, Armbruster M, Ungaro RF, Abouhamze AS, Lopez C, Baker HV, Moore FA, Ang DN, Efron PA: IDENTIFICATION AND DESCRIPTION OF A NOVEL MURINE MODEL FOR POLYTRAUMA AND SHOCK. Crit Care Med 41: 1075–1085 (2013)

36. Ghaffari-Nazari H: The known molecules involved in MSC homing and migration. J Stem Cell Res Med 3: (2018)

37. Gill SE, Yamashita CM, Veldhuizen RAW: Lung remodeling associated with recovery from acute lung injury. Cell Tissue Res 367: 495–509 (2017)

38. Glasser SW, Hagood JS, Wong S, Taype CA, Madala SK, Hardie WD: Mechanisms of Lung Fibrosis Resolution. The American Journal of Pathology 186: 1066–1077 (2016)

39. Godiska R, Chantry D, Raport CJ, Sozzani S, Allavena P, Leviten D, Mantovani A, Gray PW: Human macrophage-derived chemokine (MDC), a novel chemoattractant for monocytes, monocyte-derived dendritic cells, and natural killer cells. J Exp Med 185: 1595–1604 (1997)

40. Goodchild TT, Robinson KA, Pang W, Tondato F, Cui J, Arrington J, Godwin L, Ungs M, Carlesso N, Weich N, Poznansky MC, Chronos NAF: Bone Marrow-Derived B Cells Preserve Ventricular Function After Acute Myocardial Infarction. J Am Coll Cardiol Intv 2: 1005–1016 (2009)

41. Grommes J, Soehnlein O: Contribution of Neutrophils to Acute Lung Injury. Mol Med 17: 293–307 (2011)

42. Guidi N, Sacma M, Ständker L, Soller K, Marka G, Eiwen K, Weiss JM, Kirchhoff F, Weil T, Cancelas JA, Florian MC, Geiger H: Osteopontin attenuates aging-associated phenotypes of hematopoietic stem cells. EMBO J 36: 840–853 (2017)

43. Guillamat-Prats R, Gay-Jordi G, Xaubet A, Peinado VI, Serrano-Mollar A: Alveolar type II cell transplantation restores pulmonary surfactant protein levels in lung fibrosis. J Heart Lung Transplant 33: 758–765 (2014)

44. Gussoni E, Soneoka Y, Strickland CD, Buzney EA, Khan MK, Flint AF, Kunkel LM, Mulligan RC: Dystrophin expression in the mdx mouse restored by stem cell transplantation. Nature 401: 390–394 (1999)

45. Haas S, Hansson J, Klimmeck D, Loeffler D, Velten L, Uckelmann H, Wurzer S, Prendergast ÁM, Schnell A, Hexel K, Santarella-Mellwig R, Blaszkiewicz S, Kuck A, Geiger H, Milsom MD, Steinmetz LM, Schroeder T, Trumpp A, Krijgsveld J, Essers MAG: Inflammation-Induced Emergency

Megakaryopoiesis Driven by Hematopoietic Stem Cell-like Megakaryocyte Progenitors. Cell Stem Cell 17: 422–434 (2015)

46. Hafner S, Wagner K, Wepler M, Matallo J, Gröger M, McCook O, Scheuerle A, Huber-Lang M, Frick M, Weber S, Stahl B, Jung B, Calzia E, Georgieff M, Möller P, Dietl P, Radermacher P, Wagner F: Physiological and immune-biological characterization of a long-term murine model of blunt chest trauma. Shock 43: 140–147 (2015)

47. Han Y, Yan L, Han G, Zhou X, Hong L, Yin Z, Zhang X, Wang S, Wang J, Sun A, Liu Z, Xie H, Wu K, Ding J, Fan D: Controlled trials in hepatitis B virus-related decompensate liver cirrhosis: peripheral blood monocyte transplant versus granulocyte-colony-stimulating factor mobilization therapy. Cytotherapy 10: 390–396 (2008)

48. Havran WL, Jameson JM: Epidermal T Cells and Wound Healing. The Journal of Immunology 184: 5423–5428 (2010)

49. Hayes M, Curley GF, Masterson C, Devaney J, O'Toole D, Laffey JG: Mesenchymal stromal cells are more effective than the MSC secretome in diminishing injury and enhancing recovery following ventilator-induced lung injury. Intensive Care Medicine Experimental 3: 29 (2015)

50. Heissig B, Hattori K, Dias S, Friedrich M, Ferris B, Hackett NR, Crystal RG, Besmer P, Lyden D, Moore MAS, Werb Z, Rafii S: Recruitment of Stem and Progenitor Cells from the Bone Marrow Niche Requires MMP-9 Mediated Release of Kit-Ligand. Cell 109: 625–637 (2002)

51. Hendrix CW, Flexner C, MacFarland RT, Giandomenico C, Fuchs EJ, Redpath E, Bridger G, Henson GW: Pharmacokinetics and Safety of AMD-3100, a Novel Antagonist of the CXCR-4 Chemokine Receptor, in Human Volunteers. Antimicrob Agents Chemother 44: 1667–1673 (2000)

52. Herbrig K, Haensel S, Oelschlaegel U, Pistrosch F, Foerster S, Passauer J: Endothelial dysfunction in patients with rheumatoid arthritis is associated with a reduced number and impaired function of endothelial progenitor cells. Ann Rheum Dis 65: 157–163 (2006)

53. Hermann A, Gastl R, Liebau S, Popa MO, Fiedler J, Boehm BO, Maisel M, Lerche H, Schwarz J, Brenner R, Storch A: Efficient generation of neural stem cell-like cells from adult human bone marrow stromal cells. Journal of Cell Science 117: 4411–4422 (2004)

54. Herrmann M, Verrier S, Alini M: Strategies to Stimulate Mobilization and Homing of Endogenous Stem and Progenitor Cells for Bone Tissue Repair. Front Bioeng Biotechnol 3: (2015)

55. Hick, C. and Hick, A: Intensivkurs Physiologie (6. Auflage). Elsevier Urban und Fischer, München, pp. 24-28 (2009)

56. Hill WD, Hess DC, Martin-Studdard A, Carothers JJ, Zheng J, Hale D, Maeda M, Fagan SC, Carroll JE, Conway SJ: SDF-1 (CXCL12) is upregulated in the ischemic penumbra following stroke: association with bone marrow cell homing to injury. J Neuropathol Exp Neurol 63: 84–96 (2004)

57. Höfer C. and Lefering R.: TraumaRegister DGU - Jahresbericht 2019 (2. ergänzte Auflage). http://www.traumaregister-dgu.de/fileadmin/user_upload/traumaregister-dgu.de/docs/Downloads/Jahresbericht_2019.pdf (2019) (opened 12/28/2019)

58. Hoogduijn MJ, Lombardo E: Mesenchymal Stromal Cells Anno 2019: Dawn of the Therapeutic Era? Concise Review. STEM CELLS Translational Medicine 8: 1126–1134 (2019)

59. Huber-Lang M, Lambris JD, Ward PA: Innate immune responses to trauma. Nat Immunol 19: 327–341 (2018)

60. Hummler E, Barker P, Gatzy J, Beermann F, Verdumo C, Schmidt A, Boucher R, Rossier BC: Early death due to defective neonatal lung liquid clearance in α ENaC -deficient mice. Nat Genet 12: 325–328 (1996)

61. Imberti B, Morigi M, Benigni A: Potential of mesenchymal stem cells in the repair of tubular injury. Kidney Int Suppl (2011) 1: 90–93 (2011)

62. Ito M, Liu Y, Yang Z, Nguyen J, Liang F, Morris RJ, Cotsarelis G: Stem cells in the hair follicle bulge contribute to wound repair but not to homeostasis of the epidermis. Nat Med 11: 1351–1354 (2005)

63. Jin W, Liang X, Brooks A, Futrega K, Liu X, Doran MR, Simpson MJ, Roberts MS, Wang H: Modelling of the SDF-1/CXCR4 regulated in vivo homing of therapeutic mesenchymal stem/stromal cells in mice. PeerJ 6: (2018)

64. Jujo K, Hamada H, Iwakura A, Thorne T, Sekiguchi H, Clarke T, Ito A, Misener S, Tanaka T, Klyachko E, Kobayashi K, Tongers J, Roncalli J, Tsurumi Y, Hagiwara N, Losordo DW: CXCR4 blockade augments bone marrow progenitor cell recruitment to the neovasculature and reduces mortality after myocardial infarction. Proc Natl Acad Sci USA 107: 11008–11013 (2010)

65. Julier Z, Park AJ, Briquez PS, Martino MM: Promoting tissue regeneration by modulating the immune system. Acta Biomaterialia 53: 13–28 (2017)

66. Kamei N, Atesok K, Ochi M: The Use of Endothelial Progenitor Cells for the Regeneration of Musculoskeletal and Neural Tissues. Stem Cells Int 2017: (2017)

67. Kamei N, Kwon S-M, Alev C, Nakanishi K, Yamada K, Masuda H, Ishikawa M, Kawamoto A, Ochi M, Asahara T: Ex-vivo expanded human blood-derived CD133+ cells promote repair of injured spinal cord. J Neurol Sci 328: 41–50 (2013)

68. Kapanci Y, Weibel ER, Kaplan HP, Robinson FR: Pathogenesis and reversibility of the pulmonary lesions of oxygen toxicity in monkeys. II. Ultrastructural and morphometric studies. Lab Invest 20: 101–118 (1969)

69. Kato N, Hasegawa U, Morimoto N, Saita Y, Nakashima K, Ezura Y, Kurosawa H, Akiyoshi K, Noda M: Nanogel-based delivery system enhances PGE2 effects on bone formation. Journal of Cellular Biochemistry 101: 1063–1070 (2007)

70. Kawada H, Takizawa S, Takanashi T, Morita Y, Fujita J, Fukuda K, Takagi S, Okano H, Ando K, Hotta T: Administration of hematopoietic cytokines in the subacute phase after cerebral infarction is effective for functional recovery facilitating proliferation of intrinsic neural stem/progenitor cells and transition of bone marrow-derived neuronal cells. Circulation 113: 701–710 (2006)

71. Kawakami Y, Ii M, Matsumoto T, Kuroda R, Kuroda T, Kwon S-M, Kawamoto A, Akimaru H, Mifune Y, Shoji T, Fukui T, Kurosaka M, Asahara T: SDF-1/CXCR4 axis in Tie2-lineage cells including endothelial progenitor cells contributes to bone fracture healing. J Bone Miner Res 30: 95–105 (2015)

72. Kim C-K, Yang VW, Bialkowska AB: The Role of Intestinal Stem Cells in Epithelial Regeneration Following Radiation-Induced Gut Injury. Curr Stem Cell Rep 3: 320–332 (2017)

73. Kim J, Kim W, Le HT, Moon UJ, Tran VG, Kim HJ, Jung S, Nguyen Q-T, Kim B-S, Jun J-B, Cho HR, Kwon B: IL-33-induced hematopoietic stem and progenitor cell mobilization depends upon CCR2. J Immunol 193, 3792–3802 (2014)

74. Kim M-H, Granick JL, Kwok C, Walker NJ, Borjesson DL, Curry F-RE, Miller LS, Simon SI: Neutrophil survival and c-kit+-progenitor proliferation in Staphylococcus aureus–infected skin wounds promote resolution. Blood 117: 3343–3352 (2011)

75. King KY, Goodell MA: Inflammatory modulation of hematopoietic stem cells: viewing the hematopoietic stem cell as a foundation for the immune response. Nat Rev Immunol 11: 685–692 (2011)

76. Kitaori T, Ito H, Schwarz EM, Tsutsumi R, Yoshitomi H, Oishi S, Nakano M, Fujii N, Nagasawa T, Nakamura T: Stromal cell-derived factor 1/CXCR4 signaling is critical for the recruitment of mesenchymal stem cells to the fracture site during skeletal repair in a mouse model. Arthritis Rheum 60: 813–823 (2009)

77. Klimczak A, Kozlowska U: Mesenchymal Stromal Cells and Tissue-Specific Progenitor Cells: Their Role in Tissue Homeostasis. Stem Cells Int 2016: 4285215 (2016)

78. Knöferl MW, Liener UC, Seitz DH, Perl M, Brückner UB, Kinzl L, Gebhard F: Cardiopulmonary, histological, and inflammatory alterations after lung contusion in a novel mouse model of blunt chest trauma. Shock 19: 519–525 (2003)

79. Könnecke I, Serra A, El Khassawna T, Schlundt C, Schell H, Hauser A, Ellinghaus A, Volk H-D, Radbruch A, Duda GN, Schmidt-Bleek K: T and B cells participate in bone repair by infiltrating the fracture callus in a two-wave fashion. Bone 64: 155–165 (2014)

80. Kumar P, Rajasekaran K, Palmer JM, Thakar MS, Malarkannan S: IL-22: An Evolutionary Missing-Link Authenticating the Role of the Immune System in Tissue Regeneration. J Cancer 4: 57–65 (2012)

81. Kumar V, Abbas AK, Aster JC, Robbins SL: Inflammation and repair. Robbins Basic Pathology. Saunders Elsevier, Philadelphia, London, pp. 29–74 (2012)

82. Kyriakou C, Rabin N, Pizzey A, Nathwani A, Yong K: Factors that influence short-term homing of human bone marrow-derived mesenchymal stem cells in a xenogeneic animal model. Haematologica 93: 1457–1465 (2008)

83. Lagasse E, Connors H, Al-Dhalimy M, Reitsma M, Dohse M, Osborne L, Wang X, Finegold M, Weissman IL, Grompe M: Purified hematopoietic stem cells can differentiate into hepatocytes in vivo. Nat Med 6: 1229–1234 (2000)

84. Lapidot T, Kollet O: The essential roles of the chemokine SDF-1 and its receptor CXCR4 in human stem cell homing and repopulation of transplanted immune-deficient NOD/SCID and NOD/SCID/B2m null mice. Leukemia 16: 1992–2003 (2002)

85. Lee HM, Wysoczynski M, Liu R, Shin D-M, Kucia M, Botto M, Ratajczak J, Ratajczak MZ: Mobilization studies in complement-deficient mice reveal that optimal AMD3100 mobilization of hematopoietic stem cells depends on complement cascade activation by AMD3100-stimulated granulocytes. Leukemia 24: 573–582 (2010)

86. Leitão L, Alves CJ, Alencastre IS, Sousa DM, Neto E, Conceição F, Leitão C, Aguiar P, Almeida-Porada G, Lamghari M: Bone marrow cell response after injury and during early stage of regeneration is independent of the tissue-of-injury in 2 injury models. FASEB J 33: 857–872 (2019)

87. Leliefeld PHC, Koenderman L, Pillay J: How Neutrophils Shape Adaptive Immune Responses. Front Immunol 6: (2015)

88. Li F, Zhang K, Liu H, Yang T, Xiao D-J, Wang Y-S: The neuroprotective effect of mesenchymal stem cells is mediated through inhibition of apoptosis in hypoxic ischemic injury. World J Pediatr 16: 193–200 (2020)

89. Li M, Luan F, Zhao Y, Hao H, Liu J, Dong L, Fu X, Han W: Mesenchymal stem cell-conditioned medium accelerates wound healing with fewer scars. International Wound Journal 14: 64–73 (2017)

90. Li R, Rezk A, Healy LM, Muirhead G, Prat A, Gommerman JL, Bar-Or A, Team MCB cells in M: Cytokine-Defined B Cell Responses as Therapeutic Targets in Multiple Sclerosis. Front Immunol 6: (2016)

91. Lin W, Xu L, Zwingenberger S, Gibon E, Goodman SB, Li G: Mesenchymal stem cells homing to improve bone healing. Journal of Orthopaedic Translation 9: 19–27 (2017)

92. Lin X, Barravecchia M, Kothari P, Young JL, Dean DA: β1-Na + ,K + -ATPase gene therapy upregulates tight junctions to rescue lipopolysaccharide-induced acute lung injury. Gene Ther 23: 489–499 (2016)

93. Liu G, Ma H, Qiu L, Li L, Cao Y, Ma J, Zhao Y: Phenotypic and functional switch of macrophages induced by regulatory CD4+CD25+ T cells in mice. Immunology & Cell Biology 89: 130–142 (2011)

94. Liu H, Xue W, Ge G, Luo X, Li Y, Xiang H, Ding X, Tian P, Tian X: Hypoxic preconditioning advances CXCR4 and CXCR7 expression by activating HIF-1α in MSCs. Biochemical and Biophysical Research Communications 401: 509–515 (2010)

95. Liu J-M, Zhao K, Du L-X, Zhou Y, Long X-H, Chen X-Y, Liu Z-L: AMD3100 inhibits the migration and differentiation of neural stem cells after spinal cord injury. Sci Rep 7: 1–9 (2017)

96. Liu L, Yu Q, Fu S, Wang B, Hu K, Wang L, Hu Y, Xu Y, Yu X, Huang H: CXCR4 Antagonist AMD3100 Promotes Mesenchymal Stem Cell Mobilization in Rats Preconditioned with the Hypoxia-Mimicking Agent Cobalt Chloride. Stem Cells Dev 27: 466–478 (2018)

97. Liu Q, Li Z, Gao J-L, Wan W, Ganesan S, McDermott DH, Murphy PM: CXCR4 antagonist AMD3100 redistributes leukocytes from primary immune organs to secondary immune organs, lung, and blood in mice. European Journal of Immunology 45: 1855–1867 (2015)

98. Liu X, Zhou C, Li Y, Ji Y, Xu G, Wang X, Yan J: SDF-1 promotes endochondral bone repair during fracture healing at the traumatic brain injury condition. PLoS ONE 8: e54077 (2013)

99. Lukomska B, Stanaszek L, Zuba-Surma E, Legosz P, Sarzynska S, Drela K: Challenges and Controversies in Human Mesenchymal Stem Cell Therapy. Stem Cells Int 2019: 9628536 (2019)

100. Luo Y, Zhao X, Zhou X, Ji W, Zhang L, Luo T, Liu H, Huang T, Jiang T, Li Y: Short-term intermittent administration of CXCR4 antagonist AMD3100

facilitates myocardial repair in experimental myocardial infarction. Acta Biochim Biophys Sin (Shanghai) 45: 561–569 (2013)

101. Mansilla E, Marín GH, Drago H, Sturla F, Salas E, Gardiner C, Bossi S, Lamonega R, Guzmán A, Nuñez A, Gil MA, Piccinelli G, Ibar R, Soratti C: Bloodstream Cells Phenotypically Identical to Human Mesenchymal Bone Marrow Stem Cells Circulate in Large Amounts Under the Influence of Acute Large Skin Damage: New Evidence for Their Use in Regenerative Medicine. Transplantation Proceedings 38: 967–969 (2006)

102. Mantovani A, Gray PA, Van Damme J, Sozzani S: Macrophage-derived chemokine (MDC). J Leukoc Biol 68: 400–404 (2000)

103. Mao Sun-Zhong, Ye Xiaobing, Liu Gang, Song Dongmei, Liu Shu Fang: Resident Endothelial Cells and Endothelial Progenitor Cells Restore Endothelial Barrier Function After Inflammatory Lung Injury. Arteriosclerosis, Thrombosis, and Vascular Biology 35: 1635–1644 (2015)

104. Marchesi C, Belicchi M, Meregalli M, Farini A, Cattaneo A, Parolini D, Gavina M, Porretti L, D'Angelo MG, Bresolin N, Cossu G, Torrente Y: Correlation of circulating CD133+ progenitor subclasses with a mild phenotype in Duchenne muscular dystrophy patients. PLoS ONE 3: e2218 (2008)

105. Martin T, Möglich A, Felix I, Förtsch C, Rittlinger A, Palmer A, Denk S, Schneider J, Notbohm L, Vogel M, Geiger H, Paschke S, Huber-Lang M, Barth H: Rho-inhibiting C2IN-C3 fusion toxin inhibits chemotactic recruitment of human monocytes ex vivo and in mice in vivo. Arch Toxicol 92: 323–336 (2018)

106. Massa M, Rosti V, Ferrario M, Campanelli R, Ramajoli I, Rosso R, De Ferrari GM, Ferlini M, Goffredo L, Bertoletti A, Klersy C, Pecci A, Moratti R, Tavazzi L: Increased circulating hematopoietic and endothelial progenitor cells in the early phase of acute myocardial infarction. Blood 105: 199–206 (2005)

107. Massberg S, Konrad I, Schürzinger K, Lorenz M, Schneider S, Zohlnhoefer D, Hoppe K, Schiemann M, Kennerknecht E, Sauer S, Schulz C, Kerstan S, Rudelius M, Seidl S, Sorge F, Langer H, Peluso M, Goyal P, Vestweber D, Emambokus NR, Busch DH, Frampton J, Gawaz M: Platelets secrete stromal cell-derived factor 1alpha and recruit bone marrow-derived progenitor cells to arterial thrombi in vivo. J Exp Med 203: 1221–1233 (2006)

108. Massberg S, Schaerli P, Knezevic-Maramica I, Köllnberger M, Tubo N, Moseman EA, Huff IV, Junt T, Wagers AJ, Mazo IB, Andrian UH von: Immunosurveillance by Hematopoietic Progenitor Cells Trafficking through Blood, Lymph, and Peripheral Tissues. Cell 131: 994–1008 (2007)

109. Matsumoto T, Mifune Y, Kawamoto A, Kuroda R, Shoji T, Iwasaki H, Suzuki T, Oyamada A, Horii M, Yokoyama A, Nishimura H, Lee SY, Miwa M,

Doita M, Kurosaka M, Asahara T: Fracture induced mobilization and incorporation of bone marrow-derived endothelial progenitor cells for bone healing. J Cell Physiol 215: 234–242 (2008)

110. Mayadas TN, Cullere X, Lowell CA: The Multifaceted Functions of Neutrophils. Annu Rev Pathol 9: 181–218 (2014)

111. Medina RJ, Barber CL, Sabatier F, Dignat-George F, Melero-Martin JM, Khosrotehrani K, Ohneda O, Randi AM, Chan JKY, Yamaguchi T, Van Hinsbergh VWM, Yoder MC, Stitt AW: Endothelial Progenitors: A Consensus Statement on Nomenclature. STEM CELLS Translational Medicine 6: 1316–1320 (2017)

112. Mira JC, Nacionales DC, Loftus TJ, Ungaro R, Mathias B, Mohr AM, Moldawer LL, Efron PA: Mouse Injury Model of Polytrauma and Shock. Methods Mol Biol 1717: 1–15 (2018)

113. Montagnani S, Rueger MA, Hosoda T, Nurzynska D: Adult Stem Cells in Tissue Maintenance and Regeneration. Stem Cells Int 2016: 7362879 (2016)

114. National Cancer Institute: NCI Dictionaries – stem cell mobilization. https://www.cancer.gov/publications/dictionaries/cancer-terms/def/stem-cell-mobilization (no date) (opened 03/28/2020)

115. Niesler U, Palmer A, Fröba JS, Braumüller ST, Zhou S, Gebhard F, Knöferl MW, Seitz DH: Role of alveolar macrophages in the regulation of local and systemic inflammation after lung contusion. J Trauma Acute Care Surg 76: 386–393 (2014)

116. Oh EJ, Lee HW, Kalimuthu S, Kim TJ, Kim HM, Baek SH, Zhu L, Oh JM, Son SH, Chung HY, Ahn B-C: In vivo migration of mesenchymal stem cells to burn injury sites and their therapeutic effects in a living mouse model. J Control Release 279: 79–88 (2018)

117. Olczyk P, Mencner Ł, Komosinska-Vassev K: The role of the extracellular matrix components in cutaneous wound healing. Biomed Res Int 2014: 747584 (2014)

118. Pape H-C, Lefering R, Butcher N, Peitzman A, Leenen L, Marzi I, Lichte P, Josten C, Bouillon B, Schmucker U, Stahel P, Giannoudis P, Balogh Z: The definition of polytrauma revisited: An international consensus process and proposal of the new “Berlin definition.” J Trauma Acute Care Surg 77: 780–786 (2014)

119. Park C-H, Joa K-L, Lee M-O, Yoon S-H, Kim M-O: The combined effect of granulocyte-colony stimulating factor (G-CSF) treatment and exercise in rats with spinal cord injury. The Journal of Spinal Cord Medicine 0: 1–8 (2018)

120. Park JE, Barbul A: Understanding the role of immune regulation in wound healing. The American Journal of Surgery 187: S11–S16 (2004)

121. Pati S, Pilia M, Grimsley JM, Karanikas AT, Oyeniyi B, Holcomb JB, Cap AP, Rasmussen TE: Cellular Therapies in Trauma and Critical Care Medicine: Forging New Frontiers. Shock 44: 505–523 (2015)

122. Pati S, Rasmussen TE: Cellular therapies in trauma and critical care medicine: Looking towards the future. PLOS Medicine 14: e1002343 (2017)

123. Peled A, Grabovsky V, Habler L, Sandbank J, Arenzana-Seisdedos F, Petit I, Ben-Hur H, Lapidot T, Alon R: The chemokine SDF-1 stimulates integrin-mediated arrest of CD34(+) cells on vascular endothelium under shear flow. J Clin Invest 104: 1199–1211 (1999)

124. Pelus LM, Fukuda S: Peripheral blood stem cell mobilization: The CXCR2 ligand GROβ rapidly mobilizes hematopoietic stem cells with enhanced engraftment properties. Experimental Hematology 34: 1010–1020 (2006)

125. Perl M, Gebhard F, Braumüller S, Tauchmann B, Brückner UB, Kinzl L, Knöferl MW: The pulmonary and hepatic immune microenvironment and its contribution to the early systemic inflammation following blunt chest trauma. Crit Care Med 34: 1152–1159 (2006)

126. Petrenko Y, Vackova I, Kekulova K, Chudickova M, Koci Z, Turnovcova K, Kupcova Skalnikova H, Vodicka P, Kubinova S: A Comparative Analysis of Multipotent Mesenchymal Stromal Cells derived from Different Sources, with a Focus on Neuroregenerative Potential. Scientific Reports 10: 4290 (2020)

127. Pitchford SC, Furze RC, Jones CP, Wengner AM, Rankin SM: Differential Mobilization of Subsets of Progenitor Cells from the Bone Marrow. Cell Stem Cell 4: 62–72 (2009)

128. Porada CD, Atala AJ, Almeida-Porada G: The Hematopoietic System in the Context of Regenerative Medicine. Methods 99: 44–61 (2016)

129. Probst C, Pape H-C, Hildebrand F, Regel G, Mahlke L, Giannoudis P, Krettek C, Grotz MRW: 30 years of polytrauma care: An analysis of the change in strategies and results of 4849 cases treated at a single institution. Injury 40: 77–83 (2009)

130. Qian H, Blanc KL, Sigvardsson M: Primary Mesenchymal Stem and Progenitor Cells from Bone Marrow Lack Expression of CD44 Protein. J Biol Chem 287: 25795–25807 (2012)

131. Rafii S, Butler JM, Ding B-S: Angiocrine functions of organ-specific endothelial cells. Nature 529: 316–325 (2016)

132. Ramirez K, Witherden DA, Havran WL: All hands on DE(T)C: Epithelial-resident γδ T cells respond to tissue injury. Cellular Immunology 296: 57–61 (2015)

133. Ramírez M, Lucia A, Gómez-Gallego F, Esteve-Lanao J, Pérez-Martínez A, Foster C, Andreu AL, Martin MA, Madero L, Arenas J, García-Castro J: Mobilisation of mesenchymal cells into blood in response to skeletal muscle injury. Br J Sports Med 40: 719–722 (2006)

134. Rau C-S, Wu S-C, Kuo P-J, Chen Y-C, Chien P-C, Hsieh H-Y, Hsieh C-H: Polytrauma Defined by the New Berlin Definition: A Validation Test Based on Propensity-Score Matching Approach. Int J Environ Res Public Health 14: (2017)

135. Relja B, Land WG: Damage-associated molecular patterns in trauma. Eur J Trauma Emerg Surg [Epub ahead of print], doi: 10.1007/s00068-019-01235-w (2019)

136. Ren G, Zhang L, Zhao X, Xu G, Zhang Y, Roberts AI, Zhao RC, Shi Y: Mesenchymal Stem Cell-Mediated Immunosuppression Occurs via Concerted Action of Chemokines and Nitric Oxide. Cell Stem Cell 2: 141–150 (2008)

137. Rennert RC, Sorkin M, Garg RK, Gurtner GC: Stem cell recruitment after injury: lessons for regenerative medicine. Regen Med 7: 833–850 (2012)

138. Richter R, Forssmann W, Henschler R: Current Developments in Mobilization of Hematopoietic Stem and Progenitor Cells and Their Interaction with Niches in Bone Marrow. Transfus Med Hemother 44: 151–164 (2017)

139. Robb CT, Regan KH, Dorward DA, Rossi AG: Key mechanisms governing resolution of lung inflammation. Semin Immunopathol 38: 425–448 (2016)

140. Sadtler K, Estrellas K, Allen BW, Wolf MT, Fan H, Tam AJ, Patel CH, Luber BS, Wang H, Wagner KR, Powell JD, Housseau F, Pardoll DM, Elisseeff JH: Developing a pro-regenerative biomaterial scaffold microenvironment requires T helper 2 cells. Science 352: 366–370 (2016)

141. Scholten D, Canals M, Maussang D, Roumen L, Smit M, Wijtmans M, de Graaf C, Vischer H, Leurs R: Pharmacological modulation of chemokine receptor function. Br J Pharmacol 165: 1617–1643 (2012)

142. Seebach C, Henrich D, Wilhelm K, Barker JH, Marzi I: Endothelial progenitor cells improve directly and indirectly early vascularization of mesenchymal stem cell-driven bone regeneration in a critical bone defect in rats. Cell Transplant 21: 1667–1677 (2012)

143. Selvasandran K, Makhoul G, Jaiswal PK, Jurakhan R, Li L, Ridwan K, Cecere R: A Tumor Necrosis Factor-α and Hypoxia-Induced Secretome Therapy for Myocardial Repair. The Annals of Thoracic Surgery 105: 715–723 (2018)

144. Serrano-Mollar A, Nacher M, Gay-Jordi G, Closa D, Xaubet A, Bulbena O: Intratracheal Transplantation of Alveolar Type II Cells Reverses Bleomycin-induced Lung Fibrosis. Am J Respir Crit Care Med 176: 1261–1268 (2007)

145. Shen H, Cheng T, Olszak I, Garcia-Zepeda E, Lu Z, Herrmann S, Fallon R, Luster AD, Scadden DT: CXCR-4 desensitization is associated with tissue localization of hemopoietic progenitor cells. J Immunol 166: 5027–5033 (2001)

146. Shi M, Ishikawa M, Kamei N, Nakasa T, Adachi N, Deie M, Asahara T, Ochi M: Acceleration of skeletal muscle regeneration in a rat skeletal muscle injury model by local injection of human peripheral blood-derived CD133-positive cells. Stem Cells 27: 949–960 (2009)

147. Shibuya M: Vascular Endothelial Growth Factor (VEGF) and Its Receptor (VEGFR) Signaling in Angiogenesis. Genes Cancer 2: 1097–1105 (2011)

148. Shimode K, Iwasaki N, Majima T, Funakoshi T, Sawaguchi N, Onodera T, Minami A: Local Upregulation of Stromal Cell–Derived Factor-1 After Ligament Injuries Enhances Homing Rate of Bone Marrow Stromal Cells in Rats. Tissue Engineering Part A 15: 2277–2284 (2009)

149. Si Y, Tsou C-L, Croft K, Charo IF: CCR2 mediates hematopoietic stem and progenitor cell trafficking to sites of inflammation in mice. J Clin Invest 120: 1192–1203 (2010)

150. Silvestre-Roig C, Hidalgo A, Soehnlein O: Neutrophil heterogeneity: implications for homeostasis and pathogenesis. Blood 127: 2173–2181 (2016)

151. Singh P, Yao Y, Weliver A, Broxmeyer HE, Hong S-C, Chang C-H: Vaccinia Virus Infection Modulates the Hematopoietic Cell Compartments in the Bone Marrow. Stem Cells 26: 1009 (2008)

152. Sîrbulescu RF, Boehm CK, Soon E, Wilks MQ, Ilieş I, Yuan H, Maxner B, Chronos N, Kaittanis C, Normandin MD, Fakhri GE, Orgill DP, Sluder AE, Poznansky MC: Mature B cells accelerate wound healing after acute and chronic diabetic skin lesions. Wound Repair Regen 25: 774–791 (2017)

153. Skirecki T, Mikaszewska-Sokolewicz M, Godlewska M, Dołęgowska B, Czubak J, Hoser G, Kawiak J, Zielińska-Borkowska U: Mobilization of Stem and Progenitor Cells in Septic Shock Patients. Sci Rep 9: (2019)

154. Snapper CM, Yamaguchi H, Urban JF, Finkelman FD: Induction of Ly-6A/E expression by murine lymphocytes after in vivo immunization is strictly dependent upon the action of IFN-alpha/beta and/or IFN-gamma. Int Immunol 3: 845–852 (1991)

155. Stripp BR: Hierarchical Organization of Lung Progenitor Cells. Proc Am Thorac Soc 5: 695–698 (2008)

156. Sutherland DR, Anderson L, Keeney M, Nayar R, Chin-Yee I: The ISHAGE guidelines for CD34+ cell determination by flow cytometry. International Society of Hematotherapy and Graft Engineering. J Hematother 5: 213–226 (1996)

157. Suzuki T, Tada Y, Nishimura R, Kawasaki T, Sekine A, Urushibara T, Kato F, Kinoshita T, Ikari J, West J, Tatsumi K: Endothelial-to-mesenchymal transition in lipopolysaccharide-induced acute lung injury drives a progenitor cell-like phenotype. Am J Physiol Lung Cell Mol Physiol 310: L1185-1198 (2016)

158. Szpalski C, Butala P, Vandegrift MT, Knobel D, Allen RJ, Saadeh PB, Warren SM: Improving Senescent Wound Healing With Local and Systemic Therapies. Ann Plast Surg 81: 96–105 (2018)

159. Takizawa H, Regoes RR, Boddupalli CS, Bonhoeffer S, Manz MG: Dynamic variation in cycling of hematopoietic stem cells in steady state and inflammation. J Exp Med 208: 273–284 (2011)

160. Tang YL, Qian K, Zhang YC, Shen L, Phillips MI: Mobilizing of haematopoietic stem cells to ischemic myocardium by plasmid mediated stromal-cell-derived factor-1alpha (SDF-1alpha) treatment. Regul Pept 125: 1–8 (2005)

161. Tashiro K, Nonaka A, Hirata N, Yamaguchi T, Mizuguchi H, Kawabata K: Plasma Elevation of Vascular Endothelial Growth Factor Leads to the Reduction of Mouse Hematopoietic and Mesenchymal Stem/Progenitor Cells in the Bone Marrow. Stem Cells and Development 23: 2202–2210 (2013)

162. Tilling L, Chowienczyk P, Clapp B: Progenitors in motion: mechanisms of mobilization of endothelial progenitor cells. Br J Clin Pharmacol 68: 484–492 (2009)

163. Tomoda H, Aoki N: Bone marrow stimulation and left ventricular function in acute myocardial infarction. Clin Cardiol 26: 455–457 (2003)

164. Toupadakis CA, Granick JL, Sagy M, Wong A, Ghassemi E, Chung D-J, Borjesson DL, Yellowley CE: Mobilization of endogenous stem cell populations enhances fracture healing in a murine femoral fracture model. Cytotherapy 15: 1136–1147 (2013)

165. Toupadakis CA, Wong A, Genetos DC, Chung D-J, Murugesh D, Anderson MJ, Loots GG, Christiansen BA, Kapatkin AS, Yellowley CE: Long-term administration of AMD3100, an antagonist of SDF-1/CXCR4 signaling, alters fracture repair. J Orthop Res 30: 1853–1859 (2012)

166. TraumaRegister DGU: Jahresbericht 2009. http://www.traumaregister-dgu.de/fileadmin/user_upload/traumaregister-dgu.de/docs/Downloads/TR-DGU-Jahresbericht_2009.pdf (2009) (opened 12/28/2019)

167. Tsukada S, Kwon S-M, Matsuda T, Jung S-Y, Lee J-H, Lee S-H, Masuda H, Asahara T: Identification of mouse colony-forming endothelial progenitor cells for postnatal neovascularization: a novel insight highlighted by new mouse colony-forming assay. Stem Cell Research & Therapy 4: 20 (2013)

168. Ueda Y, Cain DW, Kuraoka M, Kondo M, Kelsoe G: IL-1RI dependent HSC proliferation is necessary for Inflammatory Granulopoiesis and Reactive Neutrophilia. J Immunol 182: 6477–6484 (2009)

169. Vogel M, Christow H, Manz I, Denkinger M, Amoah A, Schütz D, Brown A, Möhrle B, Schaffer A, Kalbitz M, Gebhard F, Mayer B, Huber-Lang M, Geiger H: Distinct Dynamics of Stem and Progenitor Cells in Blood of Polytraumatized Patients. Shock 51: 430–438 (2019a)

170. Vogel M, Moehrle B, Brown A, Eiwen K, Sakk V, Geiger H: HPRT and Purine Salvaging Are Critical for Hematopoietic Stem Cell Function. STEM CELLS 37: 1606–1614 (2019b)

171. Wada H, Yoshida S, Suzuki H, Sakairi Y, Mizobuchi T, Komura D, Sato Y, Yokoi S, Yoshino I: Transplantation of alveolar type II cells stimulates lung regeneration during compensatory lung growth in adult rats. J Thorac Cardiovasc Surg 143: 711-719.e2 (2012)

172. Walter HL, van der Maten G, Antunes AR, Wieloch T, Ruscher K: Treatment with AMD3100 attenuates the microglial response and improves outcome after experimental stroke. Journal of Neuroinflammation 12: 24 (2015)

173. Wan M, Li C, Zhen G, Jiao K, He W, Jia X, Wang W, Shi C, Xing Q, Chen Y-F, Jan De Beur S, Yu B, Cao X: Injury-Activated TGFβ Controls Mobilization of MSCs for Tissue Remodeling. Stem Cells 30: 2498–2511 (2012)

174. Wang J: Neutrophils in tissue injury and repair. Cell Tissue Res 371: 531–539 (2018)

175. Wang XX, Allen RJ, Tutela JP, Sailon A, Allori AC, Davidson EH, Paek GK, Saadeh PB, McCarthy JG, Warren SM: Progenitor cell mobilization enhances bone healing by means of improved neovascularization and osteogenesis. Plast Reconstr Surg 128: 395–405 (2011)

176. Wara AK, Croce K, Foo S, Sun X, Icli B, Tesmenitsky Y, Esen F, Rosenzweig A, Feinberg MW: Bone marrow–derived CMPs and GMPs represent highly functional proangiogenic cells: implications for ischemic cardiovascular disease. Blood 118: 6461–6464 (2011)

177. Watson, T.: Soft Tissue Repair and Healing Review. Electrotherapy. http://www.electrotherapy.org/modality/soft-tissue-repair-and-healing-review (2009) (opened 01/03/2020)

178. Weber B, Lackner I, Haffner-Luntzer M, Palmer A, Pressmar J, Scharffetter-Kochanek K, Knöll B, Schrezenemeier H, Relja B, Kalbitz M: Modeling trauma in rats: similarities to humans and potential pitfalls to consider. J Transl Med 17: (2019)

179. Weckbach S, Hohmann C, Denk S, Kellermann P, Huber-Lang MS, Baumann B, Wirth T, Gebhard F, Bachem M, Perl M: Apoptotic and inflammatory signaling via Fas and tumor necrosis factor receptor I contribute to the development of chest trauma-induced septic acute lung injury. J Trauma Acute Care Surg 74: 792–800 (2013)

180. Weckbach S, Perl M, Heiland T, Braumüller S, Stahel PF, Flierl MA, Ignatius A, Gebhard F, Huber-Lang M: A New Experimental Polytrauma Model in Rats: Molecular Characterization of the Early Inflammatory Response. Mediators Inflamm 2012: (2012)

181. Wei H-J, Liu L, Chen F-L, Wang D, Wang L, Wang Z-G, Jiang R-C, Dong J-F, Chen J-L, Zhang J-N: Decreased numbers of circulating endothelial progenitor cells are associated with hyperglycemia in patients with traumatic brain injury. Neural Regen Res 14: 984–990 (2019)

182. Wiegner R, Rudhart N-E, Barth E, Gebhard F, Lampl L, Huber-Lang MS, Brenner RE: Mesenchymal stem cells in peripheral blood of severely injured patients. Eur J Trauma Emerg Surg 44: 627–636 (2018)

183. Winkler IG, Barbier V, Wadley R, Zannettino ACW, Williams S, Lévesque J-P: Positioning of bone marrow hematopoietic and stromal cells relative to blood flow in vivo: serially reconstituting hematopoietic stem cells reside in distinct nonperfused niches. Blood 116: 375–385 (2010)

184. Wisniewski D, Affer M, Willshire J, Clarkson B: Further phenotypic characterization of the primitive lineage− CD34+CD38−CD90+CD45RA− hematopoietic stem cell/progenitor cell sub-population isolated from cord blood, mobilized peripheral blood and patients with chronic myelogenous leukemia. Blood Cancer Journal 1: e36–e36 (2011)

185. Witte SFH de, Luk F, Parraga JMS, Gargesha M, Merino A, Korevaar SS, Shankar AS, O'Flynn L, Elliman SJ, Roy D, Betjes MGH, Newsome PN, Baan CC, Hoogduijn MJ: Immunomodulation By Therapeutic Mesenchymal

Stromal Cells (MSC) Is Triggered Through Phagocytosis of MSC By Monocytic Cells. STEM CELLS 36: 602–615 (2018)

186. Wright DE, Bowman EP, Wagers AJ, Butcher EC, Weissman IL: Hematopoietic Stem Cells Are Uniquely Selective in Their Migratory Response to Chemokines. J Exp Med 195: 1145–1154 (2002)

187. Wynn TA, Vannella KM: Macrophages in Tissue Repair, Regeneration, and Fibrosis. Immunity 44: 450–462 (2016)

188. Xing J, Hou T, Jin H, Luo F, Change Z, Li Z, Xie Z, Xu J: Inflammatory Microenvironment Changes the Secretory Profile of Mesenchymal Stem Cells to Recruit Mesenchymal Stem Cells. CPB 33: 905–919 (2014)

189. Xu F, Shi J, Yu B, Ni W, Wu X, Gu Z: Chemokines mediate mesenchymal stem cell migration toward gliomas in vitro. Oncol Rep 23: 1561–1567 (2010)

190. Yamada T, Park CS, Lacorazza HD: Genetic control of quiescence in hematopoietic stem cells. Cell Cycle 12: 2376–2383 (2013)

191. Yang J, Zhu F, Wang X, Yao W, Wang M, Pei G, Hu Z, Guo Y, Zhao Z, Wang P, Mou J, Sun J, Zeng R, Xu G, Liao W, Yao Y: Continuous AMD3100 Treatment Worsens Renal Fibrosis through Regulation of Bone Marrow Derived Pro-Angiogenic Cells Homing and T-Cell-Related Inflammation. PLOS ONE 11: e0149926 (2016)

192. Ye J-S, Su X-S, Stoltz J-F, de Isla N, Zhang L: Signalling pathways involved in the process of mesenchymal stem cells differentiating into hepatocytes. Cell Prolif 48: 157–165 (2015)

193. Yin Y, Huang L, Zhao X, Fang Y, Yu S, Zhao J, Cui B: AMD3100 mobilizes endothelial progenitor cells in mice, but inhibits its biological functions by blocking an autocrine/paracrine regulatory loop of stromal cell derived factor-1 in vitro. J Cardiovasc Pharmacol 50: 61–67 (2007)

194. Yoder Mervin C.: Is Endothelium the Origin of Endothelial Progenitor Cells? Arteriosclerosis, Thrombosis, and Vascular Biology 30: 1094–1103 (2010)

195. Yu Y-RA, O'Koren EG, Hotten DF, Kan MJ, Kopin D, Nelson ER, Que L, Gunn MD: A Protocol for the Comprehensive Flow Cytometric Analysis of Immune Cells in Normal and Inflamed Murine Non-Lymphoid Tissues. PLoS ONE 11: e0150606 (2016)

196. Zhai R, Wang Y, Qi L, Williams GM, Gao B, Song G, Burdick JF, Sun Z: Pharmacological Mobilization of Endogenous Bone Marrow Stem Cells Promotes Liver Regeneration after Extensive Liver Resection in Rats. Sci Rep 8: 1–10 (2018)

197. Zhang W, Zhang G, Jin H, Hu R: Characteristics of bone marrow-derived endothelial progenitor cells in aged mice. Biochem Biophys Res Commun 348: 1018–1023 (2006)

198. Zuk A, Gershenovich M, Ivanova Y, MacFarland RT, Fricker SP, Ledbetter S: CXCR4 antagonism as a therapeutic approach to prevent acute kidney injury. American Journal of Physiology-Renal Physiology 307: F783–F797 (2014)

Table A1: *Correlation of clinical parameters, blood products and fluids with the number of SPCs, strength of decrease (d0-3 h-48 h) and strength of increase (d48 h - 120 h). Correlations with a r-value > 0.7 and a p-value < 0.05 are highlighted in red. According to: Vogel et al.: Distinct Dynamics of Stem and Progenitor Cells in Blood of Polytraumatized Patients. Shock 51: 430–438 (2019). https://journals.lww.com/shockjournal/Fulltext/2019/04000/Distinct_Dynamics_of_Stem_and_Progenitor_Cells_in.5.aspx.*

GMP d48-120h	GMP d0-48h	CMP 120h	CMP 48h	GMP 24h	GMP 0h	CMP d48-120h	CMP d0-48h	CMP 120h	CMP 48h	CMP 24h	CMP 0h	MSC d48-120h	MSC d0-48h	MSC 120h	MSC 48h	MSC 24h	MSC 0h	HSC d48-120h	HSC d0-48h	HSC 120h	HSC 48h	HSC 24h	HSC 0h		
-0,071	0,036	-0,036	0,071	0,762	0,036	-0,071	0,393	0,107	0,452	0,667	0,357	-0,071	0,286	-0,071	-0,429	0,214	-0,179	-0,571	0,321	-0,571	-0,214	0,810	0,750	Spearman	Age
0,906	0,964	0,964	0,882	0,037	0,964	0,906	0,396	0,840	0,268	0,083	0,444	0,906	0,556	0,906	0,299	0,662	0,713	0,200	0,498	0,200	0,619	0,022	0,066	p-value	
-0,571	0,036	-0,821	-0,310	-0,071	0,036	0,071	0,393	0,107	0,071	0,405	0,429	-0,500	-0,357	-0,500	-0,095	-0,107	-0,357	-0,429	0,107	-0,357	0,191	0,191	0,036	Spearman	ISS
0,200	0,964	0,034	0,462	0,882	0,964	0,906	0,396	0,840	0,882	0,327	0,354	0,267	0,444	0,267	0,840	0,840	0,444	0,354	0,840	0,444	0,665	0,665	0,964	p-value	
-0,036	0,464	-0,071	-0,500	0,214	0,464	0,071	0,679	0,143	0,357	0,286	0,714	-0,321	0,679	-0,321	-0,571	-0,393	0,179	-0,643	0,357	-0,571	-0,214	0,214	0,500	Spearman	CK shock-room
0,964	0,302	0,906	0,216	0,619	0,302	0,906	0,110	0,783	0,389	0,501	0,088	0,498	0,110	0,498	0,151	0,396	0,713	0,139	0,444	0,200	0,619	0,619	0,267	p-value	
-0,250	-0,357	-0,107	0,286	0,476	-0,357	-0,536	0,000	-0,464	0,476	0,262	0,036	0,000	0,214	0,000	-0,214	-0,571	-0,321	-0,607	-0,286	-0,143	0,071	0,476	0,214	Spearman	CK 24h
0,595	0,444	0,840	0,501	0,243	0,444	0,236	9999,0	0,302	0,243	0,536	0,964	9999,0	0,662	9999,0	0,619	0,200	0,498	0,167	0,556	0,783	0,882	0,243	0,662	p-value	
-0,286	0,000	-0,393	0,024	0,167	0,000	-0,321	0,214	-0,286	0,214	0,214	0,321	-0,214	0,321	-0,214	-0,238	-0,536	-0,107	-0,964	-0,321	-0,571	0,095	0,429	0,036	Spearman	CK 48h
0,556	9999,0	0,396	0,977	0,703	9999,0	0,498	0,662	0,556	0,619	0,619	0,498	0,662	0,498	0,662	0,582	0,236	0,840	0,003	0,498	0,200	0,840	0,299	0,964	p-value	
0,086	0,300	-0,143	-0,600	-0,029	0,300	0,600	0,200	0,543	0,257	0,143	0,600	-0,086	-0,100	-0,086	0,200	-0,100	-0,300	-0,771	-0,200	-0,314	0,257	0,371	0,300	Spearman	CK 120h
0,919	0,683	0,803	0,242	9999,0	0,683	0,242	0,783	0,297	0,658	0,803	0,350	0,919	0,950	0,919	0,714	0,950	0,683	0,103	0,783	0,564	0,658	0,497	0,683	p-value	
-0,182	0,234	-0,364	-0,711	0,072	0,234	0,564	0,523	0,509	0,494	0,362	0,703	-0,273	0,144	-0,273	-0,145	-0,564	-0,234	-0,455	0,054	0,055	0,121	0,145	0,378	Spearman	Length ICU (days)
0,698	0,620	0,429	0,055	0,871	0,620	0,197	0,240	0,249	0,218	0,379	0,086	0,562	0,757	0,562	0,737	0,197	0,620	0,305	0,919	0,924	0,780	0,737	0,406	p-value	
0,086	0,214	-0,143	-0,429	-0,393	0,214	0,257	0,000	0,086	0,000	-0,357	0,214	-0,086	0,143	-0,086	0,143	-0,771	0,107	-0,600	-0,429	0,143	0,250	-0,179	-0,214	Spearman	PRBC
0,919	0,662	0,803	0,354	0,396	0,662	0,658	9999,0	0,919	9999,0	0,444	0,662	0,919	0,783	0,919	0,783	0,103	0,840	0,242	0,354	0,803	0,595	0,713	0,662	p-value	
0,029	0,396	-0,257	-0,613	-0,505	0,396	0,143	0,234	-0,029	-0,054	-0,306	0,414	-0,200	0,324	-0,200	-0,090	-0,928	0,234	-0,543	-0,198	-0,086	0,072	-0,324	-0,198	Spearman	FFP
9999,0	0,381	0,658	0,158	0,252	0,381	0,803	0,623	9999,0	0,917	0,512	0,357	0,714	0,477	0,714	0,860	0,022	0,623	0,297	0,670	0,919	0,889	0,477	0,670	p-value	
-0,158	0,217	-0,296	-0,355	0,109	0,217	0,039	0,335	0,039	0,300	0,218	0,512	-0,217	0,217	-0,217	-0,164	-0,493	-0,099	-0,906	-0,197	-0,434	0,136	0,355	0,236	Spearman	TK
0,762	0,648	0,524	0,399	0,827	0,648	0,952	0,476	0,952	0,488	0,619	0,229	0,648	0,648	0,648	0,702	0,257	0,819	0,010	0,686	0,343	0,762	0,399	0,610	p-value	
-0,321	0,179	-0,500	-0,691	0,310	0,179	0,571	0,643	0,607	0,643	0,595	0,786	-0,429	0,143	-0,429	-0,286	-0,464	-0,357	-0,607	0,143	-0,179	0,095	0,381	0,571	Spearman	Fluid Balance
0,498	0,713	0,267	0,069	0,462	0,713	0,200	0,139	0,167	0,096	0,132	0,048	0,354	0,783	0,354	0,501	0,302	0,444	0,167	0,783	0,713	0,840	0,360	0,200	p-value	

Table A2: *Correlation of SPC numbers with the concentration of inflammatory and mobilizing factors. Correlations with a r-value > 0.7 and a p-value < 0.05 are highlighted in red. Based on: Vogel et al.: Distinct Dynamics of Stem and Progenitor Cells in Blood of Polytraumatized Patients. Shock 51: 430–438 (2019). https://journals.lww.com/shockjournal/Fulltext/2019/04000/Distinct_Dynamics_of_Stem_and_Progenitor_Cells_in.5.aspx.*

	Fractalkine								G-CSF								Gro-α								Gro-β								IL-6							
	0-3 h		24 h		48 h		120 h		0-3 h		24 h		48 h		120 h		0-3 h		24 h		48 h		120 h		0-3 h		24 h		48 h		120 h		0-3 h		24 h		48 h		120 h	
	r	p	r	p	r	p	r	p	r	p	r	p	r	p	r	p	r	p	r	p	r	p	r	p	r	p	r	p	r	p	r	p	r	p	r	p	r	p	r	p
ANSP (0-48 h)	0,29	0,56	-0,23	0,62	0,07	0,91	-0,31	0,56	-0,04	0,96	0,11	0,84	0,11	0,84	0,14	0,80	-0,07	0,91	-0,20	0,69	-0,02	0,99	0,84	0,04	0,64	0,14	-0,11	0,84	-0,21	0,66	0,71	0,14	0,04	0,96	0,21	0,66	0,11	0,84	0,26	0,66
ANSP (48 - 120 h)	-0,54	0,30	0,86	0,02	0,54	0,24	0,39	0,40	-0,60	0,24	-0,79	0,05	-0,64	0,14	-0,50	0,27	-0,83	0,06	-0,33	0,48	-0,41	0,36	-0,16	0,73	-0,43	0,42	-0,21	0,66	-0,25	0,59	0,11	0,84	-0,60	0,24	-0,89	0,01	-0,57	0,20	-0,36	0,44
HSC 0h	-0,21	0,66	0,07	0,89	-0,25	0,59	-0,37	0,50	0,50	0,27	0,43	0,35	0,43	0,35	0,26	0,66	0,36	0,44	0,49	0,26	-0,02	0,99	0,17	0,75	0,25	0,59	0,21	0,66	0,32	0,50	0,77	0,10	0,25	0,59	0,39	0,40	0,57	0,20	-0,20	0,71
HSC 24h	-0,11	0,84	-0,25	0,55	-0,55	0,17	-0,32	0,50	0,54	0,24	0,55	0,17	0,36	0,39	0,21	0,66	0,64	0,14	0,52	0,21	0,05	0,92	-0,35	0,45	0,00	1	0,17	0,70	0,31	0,46	-0,11	0,84	0,25	0,59	0,57	0,15	0,50	0,22	0,00	>0,99
HSC 48h	-0,11	0,84	0,07	0,87	0,10	0,84	0,54	0,24	0,21	0,66	-0,07	0,88	0,12	0,79	0,43	0,35	0,25	0,59	0,16	0,70	0,36	0,38	-0,44	0,34	-0,54	0,24	0,31	0,46	0,43	0,30	-0,14	0,78	0,18	0,71	0,02	0,98	0,05	0,93	-0,07	0,91
HSC 120h	-0,37	0,50	0,96	0,00	0,68	0,11	0,64	0,14	-0,20	0,71	-0,64	0,14	-0,36	0,44	-0,21	0,66	-0,37	0,50	-0,12	0,79	-0,05	0,92	-0,47	0,29	-0,71	0,14	0,07	0,91	0,18	0,71	0,00	1	-0,20	0,71	-0,75	0,07	-0,43	0,35	-0,43	0,35
HSCs d(0 - 48h)	0,14	0,78	-0,22	0,64	-0,25	0,59	-0,77	0,10	0,07	0,91	0,00	>0,99	0,00	>0,99	0,14	0,80	0,00	>0,9	-0,02	>0,99	-0,34	0,46	0,58	0,23	0,68	0,11	-0,07	0,91	-0,18	0,71	0,77	0,10	0,11	0,84	0,11	0,84	0,07	0,91	-0,20	0,71
HSCs d(48-120h)	0,03	1	0,61	0,17	0,32	0,50	0,14	0,78	-0,77	0,10	-1,00	0,00	-0,79	0,05	-0,50	0,27	-0,66	0,18	-0,59	0,17	-0,58	0,19	-0,16	0,73	0,09	0,92	0,07	0,91	0,00	>0,99	0,18	0,71	-0,54	0,30	-0,93	0,01	-0,82	0,03	-0,71	0,09
MSC 0h	0,11	0,84	-0,04	0,95	0,29	0,56	0,03	1	-0,54	0,24	-0,25	0,59	-0,25	0,59	-0,31	0,56	-0,50	0,27	-0,57	0,20	-0,04	0,95	0,55	0,27	0,29	0,56	-0,18	0,71	-0,46	0,30	0,31	0,56	-0,43	0,35	-0,18	0,71	-0,29	0,56	0,14	0,80
MSC 24h	-0,94	0,02	-0,11	0,84	-0,68	0,11	-0,20	0,71	-0,49	0,36	-0,54	0,24	-0,54	0,24	-0,37	0,50	-0,54	0,30	-0,20	0,69	-0,68	0,11	0,00	>0,99	-0,20	0,71	0,36	0,44	-0,07	0,91	0,60	0,24	-0,71	0,14	-0,25	0,59	-0,29	0,56	-0,60	0,24
MSC 48h	-0,79	0,05	0,48	0,23	0,21	0,62	0,64	0,14	-0,36	0,44	-0,45	0,27	-0,38	0,36	-0,11	0,84	-0,57	0,20	0,00	>0,99	-0,14	0,73	-0,44	0,34	-0,86	0,02	-0,12	0,79	-0,21	0,62	-0,14	0,78	-0,46	0,30	-0,50	0,22	-0,31	0,46	0,00	>0,99
MSC 120h	-0,43	0,42	0,50	0,27	0,18	0,71	0,14	0,78	-0,71	0,14	-0,29	0,56	-0,46	0,30	-0,61	0,17	-0,77	0,10	-0,16	0,76	-0,41	0,36	-0,13	0,78	-0,31	0,56	-0,46	0,30	-0,54	0,24	-0,11	0,84	-0,77	0,10	-0,54	0,24	-0,29	0,56	0,00	>0,99
MSCs d(0 - 48h)	0,64	0,14	-0,13	0,80	0,29	0,56	-0,03	1	0,04	0,96	0,32	0,50	0,32	0,50	-0,14	0,80	0,21	0,66	-0,30	0,52	0,34	0,46	0,58	0,23	0,68	0,11	0,00	1	0,04	0,96	0,31	0,56	0,11	0,84	0,32	0,50	0,14	0,78	0,26	0,66
MSCs d(48-120h)	-0,43	0,42	0,50	0,27	0,18	0,71	0,14	0,78	-0,71	0,14	-0,29	0,56	-0,46	0,30	-0,61	0,17	-0,77	0,10	-0,16	0,76	-0,41	0,36	-0,13	0,78	-0,31	0,56	-0,46	0,30	-0,54	0,24	-0,11	0,84	-0,77	0,10	-0,54	0,24	-0,29	0,56	0,00	>0,99
CMP 0h	0,21	0,66	-0,25	0,59	0,14	0,78	-0,43	0,42	0,71	0,09	0,64	0,14	0,64	0,14	0,83	0,06	0,39	0,40	0,57	0,20	0,31	0,51	0,84	0,04	0,36	0,44	-0,18	0,71	0,11	0,84	0,77	0,10	0,71	0,09	0,71	0,09	0,71	0,09	0,49	0,36
CMP 24h	0,07	0,91	-0,28	0,51	-0,45	0,27	-0,71	0,09	0,68	0,11	0,55	0,17	0,38	0,36	0,21	0,66	0,61	0,17	0,63	0,11	-0,02	0,96	-0,16	0,73	0,29	0,56	0,02	0,98	0,24	0,58	-0,04	0,96	0,57	0,20	0,57	0,15	0,55	0,17	-0,14	0,78
CMP 48h	0,14	0,78	0,11	0,81	-0,02	0,98	0,11	0,84	0,82	0,03	0,48	0,24	0,60	0,13	0,39	0,40	0,82	0,03	0,49	0,22	0,43	0,29	-0,45	0,30	0,07	0,91	0,43	0,30	0,74	0,05	0,04	0,96	0,64	0,14	0,43	0,30	0,55	0,17	-0,25	0,59
CMP 120h	-0,83	0,06	0,29	0,56	0,04	0,96	0,04	0,96	0,60	0,24	-0,07	0,91	0,21	0,66	0,50	0,27	0,03	1	0,49	0,26	0,05	0,92	0,31	0,50	-0,26	0,66	0,21	0,66	0,25	0,59	0,75	0,07	0,31	0,56	0,04	0,96	0,43	0,35	-0,07	0,91
CMPs d(0-3 h -48h)	0,36	0,44	-0,38	0,40	-0,04	0,96	-0,66	0,18	0,61	0,17	0,54	0,24	0,54	0,24	0,66	0,18	0,43	0,35	0,39	0,38	0,18	0,70	0,75	0,11	0,57	0,20	-0,07	0,91	0,14	0,78	0,71	0,14	0,64	0,14	0,64	0,14	0,57	0,20	0,26	0,66
CMPs d(48-120h)	-0,94	0,02	0,43	0,35	0,21	0,66	0,14	0,78	0,49	0,36	-0,14	0,78	0,14	0,78	0,46	0,30	-0,26	0,66	0,49	0,26	0,05	0,92	0,36	0,43	-0,49	0,36	0,04	0,96	0,07	0,91	0,71	0,09	0,26	0,66	-0,07	0,91	0,39	0,40	0,04	0,96
GMP 0h	-0,07	0,91	-0,11	0,82	0,29	0,56	-0,09	0,92	-0,04	0,96	0,11	0,84	0,11	0,84	0,31	0,56	-0,32	0,50	-0,02	>0,99	0,05	0,92	0,93	0,02	0,25	0,59	-0,29	0,56	-0,39	0,40	0,77	0,10	0,00	1	0,21	0,66	0,21	0,66	0,49	0,36
GMP 24h	0,04	0,96	-0,04	0,95	-0,45	0,27	-0,32	0,50	0,43	0,35	0,38	0,36	0,31	0,46	0,00	1	0,68	0,11	0,30	0,49	0,01	0,99	-0,49	0,27	0,21	0,66	0,43	0,30	0,55	0,17	-0,04	0,96	0,18	0,71	0,36	0,39	0,36	0,39	-0,36	0,44
GMP 48h	0,07	0,91	-0,04	0,95	-0,40	0,33	0,14	0,78	-0,54	0,24	-0,29	0,50	-0,45	0,27	-0,71	0,09	0,00	1	-0,49	0,22	-0,29	0,49	-0,87	0,02	-0,04	0,96	0,24	0,58	0,07	0,88	-0,64	0,14	-0,57	0,20	-0,33	0,43	-0,60	0,13	-0,43	0,35
GMP 120h	-0,49	0,36	0,57	0,20	0,32	0,50	0,36	0,44	-0,66	0,18	-0,46	0,30	-0,36	0,44	-0,54	0,24	-0,66	0,18	-0,47	0,29	-0,29	0,54	0,07	0,89	-0,14	0,80	-0,04	0,96	-0,18	0,71	0,29	0,56	-0,83	0,06	-0,57	0,20	-0,32	0,50	-0,14	0,78
GMPs d(0-48h)	-0,07	0,91	-0,11	0,82	0,29	0,56	-0,09	0,92	-0,04	0,96	0,11	0,84	0,11	0,84	0,31	0,56	-0,32	0,50	-0,02	>0,99	0,05	0,92	0,93	0,02	0,25	0,59	-0,29	0,56	-0,39	0,40	0,77	0,10	0,00	1	0,21	0,66	0,21	0,66	0,49	0,36
GMPs d(48- 120h)	-0,54	0,30	0,43	0,35	0,25	0,59	0,18	0,71	-0,54	0,30	-0,32	0,50	-0,32	0,50	-0,39	0,40	-0,77	0,10	-0,24	0,61	-0,31	0,51	0,29	0,54	-0,26	0,66	-0,32	0,50	-0,46	0,30	0,29	0,56	-0,66	0,18	-0,43	0,35	-0,14	0,78	0,11	0,84

	IL-8								IL-10								MCP-1								Mip-1α							
	0-3 h		24 h		48 h		120 h		0-3 h		24 h		48 h		120 h		0-3 h		24 h		48 h		120 h		0-3 h		24 h		48 h		120 h	
	r	p	r	p	r	p	r	p	r	p	r	p	r	p	r	p	r	p	r	p	r	p	r	p	r	p	r	p	r	p	r	p
ANSP (0-48h)	-0,04	0,96	-0,04	0,96	-0,04	0,96	-0,09	0,92	0,50	0,27	-0,36	0,43	0,00	>0,99	-0,06	0,94	-0,14	0,78	0,14	0,78	0,04	0,96	-0,03	>0,9	0,39	0,40	0,11	0,82	0,34	0,46	-0,09	0,92
ANSP (48 -120h)	-0,83	0,06	-0,71	0,09	-0,86	0,02	-0,82	0,03	0,09	0,92	-0,71	0,09	-0,57	0,20	-0,02	0,99	-0,77	0,10	-0,46	0,30	0,00	>0,99	-0,43	0,35	-0,09	0,92	-0,07	0,90	-0,14	0,76	-0,32	0,50
HSC 0h	0,36	0,44	0,50	0,27	0,36	0,44	0,14	0,80	0,43	0,35	0,34	0,46	0,36	0,44	0,03	0,99	0,39	0,40	0,82	0,03	0,64	0,14	-0,09	0,92	0,07	0,91	-0,02	0,99	0,50	0,25	0,66	0,18
HSC 24h	0,54	0,24	0,64	0,10	0,60	0,13	0,68	0,11	0,21	0,66	0,83	0,02	0,62	0,12	0,23	0,62	0,68	0,11	0,67	0,08	0,55	0,17	0,36	0,44	-0,25	0,59	-0,08	0,85	0,42	0,30	0,75	0,07
HSC 48h	0,29	0,56	0,00	>0,99	0,02	0,98	0,25	0,59	-0,61	0,17	0,25	0,55	-0,07	0,88	0,04	0,95	0,32	0,50	-0,14	0,75	-0,31	0,46	0,00	>0,99	-0,36	0,44	-0,08	0,85	-0,62	0,11	-0,11	0,84
HSC 120h	-0,37	0,50	-0,50	0,27	-0,61	0,17	-0,61	0,17	-0,26	0,66	-0,50	0,27	-0,46	0,30	-0,02	0,99	-0,26	0,66	-0,43	0,35	-0,11	0,84	-0,43	0,35	-0,31	0,56	0,07	0,90	-0,40	0,38	-0,29	0,56
HSCs d(0 - 48h)	-0,07	0,91	0,07	0,91	-0,07	0,91	-0,26	0,66	0,64	0,14	-0,34	0,46	-0,14	0,78	-0,41	0,44	-0,11	0,84	0,39	0,40	0,07	0,91	-0,49	0,36	0,64	0,14	0,41	0,36	0,61	0,16	0,43	0,42
HSC d(48-120h)	-0,94	0,02	-0,86	0,02	-0,96	0,02	-0,96	0,00	0,49	0,36	-0,86	0,02	-0,86	0,02	-0,36	0,43	-0,83	0,06	-0,61	0,17	-0,54	0,24	-0,86	0,02	0,43	0,42	0,51	0,25	-0,02	0,99	-0,14	0,78
MSC 0h	-0,43	0,35	-0,54	0,24	-0,43	0,35	-0,37	0,50	0,14	0,78	-0,52	0,24	-0,18	0,71	0,17	0,76	-0,54	0,24	-0,43	0,35	-0,14	0,78	0,03	>0,	0,00	>0,99	-0,25	0,58	-0,07	0,89	-0,37	0,50
MSC 24h	-0,54	0,30	-0,39	0,40	-0,54	0,24	-0,14	0,80	-0,09	0,92	0,04	0,95	-0,43	0,35	-0,03	>0,99	-0,54	0,30	0,04	0,96	-0,18	0,71	-0,26	0,66	-0,09	0,92	-0,04	0,96	-0,04	0,95	0,89	0,03
MSC 48h	-0,46	0,30	-0,33	0,43	-0,48	0,24	-0,21	0,66	-0,64	0,14	-0,11	0,81	-0,26	0,54	0,29	0,53	-0,43	0,35	-0,36	0,39	-0,05	0,93	0,11	0,84	-0,54	0,24	-0,47	0,24	-0,57	0,14	-0,29	0,56
MSC 120h	-0,77	0,10	-0,36	0,44	-0,43	0,35	-0,43	0,35	0,14	0,80	-0,21	0,66	0,00	>0,99	0,38	0,41	-0,71	0,14	-0,18	0,71	0,57	0,20	0,14	0,78	-0,31	0,56	-0,51	0,25	0,20	0,67	-0,14	0,78
MSCs d(0 - 48h)	0,21	0,66	0,04	0,96	0,21	0,66	-0,09	0,92	0,57	0,20	-0,13	0,80	0,36	0,44	0,23	0,67	0,14	0,78	-0,07	0,91	0,14	0,78	0,14	0,80	0,14	0,78	0,02	0,99	0,36	0,43	-0,26	0,66
MSC d(48-120h)	-0,77	0,10	-0,36	0,44	-0,43	0,35	-0,43	0,35	0,14	0,80	-0,21	0,66	0,00	>0,99	0,38	0,41	-0,71	0,14	-0,18	0,71	0,57	0,20	0,14	0,78	-0,31	0,56	-0,51	0,25	0,20	0,67	-0,14	0,78
CMP 0h	0,57	0,20	0,71	0,09	0,57	0,20	0,43	0,42	0,25	0,59	0,04	0,95	0,29	0,56	-0,41	0,44	0,43	0,35	0,79	0,05	0,29	0,56	0,03	>0,99	0,43	0,35	0,16	0,73	0,23	0,62	0,09	0,92
CMP 24h	0,50	0,27	0,71	0,06	0,62	0,12	0,43	0,35	0,39	0,40	0,47	0,25	0,38	0,36	-0,31	0,51	0,57	0,20	0,86	0,01	0,43	0,30	-0,04	0,96	0,43	0,35	0,37	0,36	0,61	0,12	0,79	0,05
CMP 48h	0,79	0,05	0,48	0,24	0,57	0,15	0,43	0,35	0,18	0,71	0,46	0,26	0,33	0,43	0,02	0,99	0,86	0,02	0,57	0,15	0,29	0,50	-0,04	0,96	0,00	>0,99	0,29	0,49	0,19	0,65	0,50	0,27
CMP 120h	0,26	0,66	0,14	0,78	-0,14	0,78	0,11	0,84	-0,20	0,71	-0,14	0,78	-0,29	0,56	-0,34	0,46	0,20	0,71	0,61	0,17	0,14	0,78	-0,29	0,56	0,09	0,92	0,07	0,90	-0,22	0,64	0,32	0,50
CMPs d(0 -48h)	0,50	0,27	0,61	0,17	0,50	0,27	0,26	0,66	0,43	0,35	0,00	>0,99	0,21	0,66	-0,49	0,34	0,39	0,40	0,68	0,11	0,14	0,78	-0,20	0,71	0,57	0,20	0,36	0,43	0,40	0,38	0,26	0,66
CMP d(48- 120h)	0,09	0,92	0,07	0,91	-0,25	0,59	0,00	>0,99	-0,37	0,50	-0,29	0,56	-0,36	0,44	-0,34	0,46	-0,03	>0,99	0,54	0,24	0,18	0,71	-0,25	0,59	0,03	>0,99	-0,07	0,90	-0,32	0,48	0,11	0,84
GMP 0h	-0,11	0,84	-0,04	0,96	-0,11	0,84	0,09	0,92	0,11	0,84	-0,41	0,36	-0,07	0,91	0,03	0,99	-0,29	0,56	0,21	0,66	0,11	0,84	0,20	0,71	0,18	0,71	-0,23	0,61	-0,04	0,95	-0,26	0,66
GMP 24h	0,46	0,30	0,40	0,33	0,45	0,27	0,43	0,35	0,39	0,40	0,63	0,10	0,45	0,27	0,22	0,64	0,64	0,14	0,55	0,17	0,45	0,27	0,07	0,91	-0,11	0,84	0,19	0,65	0,52	0,20	0,89	0,01
GMP 48h	-0,32	0,50	-0,29	0,50	-0,19	0,66	-0,18	0,71	0,07	0,91	0,36	0,38	0,14	0,75	0,63	0,14	-0,11	0,84	-0,57	0,15	-0,10	0,84	0,14	0,78	-0,32	0,50	-0,05	0,92	0,10	0,82	0,21	0,66
GMP 120h	-0,66	0,18	-0,68	0,11	-0,64	0,14	-0,50	0,27	0,26	0,66	-0,39	0,40	-0,14	0,78	0,43	0,33	-0,60	0,24	-0,39	0,40	0,29	0,56	-0,04	0,96	-0,37	0,50	-0,42	0,35	0,00	>0,99	-0,14	0,78
GMPs d(0- 48h)	-0,11	0,84	-0,04	0,96	-0,11	0,84	0,09	0,92	0,11	0,84	-0,41	0,36	-0,07	0,91	0,03	0,99	-0,29	0,56	0,21	0,66	0,11	0,84	0,20	0,71	0,18	0,71	-0,23	0,61	-0,04	0,95	-0,26	0,66
GMP d(48- 120h)	-0,60	0,24	-0,46	0,30	-0,54	0,24	-0,39	0,40	0,03	>0,99	-0,39	0,40	-0,14	0,78	0,27	0,56	-0,66	0,18	-0,14	0,78	0,39	0,40	0,07	0,91	-0,31	0,56	-0,53	0,23	0,02	0,99	-0,21	0,66

	Mip-1β								MDC								SDF-1α								VEGF-A							
	0-3 h		24 h		48 h		120 h		0-3 h		24 h		48 h		120 h		0-3 h		24 h		48 h		120 h		0-3 h		24 h		48 h		120 h	
	r	p	r	p	r	p	r	p	r	p	r	p	r	p	r	p	r	p	r	p	r	p	r	p	r	p	r	p	r	p	r	p
ANSP (0-48h)	0,36	0,42	0,87	0,02	0,43	0,33	0,21	0,73	-0,04	0,96	0,07	0,91	0,57	0,20	0,83	0,06	0,25	0,58	0,80	0,04	0,46	0,30	0,43	0,42	-0,29	0,56	0,50	0,27	-0,04	0,96	-0,09	0,92
ANSP (48 -120h)	-0,91	0,02	0,34	0,46	0,52	0,24	0,70	0,09	-0,77	0,10	-0,46	0,30	-0,29	0,56	0,39	0,40	-0,23	0,65	-0,24	0,63	-0,46	0,30	-0,21	0,66	0,26	0,66	-0,50	0,27	-0,71	0,09	-0,82	0,03
HSC 0h	0,20	0,67	0,37	0,43	0,09	0,86	0,52	0,35	0,18	0,71	0,11	0,84	0,46	0,30	0,49	0,36	-0,13	0,79	0,49	0,26	0,54	0,24	0,43	0,42	0,79	0,05	0,57	0,20	0,50	0,27	0,14	0,80
HSC 24h	0,22	0,65	-0,33	0,43	-0,40	0,33	-0,26	0,60	0,32	0,50	0,10	0,84	-0,19	0,66	-0,39	0,40	-0,31	0,50	0,04	0,94	0,14	0,75	0,14	0,78	0,86	0,02	0,31	0,46	0,64	0,10	0,61	0,17
HSC 48h	-0,07	0,90	-0,60	0,12	-0,20	0,63	-0,07	0,88	0,25	0,59	0,26	0,54	-0,14	0,75	-0,54	0,24	-0,05	0,92	-0,64	0,10	-0,17	0,70	-0,07	0,91	0,04	0,96	-0,43	0,30	0,00	>0,9	0,21	0,66
HSC 120h	-0,79	0,08	0,02	0,97	0,45	0,31	0,59	0,18	-0,54	0,30	-0,36	0,44	-0,29	0,56	0,04	0,96	-0,46	0,37	-0,72	0,10	-0,50	0,27	-0,29	0,56	0,37	0,50	-0,64	0,14	-0,50	0,27	-0,61	0,17
HSCs d(0 - 48h)	0,27	0,55	0,77	0,05	0,09	0,86	0,15	0,82	0,25	0,59	0,11	0,84	0,61	0,17	0,94	0,02	-0,13	0,79	0,75	0,06	0,32	0,50	0,14	0,80	0,14	0,78	0,79	0,05	0,07	0,91	0,03	>0,99
HSC d(48-120h)	-0,53	0,27	0,54	0,25	0,31	0,50	0,48	0,31	-0,26	0,66	-0,43	0,35	-0,07	0,91	0,54	0,24	-0,58	0,24	-0,30	0,55	-0,43	0,35	-0,57	0,20	0,03	>0,99	-0,14	0,78	-0,86	0,02	-0,79	0,05
MSC 0h	-0,04	0,95	0,59	0,17	0,52	0,23	0,39	0,47	-0,50	0,27	-0,11	0,84	0,18	0,71	0,60	0,24	0,56	0,21	0,56	0,20	0,11	0,84	0,26	0,66	-0,64	0,14	-0,11	0,84	-0,54	0,24	-0,54	0,30
MSC 24h	-0,70	0,13	-0,17	0,71	-0,36	0,44	0,58	0,28	0,03	>0,9	0,11	0,84	-0,07	0,91	0,71	0,14	0,14	0,80	0,28	0,56	-0,18	0,71	0,09	0,92	0,60	0,24	0,32	0,50	-0,39	0,40	-0,20	0,71
MSC 48h	-0,87	0,02	-0,55	0,18	-0,07	0,87	0,52	0,26	-0,54	0,24	0,00	>0,99	-0,40	0,33	-0,21	0,66	0,14	0,76	-0,40	0,32	-0,57	0,15	0,07	0,91	0,21	0,66	-0,69	0,07	-0,33	0,43	-0,36	0,44
MSC 120h	-0,77	0,10	0,12	0,80	0,34	0,46	0,52	0,26	-0,89	0,03	-0,50	0,27	-0,54	0,24	0,14	0,78	0,03	0,98	0,12	0,84	-0,36	0,44	0,07	0,91	0,09	0,92	-0,46	0,30	-0,36	0,44	-0,61	0,17
MSCs d(0 - 48h)	0,62	0,15	0,91	0,01	0,70	0,09	0,09	0,88	-0,14	0,78	-0,25	0,59	0,21	0,66	0,43	0,42	0,23	0,61	0,47	0,29	0,54	0,24	0,26	0,66	-0,43	0,35	0,18	0,71	0,04	0,96	-0,31	0,56
MSC d(48-120h)	-0,77	0,10	0,12	0,80	0,34	0,46	0,52	0,26	-0,89	0,03	-0,50	0,27	-0,54	0,24	0,14	0,78	0,03	0,98	0,12	0,84	-0,36	0,44	0,07	0,91	0,09	0,92	-0,46	0,30	-0,36	0,44	-0,61	0,17
CMP 0h	0,55	0,21	0,51	0,27	0,23	0,62	-0,21	0,73	0,32	0,50	0,43	0,35	0,79	0,05	0,60	0,24	-0,02	0,99	0,62	0,15	0,68	0,11	0,49	0,36	0,11	0,84	0,71	0,09	0,71	0,09	0,71	0,14
CMP 24h	0,36	0,42	-0,03	0,96	-0,35	0,40	-0,44	0,33	0,68	0,11	0,21	0,62	0,19	0,66	0,00	>0,99	-0,59	0,17	0,18	0,67	0,24	0,58	-0,14	0,78	0,75	0,07	0,69	0,07	0,71	0,06	0,68	0,11
CMP 48h	0,47	0,29	0,00	>0,99	0,02	0,96	-0,07	0,88	0,54	0,24	0,05	0,93	0,10	0,84	-0,36	0,44	-0,41	0,36	-0,37	0,36	0,33	0,43	-0,04	0,96	0,68	0,11	0,14	0,75	0,48	0,24	0,43	0,35
CMP 120h	-0,26	0,60	0,14	0,76	0,05	0,92	0,48	0,31	0,09	0,92	0,61	0,17	0,57	0,20	0,61	0,17	0,03	0,98	0,24	0,63	0,18	0,71	0,36	0,44	0,71	0,14	0,36	0,44	0,14	0,78	0,25	0,59
CMPs d(0-3 h -48h)	0,64	0,14	0,61	0,16	0,14	0,76	-0,33	0,58	0,46	0,30	0,36	0,44	0,75	0,07	0,66	0,18	-0,11	0,82	0,62	0,15	0,64	0,14	0,26	0,66	0,07	0,91	0,82	0,03	0,61	0,17	0,60	0,24
CMP d(48- 120h)	-0,50	0,31	0,14	0,76	0,18	0,70	0,56	0,22	-0,20	0,71	0,57	0,20	0,54	0,24	0,64	0,14	0,12	0,84	0,24	0,63	0,11	0,84	0,39	0,40	0,60	0,24	0,21	0,66	0,07	0,91	0,14	0,78
GMP 0h	0,07	0,90	0,63	0,12	0,47	0,29	0,33	0,58	-0,29	0,56	0,29	0,56	0,68	0,11	0,77	0,10	0,50	0,25	0,88	0,02	0,43	0,35	0,66	0,18	-0,32	0,50	0,32	0,50	-0,04	0,96	0,03	>0,99
GMP 24h	0,31	0,50	-0,03	0,96	-0,19	0,65	-0,11	0,82	0,46	0,30	-0,14	0,75	-0,17	0,70	-0,29	0,56	-0,40	0,38	-0,13	0,77	0,19	0,66	-0,07	0,91	0,82	0,03	0,29	0,50	0,40	0,33	0,36	0,44
GMP 48h	-0,20	0,67	-0,41	0,33	-0,31	0,45	0,00	>0,99	0,00	>0,99	-0,52	0,20	-0,86	0,01	-0,68	0,11	-0,20	0,67	-0,52	0,19	-0,52	0,20	-0,43	0,35	0,07	0,91	-0,43	0,30	-0,29	0,50	-0,46	0,30
GMP 120h	-0,62	0,23	0,58	0,17	0,68	0,10	0,82	0,03	-0,83	0,06	-0,54	0,24	-0,29	0,56	0,36	0,44	0,20	0,70	0,18	0,74	0,00	>0,99	0,21	0,66	0,14	0,80	-0,46	0,30	-0,68	0,11	-0,79	0,05
GMPs d(0- 48h)	0,07	0,90	0,63	0,12	0,47	0,29	0,33	0,58	-0,29	0,56	0,29	0,56	0,68	0,11	0,77	0,10	0,50	0,25	0,88	0,02	0,43	0,35	0,66	0,18	-0,32	0,50	0,32	0,50	-0,04	0,96	0,03	>0,99
GMP d(48- 120h)	-0,62	0,23	0,46	0,32	0,54	0,22	0,67	0,11	-0,89	0,03	-0,29	0,56	-0,14	0,78	0,46	0,30	0,41	0,43	0,42	0,40	0,00	>0,99	0,32	0,50	-0,03	>0,99	-0,29	0,56	-0,46	0,30	-0,57	0,20

Table A3. Correlation of clinical parameters, blood products and fluids with the concentration of inflammatory and mobilizing factors. Correlations with a r-value > 0.7 and a p-value < 0.05 are highlighted in red. *Based on: Vogel et al.: Distinct Dynamics of Stem and Progenitor Cells in Blood of Polytraumatized Patients. Shock 51: 430–438 (2019). https://journals.lww.com/shockjournal/Fulltext/2019/04000/Distinct_Dynamics_of_Stem_and_Progenitor_Cells_in.5.aspx).*

	Post	Age		ISS		CK shock-room		CK 24h		CK 48h		CK 120h		PRBC		FFP		Length ICU (days)	
		Spear-man`s r	p-value	Spear-man`s r	p-value	Spear-man`s r	p-value	Spear-man`s r	p-value	Spear-man`s r	p-value	Spear-man`s r	p-value	Spear-man`s r	p-value	Spear-man`s r	p-value	Spear-man`s r	p-value
Fractalkine (pg/ml)	0 h	0,214	0,662	-0,214	0,662	0,429	0,354	0,500	0,267	0,429	0,354	-0,700	0,233	0,000	9999,0	0,126	0,800	0,054	0,919
	24 h	-0,407	0,314	-0,551	0,163	-0,132	0,761	0,072	0,874	-0,407	0,314	-0,143	0,803	0,252	0,591	0,118	0,787	0,255	0,535
	48 h	-0,548	0,171	-0,333	0,428	0,238	0,582	0,095	0,840	-0,048	0,935	0,143	0,803	0,857	0,024	0,847	0,025	0,578	0,141
	120 h	-0,357	0,444	-0,500	0,267	0,179	0,713	0,214	0,662	0,000	9999,0	0,314	0,564	0,771	0,103	0,600	0,242	0,309	0,503
G-CSF (pg/ml)	0 h	0,357	0,444	0,429	0,354	0,571	0,200	0,464	0,302	0,607	0,167	0,700	0,233	0,429	0,354	0,469	0,290	0,883	0,014
	24 h	0,643	0,096	0,167	0,703	0,762	0,037	0,738	0,046	0,881	0,007	0,771	0,103	0,571	0,200	0,577	0,186	0,639	0,094
	48 h	0,476	0,243	-0,024	0,977	0,905	0,005	0,619	0,115	0,691	0,069	0,943	0,017	0,571	0,200	0,577	0,186	0,771	0,032
	120h	-0,036	0,964	0,536	0,236	0,571	0,200	-0,143	0,783	0,393	0,396	0,829	0,058	0,543	0,297	0,600	0,242	0,891	0,010
Gro-α (pg/ml)	0 h	0,679	0,110	-0,036	0,964	0,643	0,139	0,786	0,048	0,679	0,110	0,000	9999,0	0,071	0,906	0,072	0,889	0,396	0,383
	24 h	0,218	0,619	0,627	0,113	0,246	0,560	0,164	0,702	0,409	0,327	0,845	0,067	0,453	0,314	0,447	0,314	0,801	0,036
	48 h	0,120	0,781	-0,132	0,761	0,743	0,042	0,575	0,143	0,635	0,099	0,928	0,022	0,793	0,040	0,746	0,062	0,685	0,067
	120 h	-0,036	0,956	0,109	0,822	0,618	0,148	-0,509	0,249	0,091	0,852	0,551	0,272	0,319	0,556	0,522	0,300	0,380	0,388
Gro-β (pg/ml)	0 h	0,536	0,236	-0,214	0,662	0,464	0,302	0,143	0,783	0,000	9999,0	-0,700	0,233	-0,536	0,236	-0,360	0,426	-0,270	0,558
	24 h	0,310	0,462	-0,500	0,216	0,286	0,501	0,119	0,793	-0,167	0,703	-0,257	0,658	-0,393	0,396	-0,487	0,271	-0,253	0,544
	48 h	0,357	0,389	-0,381	0,360	0,500	0,216	0,405	0,327	0,095	0,840	-0,143	0,803	-0,036	0,964	-0,126	0,800	0,169	0,692
	120 h	0,143	0,783	-0,286	0,556	0,500	0,267	-0,500	0,267	-0,321	0,498	0,371	0,497	-0,086	0,919	-0,029	9999,0	0,236	0,606
IL-6 (pg/ml)	0 h	0,071	0,906	0,571	0,200	0,429	0,354	0,286	0,556	0,500	0,267	0,500	0,450	0,429	0,354	0,541	0,214	0,847	0,024
	24 h	0,691	0,069	0,381	0,360	0,738	0,046	0,452	0,268	0,810	0,022	0,771	0,103	0,464	0,302	0,523	0,235	0,494	0,218
	48 h	0,548	0,171	0,238	0,582	0,810	0,022	0,381	0,360	0,619	0,115	0,943	0,017	0,536	0,236	0,541	0,214	0,795	0,023
	120 h	0,000	9999,0	0,357	0,444	0,571	0,200	0,179	0,713	0,750	0,066	0,886	0,033	0,886	0,033	0,943	0,017	0,655	0,125
IL-8 (pg/ml)	0 h	0,536	0,236	0,143	0,783	0,750	0,066	0,714	0,088	0,857	0,024	0,700	0,233	0,464	0,302	0,469	0,290	0,721	0,077
	24 h	0,524	0,197	0,548	0,171	0,429	0,299	0,500	0,216	0,738	0,046	0,600	0,242	0,429	0,354	0,469	0,290	0,627	0,105
	48 h	0,619	0,115	0,238	0,582	0,667	0,083	0,762	0,037	0,857	0,011	0,600	0,242	0,464	0,302	0,469	0,290	0,603	0,121
	120 h	0,607	0,167	0,393	0,396	0,750	0,066	0,536	0,236	0,893	0,012	0,829	0,058	0,600	0,242	0,543	0,297	0,527	0,237
IL-10 (pg/ml)	0 h	0,607	0,167	-0,464	0,302	0,357	0,444	0,357	0,444	-0,107	0,840	-0,900	0,083	-0,571	0,200	-0,469	0,290	-0,180	0,698
	24 h	0,802	0,020	0,096	0,824	0,383	0,345	0,683	0,071	0,790	0,024	0,314	0,564	0,126	0,798	-0,027	0,953	0,048	0,914
	48 h	0,738	0,046	-0,095	0,840	0,595	0,132	0,881	0,007	0,905	0,005	0,486	0,356	0,429	0,354	0,342	0,458	0,277	0,507
	120 h	0,523	0,240	-0,631	0,141	0,396	0,383	0,829	0,028	0,487	0,278	0,116	0,839	0,232	0,667	0,058	0,939	-0,248	0,602
MCP-1 (pg/ml)	0 h	0,643	0,139	0,000	9999,0	0,679	0,110	0,821	0,034	0,786	0,048	0,400	0,517	0,286	0,556	0,252	0,591	0,577	0,187
	24 h	0,595	0,132	0,452	0,268	0,500	0,216	0,191	0,665	0,357	0,389	0,829	0,058	0,143	0,783	0,198	0,670	0,663	0,081
	48 h	0,571	0,151	-0,191	0,665	0,429	0,299	0,667	0,083	0,524	0,197	0,371	0,497	0,321	0,498	0,216	0,637	0,434	0,286
	120 h	0,429	0,354	0,071	0,906	0,571	0,200	0,714	0,088	0,929	0,007	0,771	0,103	0,771	0,103	0,657	0,175	0,309	0,503
Mip-1α (pg/ml)	0 h	-0,250	0,595	0,571	0,200	-0,179	0,713	-0,500	0,267	-0,500	0,267	-0,400	0,517	-0,464	0,302	-0,216	0,637	0,000	9999,
	24 h	-0,157	0,711	0,181	0,669	-0,265	0,522	-0,229	0,585	-0,518	0,193	-0,667	0,161	-0,631	0,144	-0,455	0,299	-0,128	0,754
	48 h	0,575	0,143	-0,108	0,808	0,132	0,761	0,431	0,288	0,132	0,761	-0,522	0,300	-0,631	0,143	-0,546	0,210	-0,109	0,796
	120 h	0,786	0,048	0,000	9999,0	0,036	0,964	0,179	0,713	-0,036	0,964	-0,143	0,803	-0,771	0,103	-0,829	0,058	-0,346	0,448
Mip-1β (pg/ml)	0 h	0,582	0,181	-0,036	0,951	0,782	0,048	0,564	0,198	0,655	0,129	-0,154	0,833	0,073	0,897	0,193	0,675	0,284	0,523
	24 h	0,115	0,779	-0,626	0,110	0,524	0,193	0,089	0,829	-0,243	0,571	-0,309	0,567	-0,158	0,752	0,010	0,991	0,090	0,824
	48 h	-0,120	0,780	-0,731	0,048	0,539	0,175	0,323	0,433	0,012	0,990	0,086	0,919	0,559	0,206	0,555	0,201	0,370	0,364
	120 h	-0,037	0,979	-0,778	0,045	0,074	0,879	-0,185	0,714	-0,482	0,307	-0,029	0,994	-0,030	9999,0	-0,213	0,733	-0,057	0,900
MDC (pg/ml)	0 h	0,214	0,662	0,607	0,167	0,071	0,906	-0,107	0,840	-0,036	0,964	-0,100	0,950	-0,464	0,302	-0,342	0,458	-0,054	0,919
	24 h	-0,048	0,935	0,786	0,028	0,071	0,882	-0,524	0,197	0,071	0,882	0,829	0,058	0,179	0,713	0,270	0,559	0,337	0,413
	48 h	-0,024	0,977	0,310	0,462	0,452	0,268	-0,476	0,243	-0,167	0,703	0,543	0,297	0,071	0,906	0,252	0,591	0,446	0,273
	120 h	-0,179	0,713	-0,107	0,840	-0,036	0,964	-0,893	0,012	-0,679	0,110	-0,086	0,919	-0,371	0,497	-0,200	0,714	-0,018	0,989
SDF-1α (pg/ml)	0 h	0,072	0,887	-0,162	0,729	0,342	0,456	-0,144	0,757	0,342	0,456	0,600	0,350	0,414	0,356	0,373	0,400	-0,091	0,844
	24 h	0,396	0,321	0,217	0,612	0,370	0,364	-0,319	0,450	0,115	0,800	0,372	0,467	-0,075	0,881	0,085	0,857	-0,006	0,995
	48 h	0,524	0,197	-0,214	0,619	0,952	0,001	0,310	0,462	0,405	0,327	0,543	0,297	0,286	0,556	0,342	0,458	0,434	0,286
	120 h	0,357	0,444	-0,143	0,783	0,857	0,024	0,179	0,713	0,536	0,236	0,829	0,058	0,543	0,297	0,486	0,356	0,546	0,219
VEGF-A (pg/ml)	0 h	0,536	0,236	-0,036	0,964	0,000	9999,	0,286	0,556	-0,179	0,713	0,100	0,950	-0,357	0,444	-0,469	0,290	0,180	0,698
	24 h	0,452	0,268	0,524	0,197	0,191	0,665	-0,286	0,501	-0,048	0,935	0,029	9999,	-0,464	0,302	-0,252	0,591	0,012	0,989
	48 h	0,524	0,197	0,548	0,171	0,429	0,299	0,500	0,216	0,738	0,046	0,600	0,242	0,429	0,354	0,469	0,290	0,627	0,105
	120 h	0,321	0,498	0,821	0,034	0,429	0,354	0,107	0,840	0,643	0,139	0,600	0,242	0,429	0,419	0,486	0,356	0,637	0,135

Table A4: *Correlation of the fold change from the different cell populations after TXT induction within a tissue* ***a*** *BM* ***b*** *PB and* ***c*** *lung tissue. Correlations with a r-value > 0.7 and a p-value < 0.05 are highlighted in red.*

a

BM	Early Progenitors		Late progenitors		EPCs		MSC1		MSC2		MSC3		Monocytes		Lymphocytes		Neutrophils	
	Spearman´s r	p-value	Spearman´s r	p-value	Spearman´s r	p-value	Spearman´s r	p-value	Spearman´s r	p-value	Spearman´s r	p-value	Spearman´s r	p-value	Spearman´s r	p-value	Spearman´s r	p-value
HSCs	0,89	<0,0001	0,84	<0,0001	0,49	0,00	0,30	0,02	0,29	0,03	0,42	0,00	0,43	0,00	0,66	<0,0001	0,66	<0,0001
Early Progenitors			0,90	<0,0001	0,40	0,00	0,32	0,02	0,34	0,01	0,49	0,00	0,39	0,01	0,61	<0,0001	0,60	<0,0001
Late progenitors					0,53	0,00	0,47	0,00	0,51	0,00	0,53	0,00	0,35	0,01	0,62	<0,0001	0,59	<0,0001
EPCs							0,42	0,00	0,41	0,00	0,51	0,00	0,20	0,10	0,28	0,03	0,30	0,03
MSC1									0,62	<0,0001	0,62	<0,0001	0,30	0,03	0,46	0,00	0,54	0,00
MSC2											0,66	<0,0001	0,14	0,20	0,33	0,02	0,30	0,03
MSC3													0,18	0,14	0,42	0,00	0,43	0,00
Monocytes															0,53	0,00	0,70	<0,0001
Lymphocytes																	0,75	<0,0001

b

PB	Early Progenitors		Late progenitors		EPCs		MSC1		MSC2		MSC3		Monocytes		Lymphocytes		Neutrophils	
	Spearman´s r	p-value	Spearman´s r	p-value	Spearman´s r	p-value	Spearman´s r	p-value	Spearman´s r	p-value	Spearman´s r	p-value	Spearman´s r	p-value	Spearman´s r	p-value	Spearman´s r	p-value
HSCs	0,65	<0,0001	0,60	<0,0001	0,36	0,01	0,22	0,09	0,13	0,24	0,33	0,03	0,01	0,48	0,01	0,48	0,11	0,25
Early Progenitors			0,61	<0,0001	0,35	0,01	0,13	0,21	0,29	0,06	0,28	0,06	0,08	0,31	0,02	0,44	0,06	0,35
Late progenitors					0,49	0,00	0,10	0,27	0,43	0,01	0,34	0,03	-0,30	0,03	0,04	0,40	0,15	0,18
EPCs							0,17	0,15	0,20	0,15	0,22	0,11	-0,34	0,01	0,16	0,15	0,27	0,05
MSC1									0,30	0,05	0,52	0,00	0,30	0,03	0,39	0,01	0,42	0,00
MSC2											0,40	0,02	-0,21	0,12	0,13	0,25	0,01	0,49
MSC3													-0,03	0,44	0,14	0,23	0,21	0,13
Monocytes															0,49	0,00	0,11	0,24
Lymphocytes																	0,51	0,00

c

Lung	Early Progenitors		Late progenitors		EPCs		Monocytes		Lymphocytes		Neutrophils	
	Spearman´s r	p-value	Spearman´s r	p-value	Spearman´s r	p-value	Spearman´s r	p-value	Spearman´s r	p-value	Spearman´s r	p-value
HSCs	0,53	0,00	0,36	0,01	0,29	0,03	0,017	0,46	-0,05	0,39	0,10	0,28
Early Progenitors			0,38	0,01	0,36	0,01	0,04	0,41	0,20	0,12	0,26	0,06
Late progenitors					0,08	0,3	0,19	0,13	0,32	0,03	0,37	0,01
EPCs							0,26	0,06	0,01	0,49	0,00	0,49
Monocytes									0,61	<0,0001	0,39	0,01
Lymphocytes											0,34	0,02

Table A5: *Correlation of the fold change from the distinct cell populations after TXT induction between the different tissues* ***a*** *BM versus PB and BM versus lung tissue* ***b*** *PB versus lung tissue. Correlations with a r-value > 0.7 and a p-value < 0.05 are highlighted in red.*

a

BM	PB		Lung	
	Spearman´s r	p-value	Spearman´s r	p-value
HSC	0,1177	0,2289	0,1881	0,1165
Early Progenitors	0,2088	0,0922	0,1605	0,1519
Late Progenitors	-0,1916	0,112	0,1163	0,2289
EPCs	-0,1228	0,2193	0,2111	0,0871
MSC 1	0,2285	0,078		
MSC 2	0,2625	0,0805		
MSC 3	0,1008	0,2915		
Monocytes	-0,02092	0,447	-0,1818	0,1556
Lymphocytes	0,3047	0,0222	-0,0888	0,306
Neutrophils	-0,008537	0,4789	0,3125	0,036

b

PB	Lung	
	Spearman´s r	p-value
HSC	0,1392	0,1927
Early Progenitors	0,2472	0,0572
Late Progenitors	-0,03022	0,4247
EPCs	-0,09586	0,273
Monocytes	0,2739	0,0556
Lymphocytes	0,09112	0,2986
Neutrophils	0,01485	0,4663